

การสังเคราะห์โคบอลต์บน โคบอลต์อะลูมิเนียมและสมบัติการเป็นตัวเร่งปฏิกิริยาสำหรับ
คาร์บอนมอนอกไซด์ไฮโดรจีเนชัน



นางสาว ศิริรัตน์ โรจนพิพัฒนกุล

สถาบันวิทยบริการ

จุฬาลงกรณ์มหาวิทยาลัย

วิทยานิพนธ์นี้เป็นส่วนหนึ่งของการศึกษาตามหลักสูตรปริญญาวิศวกรรมศาสตรมหาบัณฑิต

สาขาวิชาวิศวกรรมเคมี ภาควิชาวิศวกรรมเคมี

คณะวิศวกรรมศาสตร์ จุฬาลงกรณ์มหาวิทยาลัย

ปีการศึกษา 2550

ลิขสิทธิ์ของจุฬาลงกรณ์มหาวิทยาลัย

SYNTHESIS OF COBALT ON COBALT-ALUMINATE AND ITS
CATALYTIC PROPERTIES FOR CARBON MONOXIDE
HYDROGENATION



Miss Sirirat Rojanapipatkul

สถาบันวิทยบริการ
จุฬาลงกรณ์มหาวิทยาลัย

A Thesis Submitted in Partial Fulfillment of the Requirements
for the Degree of Master of Engineering Program in Chemical Engineering
Department of Chemical Engineering
Faculty of Engineering
Chulalongkorn University
Academic Year 2007
Copyright of Chulalongkorn University

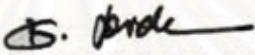
Thesis Title SYNTHESIS OF COBALT ON COBALT-ALUMINATE AND
 ITS CATALYTIC PROPERTIES FOR CARBON MONOXIDE
 HYDROGENATION

By Miss Sirirat Rojanapipatkul

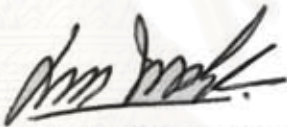
Field of Study Chemical Engineering


Thesis Advisor Assistant Professor Bunjerd Jongsomjit, Ph.D


Accepted by the Faculty of Engineering, Chulalongkorn University in Partial
Fulfillment of the Requirements for the Master's Degree


.....Dean of Faculty of Engine
(Associate Professor Boonsom Lerdhirunwong, Dr.Ing.)

THESIS COMMITTEE


..... Chairman
(Associate Professor ML Suppakanok Thongyai, Ph.D.)


..... Thesis Advisor
(Assistant Professor Bunjerd Jongsomjit, Ph.D.)


..... Member
(Assistant Professor Joongjai Panpranot, Ph.D.)


..... Member
(Associate Professor Muenduen Phisalaphong, Ph.D.)


.....External Member
(Assistant Professor Okorn Mekasuwandamrong, Ph.D.)

ศิริรัตน์ โรจนพิพัฒนกุล: การสังเคราะห์โคบอลต์บนโคบอลต์อะลูมิเนตและสมบัติการเป็นตัวเร่งปฏิกิริยาสำหรับคาร์บอนมอนอกไซด์ไฮโดรจิเนชัน (SYNTHESIS OF COBALT ON COBALT-ALUMINATE AND ITS CATALYTIC PROPERTIES FOR CARBON MONOXIDE HYDROGENATION)

อ. ที่ปรึกษา : ศศ. ดร. บรรเจิด จงสมจิตร, 120 หน้า

วิทยานิพนธ์นี้ ศึกษาถึงการสังเคราะห์โคบอลต์บนโคบอลต์อะลูมิเนตในขั้นตอนเดียวด้วยวิธีโซลโวเทอร์มอล และศึกษาความว่องไวในการเป็นตัวเร่งปฏิกิริยาสำหรับคาร์บอนมอนอกไซด์ไฮโดรจิเนชัน โดยปัจจัยในการสังเคราะห์โคบอลต์บนโคบอลต์อะลูมิเนตที่นำมาศึกษา ได้แก่ อัตราส่วนของ Co/Al เวลาและอุณหภูมิที่ใช้ในการสังเคราะห์ อุณหภูมิที่ใช้ในการเผา และชนิดสารตั้งต้นโคบอลต์ โดยตัวอย่างที่สังเคราะห์ได้จะถูกนำไปตรวจสอบคุณลักษณะโดยใช้การดูดซับทางกายภาพด้วยไนโตรเจน การกระเจิงรังสีเอ็กซ์ การส่องผ่านและส่องกราดด้วยกล้องจุลทรรศน์อิเล็กตรอน การรีดักชันแบบโปรแกรมอุณหภูมิ และการดูดซับด้วยไฮโดรเจน ปฏิกิริยาคาร์บอนมอนอกไซด์ไฮโดรจิเนชัน ($H_2/CO=10$) ถูกใช้เพื่อทดสอบความว่องไวของตัวเร่งปฏิกิริยาและการเลือกเกิดของผลิตภัณฑ์ ผลการศึกษาพบว่าเมื่อทำการสังเคราะห์โคบอลต์บนโคบอลต์อะลูมิเนตที่อุณหภูมิ 300 องศาเซลเซียส การเพิ่มอัตราส่วนของ Co/Al ทำให้ความว่องไวในการเกิดปฏิกิริยาเพิ่มขึ้น โดยที่อัตราส่วนของ Co/Al เป็น 0.5 เวลาที่ใช้ในการสังเคราะห์มีอิทธิพลมาก คือ เวลาในการสังเคราะห์ที่เพิ่มขึ้น ทำให้ความว่องไวในการเกิดปฏิกิริยาลดลง แต่เมื่อเพิ่มอัตราส่วนของ Co/Al (1.0 และ 2.0) เวลาในการสังเคราะห์ที่เพิ่มขึ้นส่งผลให้ความว่องไวในการเกิดปฏิกิริยาลดลงเล็กน้อย การสังเคราะห์โคบอลต์บนโคบอลต์อะลูมิเนตเป็นเวลา 2 ชั่วโมง พบว่าเมื่อทำการลดอุณหภูมิที่ใช้ในสังเคราะห์ลงจาก 300 เป็น 250 องศาเซลเซียส ทำให้ความว่องไวในการเกิดปฏิกิริยาเพิ่มขึ้น เมื่อทำการศึกษาอุณหภูมิที่ใช้ในการเผา (ที่ 300 400 และ 500 องศาเซลเซียส) เป็นเวลา 1 ชั่วโมง พบว่าการเผาที่อุณหภูมิ 400 องศาเซลเซียส ให้ความว่องไวในการเกิดปฏิกิริยาสูงสุด และเมื่อทำการเปรียบเทียบวิธีการสังเคราะห์โคบอลต์บนโคบอลต์อะลูมิเนตในขั้นตอนเดียว กับการฝังเคลือบโคบอลต์ลงบนอะลูมินาที่เตรียมด้วยวิธีโซลโวเทอร์มอล เมื่อมีปริมาณโคบอลต์ส่วนเกินที่เท่ากัน พบว่าวิธีการสังเคราะห์โคบอลต์บนโคบอลต์อะลูมิเนตในขั้นตอนเดียวให้ความว่องไวในการเกิดปฏิกิริยามากกว่า จากการศึกษาชนิดสารตั้งต้นโคบอลต์พบว่าความว่องไวในการเกิดปฏิกิริยาของ $CoN > CoAC > CoAA > CoCL$ สัมพันธ์กันกับขนาดของผลึก โดยผลึกใหญ่มีแรงดึงดูดระหว่างกันน้อยกว่าผลึกเล็ก แต่ $CoCL$ ให้การเลือกเกิดเป็น C_2-C_4 สูงกว่า

ภาควิชา.....วิศวกรรมเคมี..... ลายมือชื่อนิสิต.....ศิริรัตน์...โรจนพิพัฒนกุล....
สาขาวิชา.....วิศวกรรมเคมี..... ลายมือชื่ออาจารย์ที่ปรึกษา.....
ปีการศึกษา.....2550.....

##4970603921: MAJOR CHEMICAL ENGINEERING

KEY WORD: COBALT-ALUMINATE/ COBALT CATALYST/ CARBON MONOXIDE HYDROGENATION/ SOLVOTHERMAL

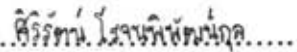
SIRIRAT ROJANAPIPAKUL: SYNTHESIS OF COBALT ON COBALT-ALUMINATE AND ITS CATALYTIC PROPERTIES FOR CARBON MONOXIDE HYDROGENATION. THESIS ADVISOR: ASST. PROF. BUNJERD JONGSOMJIT, Ph.D., 120 pp.


The study focused on synthesis of cobalt on cobalt-aluminate catalyst in one-pot via the solvothermal process and its catalytic properties for carbon monoxide hydrogenation. The influence of conditions to synthesize cobalt on cobalt-aluminate catalyst in this study was investigated such as Co/Al molar ratios, time and temperature during synthesis, temperature of calcination, and cobalt precursors. The various samples were characterized using N₂ physisorption, XRD, SEM/EDX, TEM, TPR and H₂ chemisorption. CO hydrogenation (H₂/CO = 10/1) was also performed to determine the overall activity and selectivity. It was found that when synthesized at 300°C, increased Co/Al molar ratios apparently resulted in increased activities, whereas the holding time during solvothermal synthesis seemed to have only little effect on the activities upon the high molar ratios of Co/Al (1.0 and 2.0). However, at low molar ratio of Co/Al (0.5), the increased holding time can result in dramatically decreased activity. The decreased temperature during solvothermal process for 2 h can result in increased activity. The study of calcination temperature such as 300, 400 and 500°C for 1 h revealed that the sample calcined at 400°C exhibited the highest activity among other samples. The cobalt on cobalt-aluminate catalysts apparently exhibited higher activities than that prepared from the conventional solvothermal-derived alumina-supported cobalt catalyst without any changes in product selectivity when prepared with the same amount of cobalt excess. For the study of different cobalt precursors, it revealed that the activity of CoN > CoAC > CoAA > CoCL due to large crystallite size having fewer interactions. CoCL showed higher selectivity to C₂-C₄.

Department.....Chemical Engineering...

Field of study...Chemical Engineering...

Academic year.....2007.....

Student's signature.. .....

Advisor's signature.. .....

ACKNOWLEDGEMENTS

The author would like to express her greatest gratitude and appreciation to her advisor, Asst. Prof. Dr, Bunjerd Jongsomjit for his invaluable guidance, providing value suggestions and his kind supervision throughout this study. In addition, she is also grateful to Associate Professor ML Suppakankong Thongyai, as the chairman, Assistant Professor Muenduen Phisalaphong, Assistant Professor Joongjai Panpranot and Assistant Professor Okorn Mekasuwandamrong as the members of the thesis committee. The author would like to thank the Thailand Research Fund (TFR) according to the RMU50-B. Jongsomjit project, and the Commission on Higher Education (CHE) for the financial support of this research.

The author would like to acknowledge with appreciation to Professor Piyasan Prasethdam for his kind suggestions on her research without hesitation and many thanks for kind suggestions and useful help to Miss Nitinart Chitpong, Mr. Pimchanok Tupabut, Mr. Nitikon Wongwaranon, Mr. Terachai Sirikajorn, and many friends in the petrochemical laboratory who always provide the encouragement and co-operate along the thesis study.

Most of all, the author would like to express her highest gratitude to her parents who always pay attention to her all the times for suggestions, support and encouragement.

สถาบันวิทยบริการ
จุฬาลงกรณ์มหาวิทยาลัย

CONTENTS

	page
ABSTRACT (IN THAI).....	iv
ABSTRACT (IN ENGLISH).....	v
ACKNOWLEDGMENTS.....	vi
CONTENTS.....	vii
LIST OF TABLES.....	x
LIST OF FIGURES.....	xi
CHAPTER	
I INTRODUCTION.....	1
II LITERATURE REVIEWS.....	4
2.1 Co-support compound formation.....	4
2.2 Synthesis of aluminate spinel and their application.....	8
2.3 Effect of cobalt precursors on supported cobalt catalysts.....	12
III THEORY.....	19
3.1 Fischer-Tropsch synthesis (FTS)	19
3.1.1 The surface carbide mechanism.....	22
3.1.2 The hydroxycarbene mechanism.....	24
3.1.3 The CO insertion mechanism.....	25
3.2 Alumina.....	27
3.2.1 Aluminium Oxides or Alumina (Al_2O_3).....	29
3.2.2 Aluminate.....	30
3.3 Cobalt.....	31
3.2.1 General.....	31
3.2.2 Physical properties.....	31
3.4 Cobalt aluminate and cobalt oxide.....	34
3.4.1 Cobalt aluminate (CoAl_2O_4).....	34
3.4.2 Cobalt Oxides.....	35
3.5 Cobalt-based catalysts.....	35
3.6 Cobalt-support compound formation (Co-SCF).....	36
3.4.1 Co-Aluminate Formation.....	36
3.7 Solvothermal Method.....	37

IV	EXPERIMENTS.....	39
	4.1 Catalyst preparation.....	39
	4.1.1 Chemicals.....	39
	4.1.2 Equipment.....	40
	4.1.3 Preparation of cobalt-aluminate and alumina support.....	40
	4.1.4 Preparation of alumina supported cobalt catalyst.....	41
	4.1.5 Catalyst Nomenclature.....	42
	4.2 Catalyst characterization.....	43
	4.2.1 N ₂ physisorption.....	43
	4.2.2 X-ray diffraction (XRD).....	43
	4.2.3 Scanning electron microscopy and energy dispersive X-ray spectroscopy (SEM/EDX).....	44
	4.2.4 Transmission electron microscopy (TEM).....	44
	4.2.5 Temperature-programmed reduction (TPR).....	44
	4.2.5 Hydrogen chemisorption.....	45
	4.3 Reaction study in CO hydrogenation.....	45
	4.3.1 Materials.....	45
	4.3.2 Apparatus.....	45
	4.3.3 Procedures.....	47
	Research methodology.....	50
V	RESULTS AND DISCUSSION	49
	5.1 Cobalt on cobalt-aluminate catalyst with various Co/Al molar ratios, time during synthesis, and temperature of calcination (Part I).....	51
	5.1.1 Effect of Co/Al molar ratio and holding time during synthesis.....	51
	5.1.2 Effect of temperature during solvothermal process.....	69
	5.1.3 Effect of calcination temperature.....	78
	5.2 Cobalt on cobalt-aluminate catalyst with various cobalt precursor (Part II).....	88

	ix
	page
VI CONCLUSIONS AND RECOMMENDATIONS.....	100
6.1 Conclusions.....	100
6.2 Recommendations.....	101
REFERENCES.....	102
APPENDICES.....	107
APPENDIX A: CALCULATION FOR CATALYST PREPARATION.....	108
APPENDIX B: CALCULATION FOR TOTAL H ₂ CHEMISORPTION.....	113
APPENDIX C: CALIBRATION CURVES.....	114
APPENDIX D: CALCULATION OF CO CONVERSION, REACTION RATE AND SELECTIVITY.....	117
APPENDIX E: CHEMISORPTION DATA.....	118
APPENDIX F: LIST OF PUBLICATIONS.....	119
VITA	120



สถาบันวิทยบริการ
จุฬาลงกรณ์มหาวิทยาลัย

LIST OF TABLES

Table	page
3.1 Physical properties of alumina.....	28
3.2 Physical properties of cobalt	32
4.1 Chemicals used in the preparation of catalysts.....	39
4.2 Operating condition for gas chromatograph.....	46
5.1 BET Surface areas of the calcined cobalt on cobalt-aluminate catalysts with various Co/Al molar ratios and holding time during synthesis.....	52
5.2 Reaction study of cobalt on cobalt aluminate with various Co/Al molar ratios and holding time during synthesis.....	67
5.3 BET surface areas of the calcined cobalt on cobalt-aluminate catalysts with various temperature during solvothermal process.....	69
5.4 Reaction study of cobalt on cobalt aluminate with various calcination temperature.....	77
5.5 BET surface areas of the calcined cobalt on cobalt-aluminate catalysts with various temperature during solvothermal process.....	78
5.6 H ₂ chemisorption and reaction study of cobalt on cobalt aluminate with various calcination temperature.....	87
5.7 BET surface areas of the calcined cobalt on cobalt-aluminate catalysts with various cobalt precursors.....	88
5.8 Reaction study of cobalt on cobalt aluminate with various cobalt precursors	99
C.1 Conditions use in Shimadzu modal GC-8A and GC-14B.....	114
E.1 Chemisorption data.....	119

LIST OF FIGURES

	page
3.1 Illustration of Al and O atom packing in the basal plan.....	30
3.2 Structure of cobalt aluminate.....	34
4.1 Flow diagram of CO hydrogenation system.....	49
5.1 XRD pattern of the calcined cobalt on cobalt-aluminate catalysts.....	53
5.2 SEM micrograph and EDX mapping of Co/Al _{0.5} _1h.....	55
5.3 SEM micrograph and EDX mapping of Co/Al _{0.5} _2h.....	56
5.4 SEM micrograph and EDX mapping of Co/Al _{1.0} _1h.....	57
5.5 SEM micrograph and EDX mapping of Co/Al _{1.0} _2h.....	58
5.6 SEM micrograph and EDX mapping of Co/Al _{2.0} _1h.....	59
5.7 SEM micrograph and EDX mapping of Co/Al _{2.0} _2h.....	60
5.8 SEM micrograph and EDX mapping of Co/Al ₂ O ₃ _2h.....	61
5.9 TEM micrograph of Co/Al _{0.5} _1h and Co/Al _{0.5} _2h.....	62
5.10 TEM micrograph of Co/Al _{1.0} _1h and Co/Al _{1.0} _2h.....	63
5.11 TEM micrograph of Co/Al _{2.0} _1h and Co/Al _{2.0} _2h.....	63
5.12 TEM micrograph of Co/Al ₂ O ₃ _2h	64
5.13 TPR profiles for the calcined cobalt on cobalt-aluminate catalysts with various Co/Al molar ratios and holding time during synthesis and TPR profile for alumina supported cobalt catalyst.....	66
5.14 XRD pattern of the calcined cobalt on cobalt-aluminate catalysts with various temperature during solvothermal process... ..	70
5.15 SEM micrograph and EDX mapping of Co/Al _{0.5} _250°C	72
5.16 SEM micrograph and EDX mapping of Co/Al _{1.0} _250°C	73
5.17 TEM micrograph of cobalt on cobalt-aluminate catalysts with various temperature during solvothermal process... ..	74
5.18 TPR profiles for the calcined cobalt on cobalt-aluminate catalysts with various temperature during solvothermal process... ..	76
5.19 XRD pattern of the calcined cobalt on cobalt-aluminate catalysts with various temperature during solvothermal process... ..	79
5.20 SEM micrograph and EDX mapping of Co/Al ₃₀₀ °C	81

5.21 SEM micrograph and EDX mapping of Co/Al_400°C	82
5.22 SEM micrograph and EDX mapping of Co/Al_500°C	83
5.23 TEM micrograph of cobalt on cobalt-aluminate catalysts with various calcination temperature.....	84
5.24 TPR profiles for the calcined cobalt on cobalt-aluminate catalysts with various calcination temperature.....	86
5.20 XRD pattern of the calcined cobalt on cobalt-aluminate catalysts with various cobalt precursors.....	89
5.21 SEM micrograph and EDX mapping of CoAA.....	91
5.22 SEM micrograph and EDX mapping of CoAC.....	92
5.23 SEM micrograph and EDX mapping of CoN.....	93
5.24 SEM micrograph and EDX mapping of CoCL.....	94
5.25 TEM micrograph of cobalt on cobalt-aluminate with various cobalt precursor.	95
5.26 TPR profiles for the calcined cobalt on cobalt-aluminate catalysts with various cobalt precursors.....	96
C.1 The calibration curve of methane.....	115
C.2 The calibration curve of ethylene.....	115
C.3 The chromatograms of catalyst sample from thermal conductivity detector, gas chromatography Shimadzu model 8A (Molecular sieve 5A column).....	116
C.4 The chromatograms of catalyst sample from flame ionization detector, gas chromatography Shimadzu model 14B (VZ10 column).....	116

CHAPTER I

INTRODUCTION

At present, the rapid increase of using fossil fuels or crude oil and environmental concerns are attentive problems. Fischer-Tropsch synthesis (FTS) has been considered as a part of gas-to-liquid technology, which converts natural gas that is the basis for a number of large-scale chemical industrial processes to more valuable middle distillates and clean transportation fuels. Natural gas is first transformed into synthesis gas, which is a mixture of carbon monoxide and hydrogen as the starting material to produce heavy hydrocarbons or synthetic fuels, which generally contain negligible sulfur and aromatic compounds compared to gasoline or diesel from crude oil, through carbon monoxide hydrogenation or FTS. (Mochizuki *et al.*, 2007)

Many transition metals of Group VIII can be used as catalysts for FTS such as iron (Fe), cobalt (Co), nickel (Ni), and ruthenium (Ru) (Elbashir *et al.*, 2005; Hosseini *et al.*, 2005). However, supported cobalt catalysts are preferred for FTS because of their high activity for FTS based on natural gas (Steynberg *et al.*, 2004), high selectivity for linear hydrocarbons, and low activity for the competitive water-gas shift (WGS) reaction (Steynberg, *et al.*, 1997; Brady and Pettit, 1981). To increase their activities, cobalt is usually deposited on a high surface area support to obtain a high metal dispersion. Many inorganic supports such as SiO₂, Al₂O₃, TiO₂ and zeolites (Niemela *et al.*, 1996; Jongsomjit *et al.*, 2003, 2004; Martinez., 2003) have been extensively studied for supported Co catalyst for years. It is known that in general, the catalytic properties depend on reaction conditions, catalyst composition, metal dispersion, and types of inorganic supports used. Furthermore, the catalytic performance of all FT catalysts strongly depends on the methods of catalyst preparation. The preparation of cobalt supported catalysts involves choice of the appropriate catalyst support, deposition of active phase, its promotion, oxidative and reductive treatments. The deposition of the precursor on the support surface is a complex phenomenon, which involves physical or chemical interactions between the precursor and the support. It is known that cobalt dispersion depends on the type of cobalt precursors. Loosdrecht *et al.* (1997) showed that alumina-supported cobalt catalysts prepared by incipient wetness impregnation using cobalt EDTA and cobalt

citrate precursors resulted in smaller cobalt oxide particles compared to the one prepared from cobalt nitrate. The use of cobalt oxalate, cobalt acetate, or cobalt acetylacetonate as cobalt precursors for titania-supported cobalt catalysts has been found to give higher cobalt dispersions than the catalysts prepared from cobalt nitrate (Kraum and Baerns, 1999). Rosenek and Polansky, 1991 reported that use of cobalt acetate yields higher dispersion than cobalt chloride on silica. Sun, 2000 concluded that catalysts prepared by mixed impregnation of cobalt nitrate and cobalt acetate result in higher Fischer–Tropsch synthesis activity than catalysts prepared from either monoprecursor. And recently, Soled *et al.* (2003) has presented a comprehensive model for how precursor-support interactions influence the morphology and reducibility of the fresh cobalt catalysts. A balance between dispersion-enhancing strong support–precursor interaction and metal loss by retarded reduction was suggested. However, compound formation between cobalt and the supports such as cobalt-aluminate, cobalt-silicate can occur during the catalyst activation and/or reaction conditions resulting in irreversible catalyst deactivation (Jongsomjit *et al.*, 2001).

The main objective of this thesis research was to investigate the influences of conditions and cobalt precursors to synthesize cobalt on cobalt-aluminate catalyst using single step synthesis on the characteristics and catalytic properties during CO hydrogenation. The great benefit of this study is that the cobalt on cobalt-aluminate can be prepared in only single step, plus the cobalt-aluminate as cobalt-support compound formation (Co-SCF) is not formed further (Jongsomjit *et al.*, 2001). The catalysts were characterized using various characterization techniques and tested in order to evaluate the catalytic properties during CO hydrogenation.

The study was scoped as follows:

1. Synthesize cobalt on cobalt-aluminate with various Co/Al molar ratios (Co/Al = 0.5, 1.0, and 2.0) at 300°C for 1 and 2h by solvothermal method and calcine in air at 300°C for 1h.
2. Synthesize cobalt on cobalt-aluminate (Co/Al = 0.5 and 1.0) at 250 and 300°C for 2 h by solvothermal method.

3. Synthesize cobalt on cobalt-aluminate ($\text{Co/Al} = 1.0$) at 300°C for 2 h by solvothermal method and various calcination temperature ($T = 300, 400,$ and 500°C).
4. Preparation of alumina supported cobalt catalyst (25 wt% Co) using the incipient wetness impregnation method.
5. Synthesize cobalt on cobalt-aluminate with various Co precursors (Co/Al ratio = 1.0) at 250°C for 2 h by solvothermal method and calcine in air at 300°C for 1h.
6. Characterization of the catalyst samples using BET surface area, X-ray diffraction (XRD), temperature programmed reduction (TPR), scanning electron microscopy (SEM) and energy dispersive X-ray spectroscopy (EDX), transmission electron spectroscopy (TEM) and H_2 chemisorption
7. Reaction study of the catalyst samples in carbon monoxide (CO) hydrogenation at 220°C , 1 atm and a H_2/CO ratio of 10 in order to measure catalytic activity and selectivity.

CHAPTER II

LITERATURE REVIEWS

This chapter reviews the work about several synthesis method of CoAl_2O_4 that is also of great interest in the field of heterogeneous catalysis while it has been used for catalytic application. The last section of this review shows a few research investigations about the effect of cobalt precursors on supported cobalt catalyst.

2.1 Co-support compound formation

A. Kogelbauer *et al.* (1995) studied the formation of cobalt silicates on Co/SiO_2 under hydrothermal conditions. Hydrothermal treatment at 220°C led to a catalyst with lower reducibility due to the formation of both reducible and nonreducible (at temperatures $< 900^\circ\text{C}$) Co silicates. They also showed that silicate was formed in catalysts which had been used for FT synthesis. No significant change occurred upon hydrothermal treatment of calcined catalyst. The presence of air during the hydrothermal treatment inhibited the formation of silicate and they proposed that the formation of silicate was linked to the presence of metallic cobalt.

B. Jongsomjit *et al.* (2001) studied Co-support compound formation (Co-SCF) in alumina-supported cobalt catalyst can result in lower activity of the catalysts. It has been found that water vapor present during standard reduction affects the degree of reducibility of cobalt in $\text{CoRu}/\gamma\text{-Al}_2\text{O}_3$. In this study, the impact of water vapor in the formation of Co-support compounds and the resulting characteristics of $\text{Co}/\gamma\text{-Al}_2\text{O}_3$ and $\text{CoRu}/\gamma\text{-Al}_2\text{O}_3$ catalysts were investigated to develop a better understanding of the nature of the Co-support compounds formed and the effect of noble metal promotion on their formation. The Co catalysts were reduced under differential conditions with and without added water vapor and then characterized. Co-support compound formation could not be detected by X-ray diffraction; however, Raman spectroscopy give useful information about the Co "aluminate" formed. Temperature-programmed reduction indicate that the degree of reduction of the catalyst samples was lower when additional water vapor was introduced during reduction, but to a

lesser degree when the Ru promoter was present. The Raman spectroscopic results suggest that the Co aluminate formed is not identical to CoAl_2O_4 (spinel) but is probably a surface compound deficient in Co. This compound formation is a major cause for differences seen in the degree of reducibility of Co/alumina catalyst after initial reduction, hydrogen chemisorption capacity, and Fischer-Tropsch synthesis activity.

B. jongsomjit *et al.* (2002) studied the effect of the addition of CO during H_2 reduction on Co-support compound formation in a $\text{Co}/\gamma\text{-Al}_2\text{O}_3$ catalyst was investigated. It is known that such compound formation can occur during catalyst reduction, is facilitated by the presence of water vapor, and results in a less active catalyst. In this study, a H_2 flow containing CO (1–9 vol.%) was used for standard reduction. Water vapor was also added (3 vol.%) in one series of experiments in order to examine the impact of CO when relatively high partial pressures of water vapor are also present. After reduction at various conditions, the pretreated catalyst samples were characterized and CO hydrogenation ($\text{H}_2/\text{CO} = 10/1$, 220 °C, 1.8 atm) also performed. Both initial and steady-state rates during CO hydrogenation went through a maximum for the addition of 3–5 vol.% CO during standard reduction. The maximum rate was about four times that in the case where no CO was added. A similar trend was found even where reduction occurred with a high partial pressure of water vapor. It is concluded that the addition of CO during reduction has a significant effect on activity of the catalyst due to increases in both Co reducibility and dispersion.

M. Voß *et al.* (2002) investigated the structural, chemical and electronic properties of Co and Co/Mn catalysts supported on Al_2O_3 , SiO_2 and TiO_2 by a combination of different methods such as TEM, XRD, XPS, TPR and TPO. They reported that temperature-programmed reduction and oxidation reveal the formation of various oxides in dependence on temperature. In case of the alumina- and titania-supported cobalt catalysts, the formation of high-temperature compounds CoAl_2O_4 and CoTiO_3 , respectively. Moreover, these compounds are not reducible under the

applied conditions, the degrees of reduction are only 18-20% (Co/Al₂O₃) and 77% (Co/TiO₂).

J. Lin *et al.* (2002) studied the effect of water vapor on the catalytic properties of a ruthenium promoted Co/TiO₂ catalyst during FTS operated, in a continuously stirred tank reactor (CSTR) by adding water into the feed gas at varying space velocity. They found that at higher space velocities (SV = 4 NL g cat.⁻¹h⁻¹), the addition of water did not have significant effect on the CO conversion. At lower space velocity (SV = 2 NL g cat.⁻¹h⁻¹), the addition of water decrease the CO conversion; however, the decrease was reversible with the catalyst quickly recovering the activity that it exhibited prior to water addition. Moreover, at high CO conversion (space velocity of SV = 1 NL g cat.⁻¹h⁻¹) the addition of water resulted in a catalyst permanent deactivation. The methane selectivity was not influence by water addition, but the CO₂ selectivity was increased with water addition.

G. Jacobs *et al.* (2002) investigated the effect of support, loading and promoter on the reducibility of cobalt catalysts. They have reported that significant support interactions on the reduction of cobalt oxide species were observed in the order Al₂O₃ > TiO₂ > SiO₂. Addition of Ru and Pt exhibited a similar catalytic effect by decreasing the reduction temperature of cobalt oxide species, and for Co species where a significant surface interaction with the support was present, while Re impacted mainly the reduction of Co species interaction with the support. They also suggested that, for catalysts prepared with a noble metal promoter and reduced at the same temperature, the increase in the number of active sites was due mainly to improvements in the percentage reduction rather than the actual dispersion (cluster size). Increasing the cobalt loading, and therefore the average Co cluster size, was found to exhibit improved reducibility by decreasing interactions with the support.

D.I. Enache *et al.* (2002) reported the thermal treatment, which leads to the best catalytic results, is the direct reduction of the nitrate precursor in the reactor. The effect of the pretreatment is higher in the case of zirconia supported catalyst. The direct reduction of nitrate precursors is even more effective when using a slow-temperature ramping protocol. This phenomenon is explained by the exothermicity of

the nitrate reduction. The slower the temperature ramps, the better the heat evacuation, avoiding any increase in cobalt-support interactions or particle agglomeration. The reduction of Co_3O_4 oxide is difficult and leads to an increase of the cubic crystallised cobalt at the expense of amorphous cobalt or hexagonal cobalt with stacking faults. The direct reduction of nitrate precursor increases the quantity of amorphous cobalt or hexagonal cobalt with crystallographic defects, which are active phases in this reaction. At the same time, the direct reduction leads to weaker metal-support interactions than does precalcination of catalysts. The nitrogen-flow calcination conducts to an intermediate situation. The quantity of crystallised Co_3O_4 is less important than in the case of airflow calcination and it is more reducible.

A. Sirijaruphan *et al.* (2003) was focused at getting deeper insight into the circumstances of “cobalt aluminate” formation in alumina supported cobalt catalysts. It was desired to determine which state(s) of cobalt (i.e. reduced or oxidized) and what reaction conditions play a significant role in the aluminate formation at the relatively mild conditions used for reduction or Fischer–Tropsch synthesis. Reduction and hydrothermal pretreatments were applied to influence the formation of nonreducible Co-support compounds. Temperature-programmed reduction (TPR) was used to measure the amount of reducible cobalt compounds formed in 20 wt% $\text{Co}=\text{Al}_2\text{O}_3$ catalyst. The results reveal that the presence of partially reduced cobalt in a well-dispersed form is required for the formation of cobalt aluminate. The presence of water vapor promotes cobalt aluminate formation probably by hydrating the alumina and possibly by partially reoxidizing highly dispersed cobalt.

B. jongsomjit *et al.* (2004) studied Co-support compound formation (Co-SCF) in titania-supported cobalt catalyst can occur during standard reduction resulting in a lower reducibility of catalyst. The compound of cobalt and titania formed referred as “Co-titanate” was considered to be non-reducible at temperatures $<800\text{ }^\circ\text{C}$. The “Co-titanate” formed resulted in a decrease in the reduction behaviors. It was found that the partial pressures of water vapor during reduction probably had only a slight effect on an increase in the “Co-titanate” formation. Due to its highly dispersed form, it can not be detected by XRD. However, Raman spectroscopy revealed that highly dispersed “Co-titanate” formed was likely to be different from CoTiO_3 and present as

a non-stoichiometric surface “Co-titanate” compound. The “Co-titanate” formed also resulted in decreased activities of catalyst without any changes in selectivity.

W. Chen-Bin *et al.* (2006) studied three types of supported cobalt catalysts ($\text{CoO}_x/\text{SiO}_2$, $\text{CoO}_x/\text{TiO}_2$ and $\text{CoO}_x/\text{Al}_2\text{O}_3$) were prepared by incipient wetness impregnation with aqueous $\text{Co}(\text{NO}_3)_2 \cdot 6\text{H}_2\text{O}$ solution. The phase composition and the interactions of cobalt with supports under different calcined temperatures were investigated using thermogravimetry (TG), N_2 -adsorption at -196°C , X-ray diffraction (XRD), temperature-programmed reduction (TPR) and diffuse reflectance spectroscopy (DRS). Their catalytic activities towards the CO oxidation were further studied in a continuous flow micro-reactor. The results showed that the interaction of cobalt oxide with supports was much stronger in the kinds of Al_2O_3 and TiO_2 , while no conclusive evidence of any interaction was found for SiO_2 . Besides the crystalline Co_3O_4 which was formed in three supported catalysts, both high-temperature phases CoAl_2O_4 and CoTiO_3 spinel were also detected under XRD, DRS and TPR analysis. The degree of interaction between cobalt oxide and the support not only affected the surface area and reduction behavior of the catalysts, the catalytic activity toward the CO oxidation also affected simultaneously. As the CoAl_2O_4 and CoTiO_3 spinel formed, both the surface area and catalytic activity decreased significantly.

2.2 Synthesis of aluminate spinel and their application

T. Ohgushi and S. Umeno (1987) studied low temperature synthesis of dispersed fine particle of cobalt aluminate that is a new application of zeolite. They found CoAl_2O_4 , with the spinel structure in a dispersed form, was synthesized at the 400°C by using zeolite A as a starting material. A specific surface area of products was measured by adsorption of $(\text{CH}_3)_2\text{CHCH}_3$ gas at -110°C and the mean size of the product particles was estimated to be about 14 nm. Zeolites have been used as catalyst, adsorbent or ion exchangers owing to their porous structure. In the applications, the zeolite structure is, of course, preserved. In the present work, zeolite A was used as a source of aluminium for the synthesis of cobalt aluminate.

C.O. Areal *et al.* (1999) prepared cobalt aluminate, CoAl_2O_4 , and Al_2O_3 - CoAl_2O_4 solid solutions (at Co:Al = 1:4, and Co:Al = 1:8) by hydrolysis of mixed metal alkoxides, followed by mild calcination of the resulting gels. Powder X-ray diffraction showed that all samples prepared were single phase materials having the spinel-type structure. The cubic lattice parameter, a_0 , was found to change gradually with aluminium content of the mixed metal oxides. Nitrogen adsorption-desorption isotherms, at 77 K, were used to determine surface area and pore texture. The BET surface area was found to be $235 \text{ m}^2 \text{ g}^{-1}$ for CoAl_2O_4 , and higher values (up to $365 \text{ m}^2 \text{ g}^{-1}$) were found for the Al_2O_3 - CoAl_2O_4 solid solutions. Samples having the same composition were also prepared by the classical ceramic method (starting from mechanical mixtures of the parent metal oxides); for these materials the corresponding surface areas were found to be in the range 1.7 – $3.3 \text{ m}^2 \text{ g}^{-1}$. The sol-gel method, starting from mixed metal alkoxides, was thus shown to be a convenient route to prepare cobalt aluminate spinels in a very high surface area form.

F. Mayer *et al.* (1999) searched size-controlled of nanoscaled aluminium spinels using heterobimetallic alkoxide precursors via water/oil microemulsions. They prepared nanosized spinels of type MAl_2O_4 ($\text{M} = \text{Mg}, \text{Co}, \text{Ni}, \text{Cu}$) by a sol-gel type hydrolysis of alkoxides in the inverse micelles of w/o microemulsions. Heterobimetallic alkoxides $\text{M}[\text{Al}(\text{OPr}^i)_4]_2$ containing both metallic elements in the desired stoichiometric in the molecules was established by single crystal X-ray diffraction analysis. By varying the hydrophilic chain length of detergent, the diameter of the water droplets can be tuned in the nanometer range, as determined by dynamic light scattering. The size of the resulting spinel nano-particles as evaluated from XRD peak profile analysis, correlates to the droplet size. The results of ceramic syntheses using the different types of alkoxide precursors were compared which reveal the advantage of single source approach.

W.S. Cho and M. Kakihana (1999) synthesized ceramic pigment CoAl_2O_4 nanocrystals by a polymerized complex technique. Cobalt nitrate, aluminum nitrate, citric acid and ethylene glycol were used as precursor materials. The formation of pure crystallized CoAl_2O_4 nanocrystals occurred when the precursors was heat-treated at 350°C in air for 2 h. They propose a model for CoAl_2O_4 formation from the

polymeric precursor. The model contains a series of steps such as the transformation of the precursor to amorphous cobalt aluminate, three-dimensional nucleation and growth, and solid-state reaction.

S. Chamtal *et al.* (2000) prepared cobalt spinel CoAl_2O_4 by the technique of colloidal solution destabilization using as the sol-gel process. The powder obtained from the dried gel was characterized by thermal analysis (Thermogravimetric and differential), X-ray diffraction, infrared spectroscopy, and specific surface properties (surface charge and electrophoretic mobility) of the spinel powder fired at 600°C , in suspension in different electrolyte solutions (10^{-3} molar ionic strength), shows that the spinel material charge depends on the pH of solution. The spinel sol was used for the preparation of membrane by the slip-casting method.

M. Zayat and D. Lavy (2000) prepared bright blue CoAl_2O_4 particles by the sol-gel and citrate-gel methods using aluminum sec-butoxide, cobalt salts and citric acid as oxides precursors. Both methods start from sols of the precursor alkoxides and salts, and involve formation of heterogeneous solid intermediates, reducing atomic diffusion processes during thermal treatment. This important feature results in a substantial lowering of the time and temperature needed for the formation of the desired compounds. The stages of the formation of CoAl_2O_4 , as well as the characterization of the resulting compounds were done using XRD, FTIR, UV-VIS, SEM, and TGA/DTA techniques. The structure, coloration, particle size, and temperature of formation of the resulting CoAl_2O_4 phases were found to depend on the precursors and methods used for preparation and the calcinations temperature. The lowest temperature for preparation of cobalt aluminate of about 700°C was obtained using the citrate-gel method. This Temperature is much lower than that needed for preparation of the compound through traditional solid-state reactions (above 100°C).

P. Thormahlen *et al.* (2000) studied a preparation method for making a high temperature stable monolith catalyst, using a cobalt-rich cobalt-aluminate spinel ($\text{Co}_{1.66}\text{Al}_{1.34}\text{O}_4$) as the active material, was proposed. This catalyst, which was known for being active for CO oxidation at low temperature, was prepared and characterized by BET, SEM, XRD, XPS and CO-TPD. The catalyst was tested for its capacity to

oxidize carbon monoxide using oxygen only and oxygen in combination with other compounds typically present in cold start exhausts from Otto engines, i.e. CO₂, C₃H₆, NO, H₂, H₂O or SO₂. When the catalyst activity was tested with only CO and O₂ present in the feed gas, complete conversion was reached at room temperature. When other compounds were present in the gas mixture, they inhibited the Co oxidation to various degree. The degree of inhibition for the compounds investigated was found to be: SO₂ > H₂O > NO > C₃H₆ > H₂ > CO₂. The main reason for the loss of activity is suggested to origin from the compounds adsorption and formation of different species on the cobalt oxide surface, which seems to inhibit the reduction and/or re-oxidation process of the metal oxide surface and/or the adsorption of CO

A. Kanyanucharat *et al.* (2002) synthesized CoAl₂O₄, ZnAl₂O₄ and NiAl₂O₄ by solvothermal method by using toluene as a solvent at various reaction temperatures for 2 h with the molar ratio was 0.5. It was found that the reaction temperature in the synthesis and the calcinations temperature affected the thermal stability of each metal aluminate spinels that result in the change of crystallite size and BET surface area. The varying of divalent ions in tetrahedral sites of metal aluminate spinels affected the thermal stability that revealed in the order of NiAl₂O₄ > CoAl₂O₄ > ZnAl₂O₄. That is the result of the difference in bond dissociation energy of metal oxides and cation distribution over sites with tetrahedral coordination in the spinel type structure

M. Zayat and D. Levy (2002) prepared cobalt aluminate particles by the sol-gel method, starting from aluminum sec-butoxide and cobalt salts with a Co:Al ratio of 1:3. Samples with the same composition were also prepared by the citrate-gel method from cobalt and aluminum nitrates and citric acid. The particles were calcined to temperatures between 400 and 1000°C, for the formation of the mixed oxide having spinel structure. The surface properties of the different samples (BET surface area and pore size distribution) were measured. The highest BET surface area obtained (about 339 m²/g) corresponds to a sample prepared by cobalt acetate and aluminum sec-butoxide, calcined at 400°C. The surface area of the sample is reduced progressively as the sample is calcined to higher temperatures (to about 65 m²/g at 1000°C). Narrow pore size distributions were observed with average pore radius ranging from 17–20 Å, for samples heated to 400°C, to about 55–65 Å for samples heated to 1000°C.

D.M.A. Melo *et al.* (2003) studied CoAl_2O_4 powder that was obtained from a mixture of Co and Al oxalates at a ratio of 1:8 (Co:Al). In the present investigation, CoAl_2O_4 was prepared and calcinated at different temperatures aiming at obtaining a cost-effective and thermally stable compound useful to ceramic tile dyeing. The calcining temperature affects the color of the pigments on glassy ceramic coatings. The best results were obtained calcining the spinel CoAl_2O_4 phase at 1000 or 1200 C. Different temperatures also resulted in the formation of crystalline phases but with unsatisfactory coloring effects on ceramic tiles.

N.K. Nga and D.K. Chi (2004) studied CoAl_2O_4 and NiAl_2O_4 spinels that were prepared by sol-gel method with citric acid. By powder X- ray diffraction the formation of CoAl and NiAl spinels was investigated, changing the calcination temperatures and the molar ratio of citric acid to the metals. These catalysts were characterized by temperature-programmed reduction, temperature-programmed desorption of CO and nitrogen adsorption. The catalysts have been tested for the selective reduction of NO_x with n- hexane in a continuous flow microreactor at constant pressure of 1 atm. The results CoAl_2O_4 and NiAl_2O_4 spinels were successfully prepared at comparatively low temperatures by citrate gel method. The XRD and TPR results confirm that the prepared spinels have high crystallinity and trace impurities. n-Hexane- SCR of NO_x performs at the low temperatures over the prepared spinels. The chemisorption and activity test results correspond to NiAl spinel at high NO_x conversion at lower temperatures than CoAl spinel to having a larger number of the weak adsorptive sites compared to the other. However, BET surface area of the first does not strongly differ from that of the latter. So the difference in adsorptive properties between two spinels may be due to different electron configurations of nickel and cobalt in these spinels.

2.3 Effect of cobalt precursors on supported cobalt catalysts

M.P. Rosynek and C.A. Polansky (1991) studied the effect of cobalt source on the reduction properties of silica-supported cobalt catalysts. TPR, XPRD, and XPS were use to characterize the reduction, calcinations, and catalytic behaviors of a series of 6 %wt Co/ SiO_2 catalysts prepared from nitrate, chloride, and acetate precursors.

The bulk reduction properties of the silica-supported, uncalcined nitrate and acetate precursors are similar; both involve multiple steps and are much more resistance to complete reduction by H₂ to metallic than are the corresponding unsupported salt. By contrast, reduction of CoCl₂/SiO₂ occurs in a single step that is virtually unaffected by the presence of the silica support.

M.K. Niemela *et al.* (1996) reported the effect of the precursor in the characteristics of the Co/SiO₂ catalysts prepared from Co(NO₃)₂, Co₂(CO)₈ and Co₂(CO)₁₂. The hydrogen chemisorption, CO desorption, XRD and XPS measurements indicated that the dispersion of the metallic species decreased in the precursor order Co₂(CO)₈ > Co₂(CO)₁₂ >> Co(NO₃)₂

E.V. Steen *et al.* (1996) investigated the influence of different steps in the preparation of impregnated Co/SiO₂ catalysts by incipient wetness on the reducibility of the catalyst precursor and on the formation of cobalt silicates. The TPR spectra of cobalt catalysts starting from chloride or sulphate are essentially the same as for the unsupported metal salt showing negligible interaction between the support and the salt. In the case of the nitrate or acetate precursor, however, a number of peaks can be seen in the TPR-spectra indicating the formation of different cobalt species during the preparation steps. The TPR-spectra of the nitrate and acetate precursors are very similar, with only the intensities of the peaks differing markedly.

M. Kraum and M. Bearn (1999) studied the dependence of the activity of cobalt-based catalysts for Fischer–Tropsch synthesis on the type of cobalt precursor and support material. Titania-supported catalysts were prepared by means of incipient wetness impregnation (IW), precipitation (PR) and spreading (SP) techniques. All catalysts were characterised by XRD, XPS, TPR and CO pulse experiments. The catalytic performance of the catalysts was examined at a total pressure of 20 bar, a temperature of 200°C, a space velocity (GHSV) of 1200 h⁻¹ and using a syngas having a H₂ to CO ratio equal to 2. For titania-supported catalysts, the use of oxalate, acetate and acetyl acetonate as cobalt precursors resulted in a higher activity compared with the reference catalyst prepared from nitrate. The activities determined can be slightly correlated with an increasing cobalt dispersion, which was affected by the preparation

procedure and type of precursor. The range of chain growth probabilities increased in the following order: cobalt(III) acetyl acetonate ($\alpha = 0.71$) < cobalt acetate ($\alpha = 0.74$) < cobalt(II) acetyl acetonate, cobalt oxalate, cobalt nitrate, cobalt-EDTA ($\alpha = 0.82$ – 0.84). On adding 0.1 wt.% Ru to the catalyst made from cobalt(III) acetyl acetonate, α increased from 0.71 to 0.80. For catalysts prepared by incipient wetness impregnation, ceria and zirconia were additionally used as supports. The activity changed in the following order: ZrO₂ < TiO₂ < CeO₂. The α -value for ceria- and zirconia-supported cobalt catalysts amounted to 0.81 and 0.69, respectively.

C.J. Huang *et al.* (2000) reported the cobalt precursors affects the catalytic performance of Co/SiO₂ catalyst remarkably for CO₂ reforming of CH₄. This paper compared the activity between cobalt nitrate/SiO₂ and cobalt acetate/SiO₂ catalysts at different cobalt contents and reaction temperature. It was found that the activity of Co(A)/SiO₂ is higher than Co(N)/SiO₂ especially at high cobalt content and low temperature.

J. Panpranot *et al.* (2003) prepared Co/MCM-41 catalysts using the incipient wetness impregnation technique with aqueous solutions of different cobalt compounds such as cobalt nitrate, cobalt chloride, cobalt acetate, and cobalt acetylacetonate. MCM-41 is known to have a restricted pore structure; however, using organic precursors such as cobalt acetate and cobalt acetylacetonate resulted in very small cobalt oxide particles that could not be detected by XRD even for a cobalt loading as high as 8 wt%. These cobalt particles were small enough to fit into the pores of MCM-41. However, they were found to chemisorb CO in only relatively small amounts and to have low activities for CO hydrogenation, probably due to the formation of cobalt silicates. The use of cobalt chloride resulted in very large cobalt particles/clusters and/or residual Cl⁻ blocking active sites, and consequently, very small active surface area was measurable. The use of cobalt nitrate resulted in a number of small cobalt particles dispersed throughout MCM-41 and some larger particles located on the external surface of MCM-41. Cobalt nitrate appeared to be the best precursor for preparing high-activity MCM-41-supported cobalt Fischer-Tropsch synthesis catalysts.

A. Martinez *et al.* (2003) investigated the influence of cobalt loading (10-40 wt%Co), cobalt precursor, and promoters (Re, Mn) on the physico-chemical and catalytic properties of mesoporous Co/SBA-15 catalysts for Fischer-Tropsch Synthesis reaction ($T = 493 \text{ K}$, $P = 20 \text{ bar}$, $\text{H}_2/\text{CO} = 2$). Catalysts were characterized by N_2 and Ar adsorption, X-ray diffraction (XRD), transmission electron microscopy (TEM), X-ray photoelectron spectroscopy (XPS), and temperature programmed reduction (TPR). For Co/SBA-15 catalysts prepared from Co (II) nitrate the dispersion decreased and the extent of cobalt reduction increased with cobalt loading. A maximum CO conversion was found for the sample with ca. 30 %wt Co loading, though the intrinsic activity of Co remained constant in the range of Co loading studied. More methane and less C_5^+n -paraffins were produced over the less reducibility 10 wt% Co loading sample. The addition of ca. 1 wt% Re enhanced the reducibility of cobalt oxides and increased the catalyst activity, though the intrinsic activity of cobalt sites was not altered. Rhenium also favored the formation of long chain n -paraffins (C_{10}^+) while decreasing methane selectivity. Promotion of cobalt with ca. 2 wt% Mn significantly improved cobalt dispersion but decreased its reducibility, producing catalysts that were less active than the unpromoted one. At similar cobalt loading (ca. 20 wt%), a much better dispersion and a stronger cobalt-support interaction leading to the formation of low reducible cobalt silicates was observed for oxidized samples prepared from acetate and acetylacetonate precursors as compared to that derived from cobalt (II) nitrate, as evidenced by TEM, XPS, and TPR. The former catalysts were characterized by a low FTS activity and a product distribution shifted toward the formation of lighter products. Finally, at comparable Co loading Co/SBA-15 catalysts (nitrate precursor) were about 1.5 times more active per weight of total Co than a Co/SiO₂ sample, with only minor differences in product selectivity.

Y. Ohtsuka *et al.* (2004) studied mesoporous molecular sieves (MCM-41 and SBA-15) with different pore diameters as supports of high loading of Co catalysts, and the performances in FT synthesis have been examined with a fixed bed stainless steel reactor at 2.0 MPa for the purpose of efficient production of C_{10} - C_{20} fraction as the main component of diesel fuel. The method of exchanging template ions in uncalcined MCM-41 with Co^{2+} ions is effective for holding 10-20% Co within the

mesopores while keeping the structure regularity of MCM-41 to some extent, compared with the conventional impregnation method using calcined MCM-41. At 523 K, CO conversion and selectivity to C₁₀-C₂₀ hydrocarbons are both higher at larger loading of 20% Co for the exchanged catalysts with pore diameters of 2.7-2.9 nm. When four kinds of 20% Co/SBA-15 with the diameters of 3.5-13 nm, prepared by the impregnation method using an ethanol solution of Co acetate, are used in FT synthesis at 523 K, the catalyst with the diameter of 8.3 nm shows the largest CO conversion, which is higher than those over MCM-41 supported Co catalysts. At a lower temperature of 503 K, however, the acetate-derived Co is almost inactive. In contrast, the use of Co nitrate alone or an equimolar mixture of the acetate and nitrate as Co precursor drastically enhances the reaction rate and consequently provides high space-time yield (260-270 g C/kgcat h) of C₁₀-C₂₀ hydrocarbons. The X-ray diffraction and temperature-programmed reduction measurements show that the dependency of the catalytic performance of 20% Co/SBA-15 on its precursor originates probably from the differences in not only the reducibility of the calcined catalyst but also the dispersion of metallic Co. Catalyst characterization after FTS strongly suggests the high stability of the most effective Co/SBA-15 in the dispersion and reducibility of the oxide species and in the mesoporous structure.

J. Panpranot *et al.* (2005) studied the effect of pore size and pore structure of the supports on cobalt dispersion (Co/SiO₂ and Co/MCM-41), reduction behavior, and catalytic properties for the Fischer-Tropsch synthesis. It was reported that the pore structure has little influence on the metal-support interaction in silica supported cobalt catalysts. Cobalt dispersion, reduction behavior, and catalytic properties for Fischer-Tropsch synthesis were primarily affected by the metal particle size. The XRD patterns of the catalysts prepared from cobalt nitrate and cobalt chloride (inorganic precursors) exhibited the diffraction peaks that indicated the present of Co₃O₄ but the catalysts prepared from cobalt acetate and cobalt acetylacetonate (organic precursors) did not exhibit any distinct XRD patterns. This suggests that the crystallite sizes of Co₃O₄ prepared from organic precursors were much smaller than those prepared from inorganic ones. The TPR profiles of silica supported Co catalysts used in this study were found to be dependent on the type of cobalt precursors. Using organic cobalt precursors which could result in very small cobalt particles and stronger metal-

support interaction showed a large portion of Co species that was reduced at higher reduction temperature. However, for a given Co precursor, Co/SiO₂ and Co/MCM-41 exhibited similar TPR profiles. It suggested that pore structure of the supports has little influence on the metal-support interaction on silica supported Co catalysts. The result of CO hydrogenation reaction was found that the catalyst prepared from cobalt nitrate showed very high activities due to their high Co dispersion. The catalyst prepared from cobalt chloride showed very low activities due to their low Co dispersion and maybe residual Cl⁻ blocking Co active site. The low activities of the ones prepared from cobalt acetate and cobalt acetyl acetonate were due probably to the unstable small Co particles forming Co silicates during reduction in H₂ and reaction.

J.S. Girardon *et al.* (2005) studied the effect of cobalt precursor and pretreatment conditions on the structure of cobalt species in silica-supported Fischer–Tropsch catalysts with a combination of characterization techniques (X-ray diffraction, UV–visible, X-ray absorption, X-ray photoelectron spectroscopies, DSC–TGA thermal analysis, propene chemisorption, and temperature-programmed reduction combined with in situ magnetic measurements). The catalysts were prepared via aqueous impregnation of silica with solutions of cobalt nitrate or acetate followed by oxidative pretreatment in air and reduction in hydrogen. It was found that after impregnation and drying cobalt exists in octahedrally coordinated complexes in catalysts prepared from cobalt nitrate or cobalt acetate. Decomposition of the octahedral complexes results in the appearance of Co₃O₄ crystallites and cobalt silicate species. Cobalt repartition between crystalline Co₃O₄ and the cobalt silicate phase in the oxidized samples depends on the exothermicity of salt decomposition in air and the temperature of the oxidative pretreatment. Co₃O₄ crystallite is the dominant phase in the samples prepared via endothermic decomposition of supported cobalt nitrate. Significantly higher cobalt dispersion is found in the catalyst prepared via low-temperature cobalt nitrate decomposition. The uncovered enhanced cobalt dispersion is associated with lower cobalt reducibility. The high exothermicity of cobalt acetate decomposition leads primarily to amorphous, barely reducible cobalt silicate. A more efficient heat flow control at the stage of cobalt acetate decomposition significantly increases the concentration of easy reducible Co₃O₄ in the

oxidized catalysts and the number of cobalt metal active sites after reduction. The catalytic measurements show that FT reaction rates depend on the number of cobalt surface metal sites; a higher concentration of cobalt metal sites in the catalysts prepared from cobalt nitrate or with the use of soft cobalt acetate decomposition results in higher catalytic activity in FT synthesis.

N. Nobuntu *et al.* (2005) prepared a series of Co (10%)/Zn (x%)/TiO₂ (x = 0, 5) catalysts from difference nitrate and acetate precursors. TPR and chemisorption techniques revealed that a mixture of cobalt precursors (cobalt acetate and cobalt nitrate) on titania were more easily reduced when compared to Co (10%)/TiO₂ catalysts prepared from either cobalt acetate or cobalt nitrate. By contrast, after addition of zinc, catalysts prepared from zinc acetate and cobalt nitrate had the most highly dispersed cobalt species when compared to catalysts prepared from the other combinations of nitrate and acetate precursors of zinc and cobalt. Mixed precursors of zinc and cobalt were also more active and had higher CO conversion in Fischer-Tropsch synthesis when compared to catalysts prepared from: (i) both nitrate precursors or (ii) both acetate precursors of zinc and cobalt. However, the catalyst prepared from zinc nitrate and cobalt nitrate produced more wax (>C16) when compared to the other catalysts studied (50% versus 12-32% wax). Data suggest that larger Co particles correlate with wax production as well as reduced CO conversion. CO chemisorption data correlated better with the FT activity data than did Co XPS data.

CHAPTER III

THEORY

This chapter focuses on the fundamental theory of the Fischer-Tropsch Synthesis (FTS) which is well known as one type of carbon monoxide (CO) hydrogenation using Co-based catalysts. The chapter consists of the basic details of Fischer-Tropsch Synthesis (FTS), alumina properties, cobalt properties, details of Co-based catalysts and cobalt-support compound formation (Co-SCF), and solvothermal method synthesis.

3.1 Fischer-Tropsch synthesis (FTS)

Fischer-Tropsch synthesis (FTS) that discovered by Fischer and Tropsch over 80 years ago, as an alternate process, can convert the synthesis gas (H_2/CO) derived from carbon sources such as coal, peat, biomass and natural gas, into hydrocarbons and oxygenates. During the past decades, FTS has been developed continuously by many researchers, although the rise and fall in research intensity on this process has been highly related to the demands for liquid fuels and relative economics. This synthesis is basically the reductive polymerization (oligomerization) of carbon monoxide by hydrogen to form organic products containing mainly hydrocarbons and some oxygenated products in lesser amounts.

By manipulation of the reaction conditions, the process may be designed to produce heavier saturated hydrocarbons or lower olefins or oxygenated hydrocarbons as we shall see in the following discussion.

Metals that have significant activity for Fischer-Tropsch synthesis include iron, cobalt, nickel and ruthenium. Iron has proved so far to be the best. It is superior to cobalt with respect to conversion rate, selectivity and flexibility. Nickel has disadvantage of producing appreciable amounts of methane. Ruthenium enhance the formation of high molecular weight alkanes and catalyzes polymerization to

polymethane. Other group VIII metals are of low activity. Copper does not catalyze Fisher-Tropsch synthesis.

The catalyst is usually prepared by fusion or precipitation over a silica, alumina or kieselguhr support. Small amounts of promoters such as alkali metal or copper salts are included in the catalytic mix. Copper is believed to facilitate the reduction of the catalyst, alkali metal salt, particularly K_2O_2 enhance activity and olefins selectivity. The support increased the surface area of the catalyst metal thus extremely increasing in dispersion.

Sulfur compounds generally poison the catalyst and they must be removed from the synthesis gas feed stream. However, partial sulfur poisoning may have favorable effects. Thus, it has been found that deliberate slight sulfur poisoning of the iron/manganese catalyst enhances selectivity to short chain olefins.

Three main types of reactors are currently in use in the Fischer-Tropsch processes: Fixed-bed, fluidized-bed and slurry bed reactors. Fixed-bed reactors are usually tubular, each tube having 50 mm ID and 12 m length. A single reactor may contain as many as 2000 such tubes. Fluidized-bed reactors provide for better heat transfer and continuous regeneration of the catalyst. The catalyst used in fluidized-bed reactors must have high physical stability. SASOL (in South Africa), uses fluidized-bed reactors 46 m high, 230 cm in diameter with reaction temperature of 320-360°C and pressure. In the slurry-bed reactors the feed gas is bubbled through a suspension of finely divided catalyst particles. It has the advantage of good temperature control thus providing greater flexibility of reaction conditions.

Each type of reactor is better suited for certain product composition. Fixed-bed reactors, for example, produce high boiling straight-chain hydrocarbons consisting, typically, of 33% gasoline hydrocarbons (C_5-C_{11}), 17% diesel and 40% heavy paraffins and higher waxes. The gasoline fraction is of low octane value and requires further treatment (isomerization or blending) before use. Fluidized-bed reactors are the best when lighter hydrocarbons are desired. A typical product composition is 72% lower molecular weight gasoline-range hydrocarbons rich in olefins and 14%

oxygenated hydrocarbons. However, the product is low in diesel. Thus two or more different reactors may be operated in parallel to provide an integrated fuel plant.

The demands on selectivity of Fischer-Tropsch reactions are ever-increasing. In the earlier days of the process the concern was to improve selectivity with respect to better gasoline grade and/or diesel oil chemicals. With the realization of feasible route of converting synthesis gas to industrial intermediates, more stringent conditions are being imposed on the reaction parameters to make the process more selective.

Selectivity improvement is sought with respect to product properties such as chain length, chain branching, olefin content, alcohol content and methane content. Reaction conditions that particularly eliminate or minimize carbon deposition are desirable. In order to achieve and improve product selectivity the optimization of the following reaction parameters has been investigated: reaction temperature and pressure, H_2/CO ratio, conversion, space velocity, amount and type of promoters, nature of the catalyst, size of catalyst particles and mode of its deposition, type of support, and type of reactor.

We have already seen examples of how the choice of the metal catalyst and support affects the product distribution. The effect of the choice of the reactor type on the nature of the reaction products has also been demonstrated.

Selectivity to olefins may be enhanced by addition of promoters such as K_2O , Ti, Mn or V. Selectivity of greater than 70% to C_2-C_4 olefins at high conversion rate has been achieved.

The search for selectivity to lower olefins by controlling the chain growth and inhibiting hydrogenation has been followed in three directions:

- (a) The use of highly dispersed catalyst either by improving the method of deposition or using special dispersing supports.
- (b) The use of bimetallic catalyst eg. With Mn/Fe ratio of 9:1 at 330 °C up to 90% olefin selectivity has been achieved. However, the activity of the catalyst and its life-time are low.

(c) The use of shape-selective catalyst.

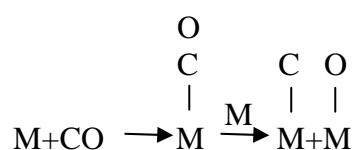
Since the Fischer-Tropsch process was originally intended for the production of hydrocarbons, little attention was paid in the early phases of the application of the process to the oxygenated products obtained as co-products. With the search for more economical sources of the oxygenated hydrocarbons, the possibility of tuning the Fischer-Tropsch process for the production such as oxygenates has been investigated. It has been found that with a nitrated iron catalyst, selectivity for alcohols may exceed 80%. A Rh/Hg/SiO₂ catalyst system gave 75% selectivity with respect to ethanol. The major side products are olefins.

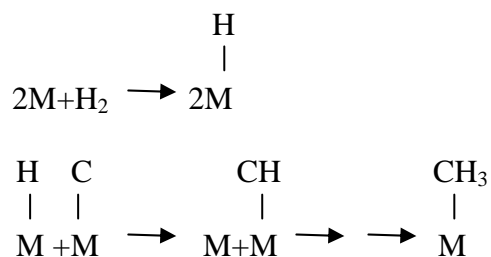
The Fischer-Tropsch process may be defined as being the hydrogenative oligomerization of CO over heterogeneous catalyst to produce alkanes, alkenes oxygenated hydrocarbons and water. A complete mechanism must account for the formation of all products observed. The first attempt at elucidating the mechanism of the process was made by the inventors of the process themselves, Fischer and Tropsch.

3.1.1 The surface carbide mechanism

Fischer and Tropsch apparently were trying to explain the formation of alkanes and alkenes rather than introduce a mechanism for whole line of the products that could be formed from the process. They observed that hydrocarbon formation occurred with heterogeneous metal catalysts (Ni, Fe, Co, Ru) that tend to absorb CO dissociatively to form surface carbide species. Their mechanism consists of the following steps:

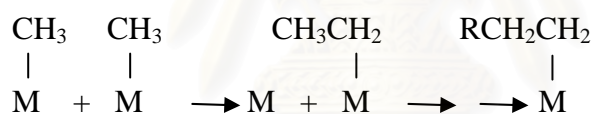
(i) **Initiation:**



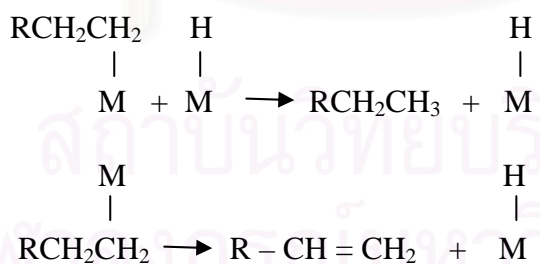


Note: M-X means species X chemisorbed on the metal surface atom M. The hyphen has no implication with respect to the strength of the M-X interaction or the order of the bond. More recently it has been suggested, based spectroscopic evidence, that in order to for an absorbed CO to undergo dissociation it must be bonded side-on to the metal, not end-on.

(ii) Propagation:

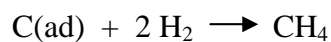
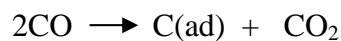


(iii) Termination:



The carbide mechanism has survived the several decades since its introduction. Several items of evidence arising from recent investigation support this mechanism e.g.

(a) In the hydrogenation of CO over clean Ni surface it has been observed that CO_2 evolution proceeds that CH_4 thus



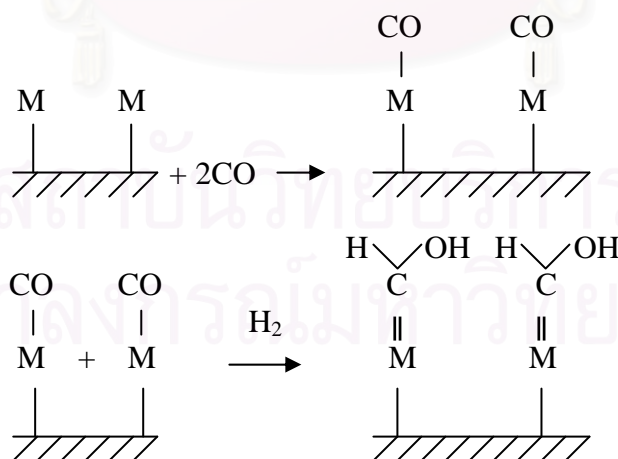
(b) Decomposition of diazomethane (CH_2N_2) at 200°C in the presence of H_2 over Co, Fe and Ru catalysts gives linear alkanes and olefins with distribution similar to that obtained from CO/H_2 reaction over the same catalyst.

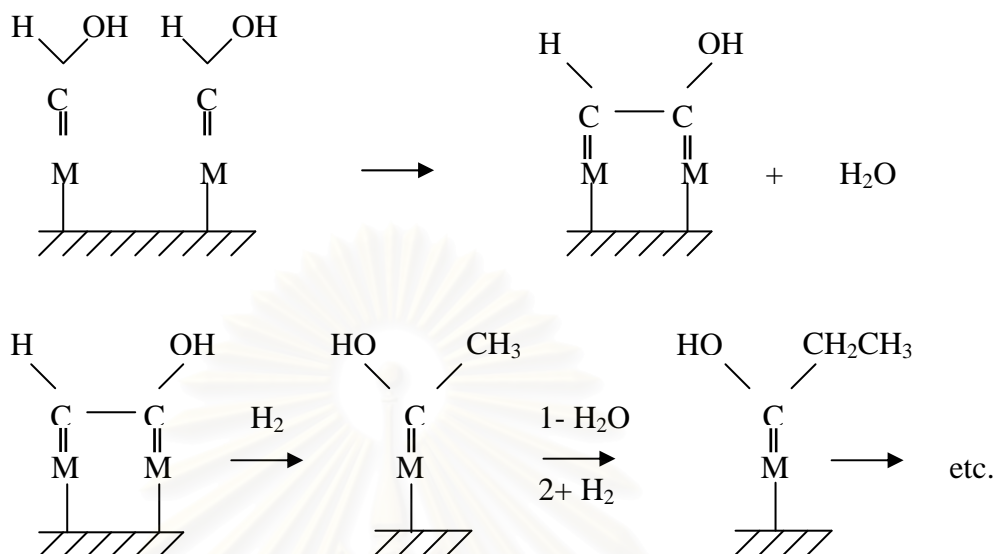
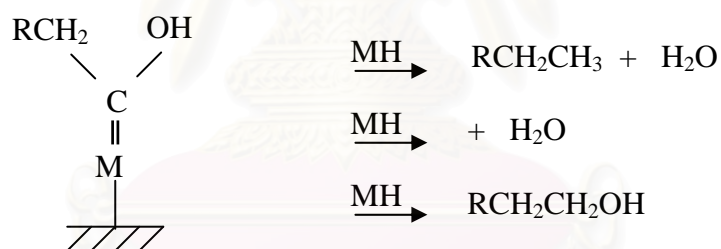
(c) Distribution of ^{13}C in $\text{CH}_2=\text{CH}$ formed when ^{13}CO , H_2 - and $^{12}\text{CH}_2\text{N}_2$ were reacted under Fischer-Tropsch conditions is consistent with the distribution predicted based on the carbided mechanism and inconsistent with other proposed mechanism.

However, a drawback of this mechanism is that it does not explain the formation of oxygenated products.

3.1.2 The hydroxycarbene mechanism

(i) Initiation:

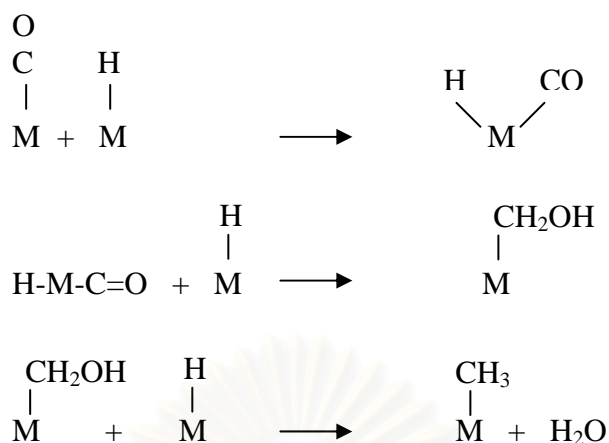


(ii) Propagation:**(iii) Termination:**

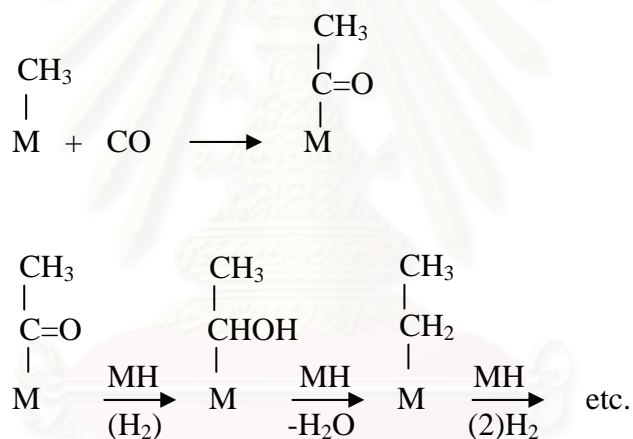
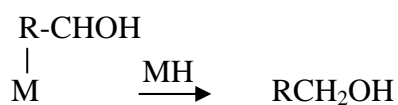
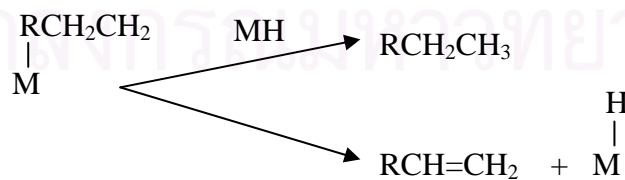
This mechanism explains the formation of alkanes, and olefins as well as oxygenated hydrocarbons. However, it precludes the dissociation of CO, which is not consistent with many experimental observations.

3.1.3 The CO insertion mechanism.**(i) initiation :**

The initiation of active species is similar to that of the carbide mechanism although the mechanism of its formation is different.

**(ii) Propagation:**

propagation proceeds via CO insertion rather than $-\text{CH}_2-$ insertion.

**(iii) Termination:**

Normally, catalysts used for FTS are group VIII metals. By nature, the hydrogenation activity increases in order of $\text{Fe} < \text{Co} < \text{Ni} < \text{Ru}$. Ru is the most active. Ni forms predominantly methane, while Co yields much higher ratios of paraffins to olefins and much less oxygenated products such as alcohols and aldehydes than Fe does.

The current main goal in FTS is to obtain high molecular weight, straight chain hydrocarbons. However, methane and other light hydrocarbons are always present as less desirable products from the synthesis. According to the Anderson-Schulz-Flory (ASF) product distribution, typically 10 to 20% of products from the synthesis are usually light hydrocarbon ($\text{C}_1\text{-C}_4$). These light alkanes have low boiling points and exist in the gas phase at room temperature, which is inconvenient for transportation. Many attempts have been made to minimize these by-products and increase the yield of long chain liquid hydrocarbons by improving chain growth probability. It would be more efficient to be able to convert these less desirable products into more useful forms, rather than re-reforming them into syngas and recycling them (Farrauto and Bartholomew, 1997). Depending upon the type of catalyst used, promoters, reaction conditions (pressure, temperature and H_2/CO ratios), and type of reactors, the distribution of the molecular weight of the hydrocarbon products can be noticeably varied.

3.2 Aluminum

Alumina (Al) is a silver-white metallic element in group IIIA of Periodic Table having an electronic configuration of $1s^2 2s^2 2p^6 3s^2 3p^1$. Aluminum exhibits a valance of +3 in all compounds except high temperature gaseous species in which the aluminum may be monovalant or divalant. Nearly all rocks, particularly igneous rocks, contain aluminum as aluminosilicate minerals.

The properties of aluminum vary significantly to purity and alloying.

- Physical properties of aluminum of 99.99% purity

Physical properties of aluminum of 99.99% purity are summarized in Table 3.1. Although, a number of radioactive isotopes have been artificially produced, naturally occurring aluminum consists of a single stable isotope. Aluminum crystallizes in the face-centered cubic system having a unit cell of 0.40496 nm at 20 °C. The unit cell contains four atoms and has coordination number of 12. The distance of closest approach of atoms is 0.2863 nm.

- Chemical properties

Aluminum reacts with oxygen, O₂ having a heat of reaction of -1675.7 kJ/mol (-400.5 kcal/mol), Al₂O₃ produced.

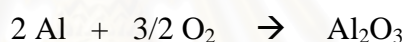


Table 3.1 Physical properties of aluminum

Property	Value
atomic number	13
atomic weight	26.9815
density at 25°C, kg/m ³	2,698
melting point, °C	660.2
boiling point, °C	2,494
thermal conductivity at 25°C, W/(mK)	234.3
latent heat of fusion, J/g ^a	395
latent heat of vaporization at bp, ΔH _v kJ/g ^a	10,777
electrical conductivity	65% IACS ^b
electrical resistivity at 20°C, Ω m	2.6548 x 10 ⁻⁸
temperature coefficient of electrical resistivity Ω m/°C	0.0043
electrochemical equivalent, mg/°C	0.0932

Table 3.1 Physical properties of aluminum (cont.)

Property	Value
electrode potential, V	-1.66
magnetic susceptibility, g ⁻¹	0.6276 x 10 ⁻⁶
Young's modulus, MPa ^c	65,000
Tensile strength, MPa ^c	50

^aTo convert J to cal, divided by 4.184.

^bInternational Annealed Copper Standard.

^cTo convert MPa to psi , multiply by 145.

3.2.1 Aluminium Oxides or Alumina (Al₂O₃)

Aluminum oxides, which are a term of alumina compounds, had transition phase and alpha phase alumina.

- Transition alumina

The partial dehydration of aluminum hydroxides and oxyhydroxides leads to compounds with the crude formula Al₂O₃ x H₂O with 0<x<1, which generally are poorly crystallized. These compounds are used to apply as catalyst supports, claus catalysts, and adsorbents. There are six principle phases designated by the Greek letters chi, kappa, eta, theta, delta, and gamma. The nature of the product obtained by calcination depends on the starting hydroxide (Gibbsite, boehmite and others) and on the calcination conditions. In effect, there exist several sequences during dehydration. In all, the ultimate product of dehydration is corundum (Al₂O₃). An excellent bibliographical review of transition alumina has been compiled by Leonard (1967). The situation can be reduced to a sample one on the basis of crystallographiscs, once one becomes aware that there are only two types of structures; spinel, for eta, gamma, delta, and theta and hexagonal, for chi and kappa.

- Alpha alumina

The structure of α -alumina consists of close packed planes of the large oxygen ions stacking in A-B-A-B sequence, thus forming hexagonal close packed array of anions. The aluminium cations are located at octahedral sites of this basic array and from another type of close packed planes between the oxygen layer. To maintain neutral charge, however, only two third of the available octahedral sites are filled with cation. Figure 3.2 illustrates the packing of Al and O atom in the basal plane. Since the vacant octahedral sites also form regular hexagonal array, three different types of cation layer can be defined, namely a, b, and c layer, depending on the position of the vacant cation site within the layer. These layers are stacked in a-b-c-a-b-c sequence in the structure of alumina.

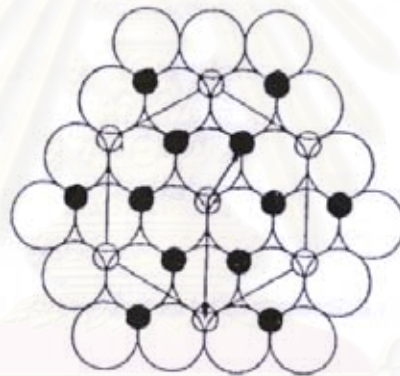


Figure 3.1 Illustration of Al and O atom packing in the basal plan

Alumina can exist in many metastable phase before transforming to the stable α -alumina (corundum form). Normally, transition alumina start to lose their surface area even at temperature below 800°C due to the elimination of micro-pores. However, drastic loss occurs at temperature higher than 1000°C when the crystallization to the thermodynamically stable α - alumina occurs.

3.2.2 Aluminate

A negative ion are usually given the formula AlO_2^- and derive from aluminum hydroxide. Solutions of aluminates are strongly basic.

3.3 Cobalt (Young 1960; Othmer, 1991)

3.3.1 General

Cobalt, a transition series metallic element having atomic number 27, is similar to silver in appearance.

Cobalt and cobalt compounds have expanded from use colorants in glasses and ground coat frits for pottery to drying agents in paints and lacquers, animal and human nutrients, electroplating materials, high temperature alloys, hard facing alloys, high speed tools, magnetic alloys, alloys used for prosthetics, and used in radiology. Cobalt is also as a catalyst for hydrocarbon refining from crude oil for the synthesis of heating fuel.

3.3.2 Physical Properties

The electronic structure of cobalt is $[\text{Ar}] 3d^7 4s^2$. At room temperature the crystalline structure of the α (or ϵ) form, is close-packed hexagonal (cph) and lattice parameters are $a = 0.2501$ nm and $c = 0.4066$ nm. Above approximately 417°C , a face-centered cubic (fcc) allotrope, the γ (or β) form, having a lattice parameter $a = 0.3544$ nm, becomes the stable crystalline form. Physical properties of cobalt are listed in Table 3.2.

The scale formed on unalloyed cobalt during exposure to air or oxygen at high temperature is double-layered. In the range of 300 to 900°C , the scale consists of a thin layer of mixed cobalt oxide, Co_3O_4 , on the outside and cobalt (II) oxide, CoO , layer next to metal. Cobalt (III) oxide, Co_2O_3 , may be formed at temperatures below 300°C . Above 900°C , Co_3O_4 decomposes and both layers, although of different appearance, are composed of CoO only. Scales formed below 600°C and above 750°C appear to be stable to cracking on cooling, whereas those produced at 600 - 750°C crack and flake off the surface.

Cobalt forms numerous compounds and complexes of industrial importance. Cobalt, atomic weight 58.933, is one of the three members of the first transition series of Group 9 (VIIB). There are thirteen known isotopes, but only three

are significant: ^{59}Co is the only stable and naturally occurring isotope; ^{60}Co has a half-life of 5.3 years and is a common source of γ -radioactivity; and ^{57}Co has a 270-d half-life and provides the γ -source for Mössbauer spectroscopy.

Cobalt exists in the +2 or +3 valance states for the major of its compounds and complexes. A multitude of complexes of the cobalt (III) ion exists, but few stable simple salt are known. Octahedral stereochemistries are the most common for cobalt (II) ion as well as for cobalt (III). Cobalt (II) forms numerous simple compounds and complexes, most of which are octahedral or tetrahedral in nature; cobalt (II) forms more tetrahedral complex than other transition-metal ions. Because of the small stability difference between octahedral and tetrahedral complexes of cobalt (II), both can be found equilibrium for a number of complexes. Typically, octahedral cobalt (II) salts and complexes are pink to brownish red; most of the tetrahedral Co (II) species are blue.

Table 3.2 Physical properties of cobalt (Othmer, 1991)

Property	Value
atomic number	27
atomic weight	58.93
transformation temperature, °C	417
heat of transformation, J/g ^a	251
melting point, °C	1493
latent heat of fusion, ΔH_{fus} J/g ^a	395
boiling point, °C	3100
latent heat of vaporization at bp, ΔH_{vap} kJ/g ^a	6276
specific heat, J/(g·°C) ^a	
15-100°C	0.442
molten metal	0.560
coefficient of thermalexpansion, °C ⁻¹	
cph at room temperature	12.5
fcc at 417°C	14.2

Table 3.2 Physical properties of cobalt (cont.)

Property	Value		
thermal conductivity at 25 °C, W/(m·K)	69.16		
thermal neutron absorption, Bohr atom	34.8		
resistivity, at 20 °C ^b , 10 ⁻⁸ Ω·m	6.24		
Curie temperature, °C	1121		
saturation induction, 4πI _s , T ^c	1.870		
permeability, μ			
initial	68		
max	245		
residual induction, T ^c	0.490		
coercive force, A/m	708		
Young's modulus, Gpac	211		
Hardness ^f , diamond pyramid, of %Co	99.9	99.98 ^e	
At 20 °C	225	253	
At 300 °C	141	145	
At 600 °C	62	43	
At 900 °C	22	17	
strength of 99.99 %cobalt, MPa ^g	as cast	annealed	sintered
tensile	237	588	679
tensile yield	138	193	302
compressive	841	808	
compressive yield	291	387	

^aTo convert J to cal, divided by 4.184.

^bconductivity = 27.6 % of International Annealed Copper Standard.

^cTo convert T to gauss, multiply by 10⁴.

^dTo convert GPa to psi , multiply by 145,000.

^eZone refined.

^fVickers.

^gTo convert MPa to psi , multiply by 145.

3.4 Cobalt aluminate and cobalt oxide

3.4.1 Cobalt aluminate (CoAl_2O_4)

CoAl_2O_4 is a binary oxide consisting of cobalt oxides and aluminum oxides that crystallize in spinel structure. The unit cell of spinels is represented by formula of AB_2O_4 . the Co^{2+} ions occupy the tetrahedrally coordinated A site and Al^{3+} ions occupy the octahedrally coordinated B site. The structure of cobalt aluminate is shown in Figure 1

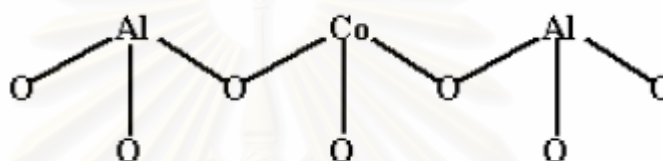


Figure 3.2 Structure of cobalt aluminate

Spinel-type structures are usually synthesized at high temperature from a mixture at solid state of the two oxide components. In this spinel-type structure, the metal aluminates seem to be a good option because of their properties such as greater thermal stability, high resistance to acids and alkalis, hydrophobicity, low surface acidity, high melting points and surface area, lower temperature sinterability, increase hardness, ductility, better diffusion, etc (Edelstein, 1999). These properties make it interesting materials as catalysts and carriers for active metals to substitute the more traditional systems. CoAl_2O_4 has received special interest due to their technological applications as inorganic ceramic blue pigment (Cho and Kakihana, 1999; Mimani, 2001; Zayat and Lavy, 2000; Bacon and Roberts, 1953). CoAl_2O_4 is also of great interest in the field of heterogeneous catalysis while it has been used for catalytic application (Chokkaram *et al.*, 1997; Arian *et al.*, 1998). Recently, CoAl_2O_4 has been prepared by several methods, such as co-precipitated method, sol-gel method, hydrothermal method, polymerized complex methods and solvothermal method

3.4.2 Cobalt Oxides

Cobalt has three well-known oxides:

Cobalt (II) oxide, CoO , is an olive green, cubic crystalline material. Cobalt (II) oxide is the final product formed when the carbonate or the other oxides are calcined to a sufficiently high temperature, preferably in a neutral or slightly reducing atmosphere. Pure cobalt (II) oxide is a difficult substance to prepare, since it readily takes up oxygen even at room temperature to re-form a higher oxide. Above about 850°C , cobalt (II) oxide form is the stable oxide. The product of commerce is usually dark gray and contains 75-78 wt % cobalt. Cobalt (II) oxide is soluble in water, ammonia solution, and organic solvents, but dissolves in strong mineral acids. It is used in glass decorating and coloring and is a precursor for the production of cobalt chemical.

Cobalt (III) oxide, Co_2O_3 , is formed when cobalt compounds are heated at a low temperature in the presence of an excess of air. Some authorities told that cobalt (III) oxide exists only in the hydrate form. The lower hydrate may be made as a black powder by oxidizing neutral cobalt solutions with substances like sodium hypochlorite. Co_2O_3 or $\text{Co}_2\text{O}_3 \cdot \text{H}_2\text{O}$ is completely converted to Co_3O_4 at temperatures above 265°C . Co_3O_4 will absorb oxygen in a sufficient quantity to correspond to the higher oxide Co_2O_3 .

Cobalt oxide, Co_3O_4 , is formed when cobalt compounds, such as the carbonate or the hydrated sesquioxide, are heated in air at temperatures above approximately 265°C and not exceeding 800°C .

3.5 Co-based Catalysts

Supported cobalt (CO) catalysts are the preferred catalysts for the synthesis of heavy hydrocarbons from natural gas based syngas (CO and H_2) because of their high Fischer-Tropsch (FT) activity, high selectivity for linear hydrocarbons and low activity for the water-gas shift reaction. It is known that reduced cobalt metal, rather

than its oxides or carbides, is the most active phase for CO hydrogenation in such catalysts. Investigations have been done to determine the nature of cobalt species on various supports such as alumina, silica, titania, magnesia, carbon, and zeolites. The influence of various types of cobalt precursors used was also investigated. It was found that the used of organic precursors such as CO (III) acetyl acetate resulting in an increase of CO conversion compared to that of cobalt nitrate.(Kraum and Baerns, 1999)

3.6 Cobalt-Support Compound Formation (Co-SCF)

Compound formation between cobalt metal and the support can occur under pretreatment and/or reaction conditions, leading to catalyst deactivation. The compound formation of cobalt metal with support materials, however, is difficult to predict because of the lack of sufficient thermodynamic data. Co-support compound formation can be detected evidentially.

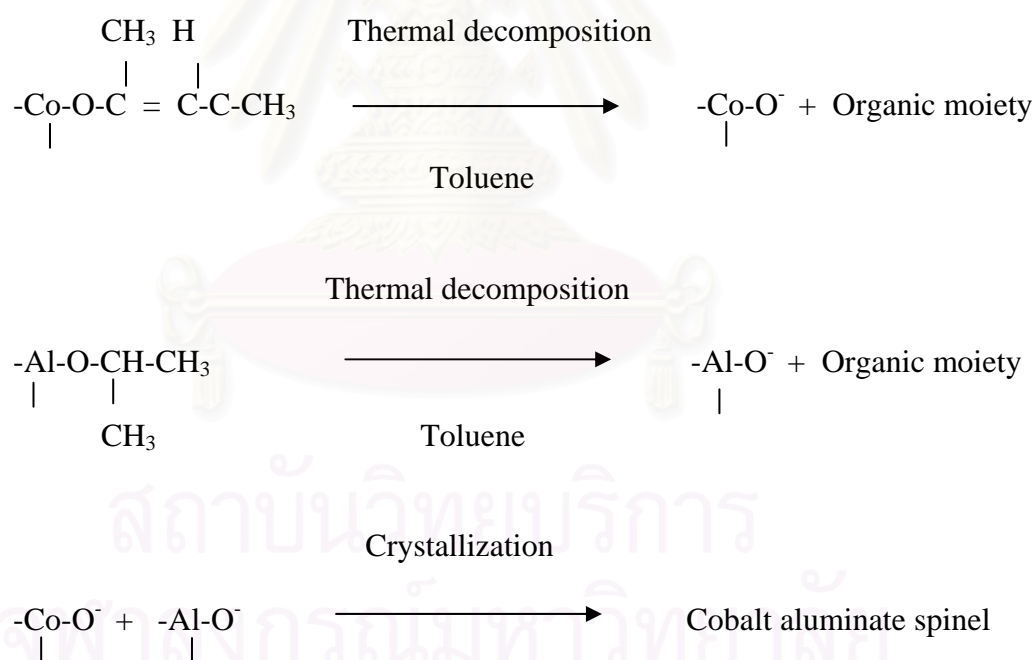
3.6.1 Co-Aluminate Formation

Interaction of cobalt with its alumina support has been observed by many authors using various techniques including TPR, XRD, EXAFS, and XPS (ESCA). The migration of cobalt ions into alumina lattice sites of octahedral or tetrahedral symmetry is limited to the first few layers of the support under normal calcination conditions. The reaction of Co with γ -Al₂O₃ can form a surface spinel in Co/ γ -Al₂O₃ catalysts. The surface spinel structure can not be observed by X-ray diffraction because it does not have long range, three dimensional order. It has been suggested that cobalt ions occupying surface octahedral site of γ -Al₂O₃ are reducible while cobalt ions occupying tetrahedral sites are non-reducible, at least at temperatures $\leq 900^\circ\text{C}$. At lower calcination temperatures, filling of the octahedral sites is more favorable. Filling of the tetrahedral site of γ -Al₂O₃ may be enhanced by an increase in calcination temperature.

3.7 Solvothermal Method

Solvothermal synthesis is improved from the hydrothermal synthesis by using organic solvent as the reaction medium instead of water. This method is based on the decomposition of metal alkoxide at elevated temperature (200-300°C) under autogeneous pressure. It is particularly suited for the synthesis of alumina in phase that is unstable at high temperature. It is also a useful technique for growing single crystals. In this method, parts or all of the reactants can dissolve in the organic solvent under high pressure. This feature enables the reaction to take place at lower temperature.

The thermal decomposition mechanism of cobalt acetylacetonate and aluminum isopropoxide in toluene can be proposed as follow (Sangthonganothai *et al.*, 2000)



Alumina can also be synthesized inorganic materials by using organic media at elevated temperature (200-300°C) under autogeneous pressure of organic for many years (1988-2002). It has been found that many oxides and mixed oxides can be crystallized in organic media at temperature lower than that required by the hydrothermal reaction. In 1988, they have reported that the glycothermal treatment

(the use of glycol instead of water for hydrothermal treatment) of gibbsite at 250°C yielded glycol derivative of boehmite. In 1992, they have found that the reaction of aluminum isopropoxide (AIP) in toluene at 300°C resulted in λ -alumina. Mekasuwandumrong et al., (2003) have reported that thermal decomposition of aluminum isopropoxide in mineral oil at 250-300°C over 2 h resulted in λ -alumina powder having high thermal stability and could be transformed directly to α -alumina at temperature higher than 1000°C.



สถาบันวิทยบริการ
จุฬาลงกรณ์มหาวิทยาลัย

CHAPTER IV

EXPERIMENTAL

This chapter consists of experimental systems and procedures used in this work which is divided into three parts including catalyst preparation, catalyst characterization and reaction study in CO hydrogenation.

The first part (section 4.1) is described catalyst preparation such as cobalt on cobalt-aluminate consisting of various Co/Al molar ratios, temperature and time during solvothermal process, temperature of calcination and cobalt precursors, and alumina supported cobalt catalysts. The catalyst nomenclature is given in this section. The second part (section 4.2) is explained catalyst characterization by various techniques including of BET surface area, TPR, XRD, SEM/EDX, TEM and H₂ Chemisorption. Finally, the last part (section 4.3) is illustrated catalyst activity measurement in CO hydrogenation.

4.1 Catalyst preparation

4.1.1 Chemicals

The details of chemicals used in this experiment are shown in Table 4.1.

Table 4.1 Chemicals used in the preparation of catalysts.

Chemical	Supplier
Aluminium Isopropoxide 98%+	Aldrich
Cobalt (II) acetylacetonate 97%	Aldrich
Cobalt (II) acetate tetrahydrate 98%+	APS
Cobalt (II) nitrate hexahydrate 98%+	Aldrich
Cobalt (II) chloride hexahydrate 98%+	Fluka
Toluene 99.5%	Carlo Erba Reagenti
Methanol	Aldrich

4.1.2 Equipment

Cobalt on cobalt-aluminate and alumina support preparation by solvothermal method requires an autoclave reactor with the following specifications.

Autoclave reactor

- Made from stainless steel
- Volume of 1000 cm³
- Maximum temperature of 350°C
- Pressure gauge in the range of 0-300 bar
- Test tube was used to contain the reagent and solvent
- A temperature program controller was connected to a thermocouple attached to the reagent in the autoclave.
- Electrical furnace (heater) supplied the required heat to the autoclave for the reaction.
- Nitrogen was set with a pressure regulator (0-150 bar) and needle valves are used to release gas from autoclave.

4.1.3 Preparation of cobalt-aluminate and alumina support

Part I Cobalt on cobalt-aluminate was synthesized by solvothermal method. It was prepared using the mixture of aluminium isopropoxide (AIP, [(CH₃)₂CHO]₃Al), 15.0 g (0.0734 mole) and appropriate amount of cobalt (II) acetylacetonate that depended on the molar ratio of Co/Al. The starting materials were suspended in 100 mL of toluene in a beaker, and then set up in 1000 mL autoclave. In the gap between the beaker and autoclave wall, toluene (40 mL) was added. After the autoclave completely purged with nitrogen, the suspension was heated to desire temperature at the rate of 2.5 °C/min and was hold at that temperature for desire time. Autogenous pressure during the reaction gradually increased as temperature was raised. Then the autoclave was cooled to room temperature. After the

autoclave was cooled, the resulting product was washed repeatedly with methanol by centrifugation with 300 rpm for 5 times (10 min/time) and dried at 110 °C for 24 h. The calcination of the obtained product was carried out in a furnace. The product was heated at the rate of 10 °C/min at desire temperature for 1h.

- the synthesis was performed at various Co/Al molar ratios (0.5, 1.0, and 2.0) at 300 °C for 1 and 2 h and calcined at 300 °C for 1h.
- the synthesis was performed with Co/Al = 0.5 and 1.0, at 250 and 300 °C for 2 h and calcined at 300 °C for 1h.
- the synthesis was performed with Co/Al = 1.0, at 300 °C for 2 h and calcined at various temperature (300, 400 and 500 °C) for 1h
- the alumina support was performed without using mixture of cobalt (II) acetylacetonate at 300 °C for 2 h and calcined at 300 °C for 1h and loaded 25%wt Co by incipient wetness impregnation method.

Part II Cobalt on cobalt-aluminate was synthesized by solvothermal method which was prepared using the same method as part I. The synthesis was performed at various cobalt precursors (Cobalt (II) acetylacetonate, Cobalt (II) acetate tetrahydrate, Cobalt (II) nitrate hexahydrate, and Cobalt (II) chloride hexahydrate) which Co/Al = 1, the suspension was heated to 250 °C and was hold at that temperature for 2 h. The calcination of the obtained product was carried out in a furnace at 300 °C for 1h.

4.1.4 Preparation of alumina supported cobalt catalyst

A alumina supported cobalt catalyst was prepared by incipient wetness impregnation method. A designed amount of cobalt (II) acetylacetonate was dissolved in ethanol and then impregnated into the alumina support with 25 wt % cobalt by calculating of the required amounts of Co loading (see Appendix A). The catalyst was dried at 110°C for 24 h and calcined in air at 500 °C for 4 h.

4.1.5 Catalyst Nomenclature

The nomenclature used for the catalyst samples in this study is following:

Part I

- **Co/Al_a_bh**
- **Co/Al_a_c°C**
- **Co/Al₂O₃_bh**
- **Co/Al_d°C**

Co/Al refers to the cobalt on cobalt-aluminate catalyst using single step synthesis

Co/Al₂O₃ refers to the alumina-supported cobalt catalyst using the conventional impregnation method having 25 %wt of cobalt

a refers to the Co/Al ratio

b refers to the holding time during synthesis (h)

c refers to the temperature during synthesis (°C)

d refers to the calcination temperature (°C)

Part II

- **CoAA** refers to the cobalt on cobalt-aluminate catalyst synthesized from the cobalt (II) acetylacetonate precursor.
- **CoAC** refers to the cobalt on cobalt-aluminate catalyst synthesized from the cobalt (II) acetate precursor.
- **CoN** refers to the cobalt on cobalt-aluminate catalyst synthesized from the cobalt (II) nitrate precursor.
- **CoCL** refers to cobalt on cobalt-aluminate catalyst that synthesized from the cobalt (II) chloride precursor.

4.2 Catalyst characterization

Various characterization techniques were used in this studied in order to clarify the catalyst structure and morphology, and surface composition of catalysts.

4.2.1 N₂ physisorption

Surface area measurements were carried out by low temperature nitrogen adsorption in a Micromeritic ChemiSorb 2750 system. Calculations were performed on the basis of the BET isotherm. 0.2 grams of sample was loaded into u-shape cell made from Pyrex and heated in helium to 200°C for 1 h in order to eliminate trace amount of water adsorbed on surface, then cooled down to room temperature. The analysis gas consist of 30%N₂ in helium was introduced to Pyrex cell. Sample adsorbed nitrogen at low temperature by dipped cell into liquid nitrogen dewar until it's surface was satuated with nitrogen and desorbed nitrogen at room temperature by moved away the dewar. The nitrogen that was desorbed from sample was measured by TCD detector.

4.2.2 X-ray diffraction (XRD)

XRD were performed to determine the bulk crystalline phases of catalyst. It was conducted using a SIEMENS D-5000 X-ray diffractometer connected with a computer with Diffract ZT version 3.3 program for fully control of the XRD analyzer. The experiments were carried out by using CuK_α ($\lambda = 1.54439 \text{ \AA}$) radiation with Ni filter in the range $2\theta = 20\text{-}80^\circ$ resolution 0.04.

4.2.3 Scanning electron microscopy and energy dispersive X-ray spectroscopy (SEM/EDX)

SEM and EDX were used to determine the catalyst morphologies and elemental distribution throughout the catalyst granules, respectively. The SEM of JEOL mode JSM-5410LV was applied using the secondary electron mode at 15 kV. EDX was performed using Link Isis series 300 program.

4.2.4 Transmission electron microscopy (TEM)

The morphology and size of the catalysts were determined using a JEOL-TEM 200CX transmission electron spectroscopy operated at 160 kV at the Scientific and Technological Research Equipment Center (STREC), Chulalongkorn University.

4.2.5 Temperature-programmed reduction (TPR)

TPR was used to determine the reduction behaviors of the samples using a Micromeritics Chemisorb 2750.

1. The catalyst sample 0.2 g used in the sample cell.
2. Prior to operation, the catalysts were heated up to 200 °C in flowing nitrogen and held at this temperature for 1 h.
3. After the catalyst sample was cooled down to room temperature, the carrier gas was 5% H₂ in Ar (30 CC/min) were ramping from 35 to 800 °C at 10 °C/min.
4. A cold trap was placed before the detector to remove water produced during the reaction.
5. A thermal conductivity detector (TCD) was used to determine the amount of hydrogen consumption during TPR. The operating condition of the TCD is shown in Table 4.2.

4.2.3 Hydrogen chemisorption

Static H₂ chemisorption at 100 °C on the reduced cobalt catalysts was used to determine the number of reduced surface cobalt metal atoms. This is related to the overall activity of the catalysts during CO hydrogenation. Gas chemisorption at 100 °C was performed using the method described by Reuel and Bartholomew. The experiment was performed in a Micromeritics Pulse Chemisorb 2700 instrument at the Analysis Center of Department of Chemical Engineering, Faculty of Engineering, Chulalongkorn University

4.3 Reaction study in CO hydrogenation

4.3.1 Materials

The reactant gas used for the reaction study was the carbon monoxide in hydrogen feed stream as supplied by Thai Industrial Gas Limited (TIG). The gas mixture contained 9.73 vol % CO in H₂ (22 CC/min). The total flow rate was 30 CC/min with the H₂/CO ratio of 10/1. Ultra high purity hydrogen (50 CC/min) and high purity argon (8 CC/min) manufactured by Thai Industrial Gas Limited (TIG) were used for reduction and balanced flow rate

4.3.2 Apparatus

Flow diagram of CO hydrogenation system is shown in Figure 4.1. The system consists of a reactor, an automatic temperature controller, an electrical furnace and a gas controlling system.

4.3.2.1 Reactor

The reactor was made from a stainless steel tube (O.D. 3/8"). Two sampling points were provided above and below the catalyst bed. Catalyst was placed between two quartz wool layers.

4.3.2.2 Automation Temperature Controller

This unit consisted of a magnetic switch connected to a variable voltage transformer and a solid-state relay temperature controller model no. SS2425DZ connected to a thermocouple. Reactor temperature was measured at the bottom of the catalyst bed in the reactor. The temperature control set point is adjustable within the range of 0-800°C at the maximum voltage output of 220 volt.

4.3.2.3 Electrical Furnace

The furnace supplied heat to the reactor for CO hydrogenation. The reactor could be operated from temperature up to 800°C at the maximum voltage of 220 volt.

4.3.2.4 Gas Controlling System

Reactant for the system was each equipped with a pressure regulator and an on-off valve and the gas flow rates were adjusted by using metering valves.

4.3.2.5 Gas Chromatography

The composition of hydrocarbons in the product stream was analyzed by a Shimadzu GC14B (VZ10) gas chromatograph equipped with a flame ionization detector. A Shimadzu GC8A (molecular sieve 5A) gas chromatography equipped with a thermal conductivity detector was used to analyze CO and H₂ in the feed and product streams. The operating conditions for each instrument are shown in the Table 4.2.

Table 4.2 Operating condition for gas chromatograph

Gas Chromatograph	SHIMADZU GC-8A	SHIMADZU GC-14B
Detector	TCD	FID
Column	Molecular sieve 5A	VZ10
- Column material	SUS	-
- Length	2 m	-
- Outer diameter	4 mm	-

Table 4.2 Operating condition for gas chromatograph (cont.)

Gas Chromatograph	SHIMADZU GC-8A	SHIMADZU GC-14B
- Inner diameter	3 mm	-
- Mesh range	60/80	60/80
- Maximum temperature	350 °C	80 °C
Carrier gas	He (99.999%)	H ₂ (99.999%)
Carrier gas flow	20 cc/min	-
Column gas	He (99.999%)	Air, H ₂
Column gas flow	20 cc/min	-
Column temperature		
- initial (°C)	60	70
- final (°C)	60	70
Injector temperature (°C)	100	100
Detector temperature (°C)	100	150
Current (mA)	80	-
Analysed gas	Ar, CO, H ₂	Hydrocarbon C ₁ -C ₄

4.3.3 Procedures

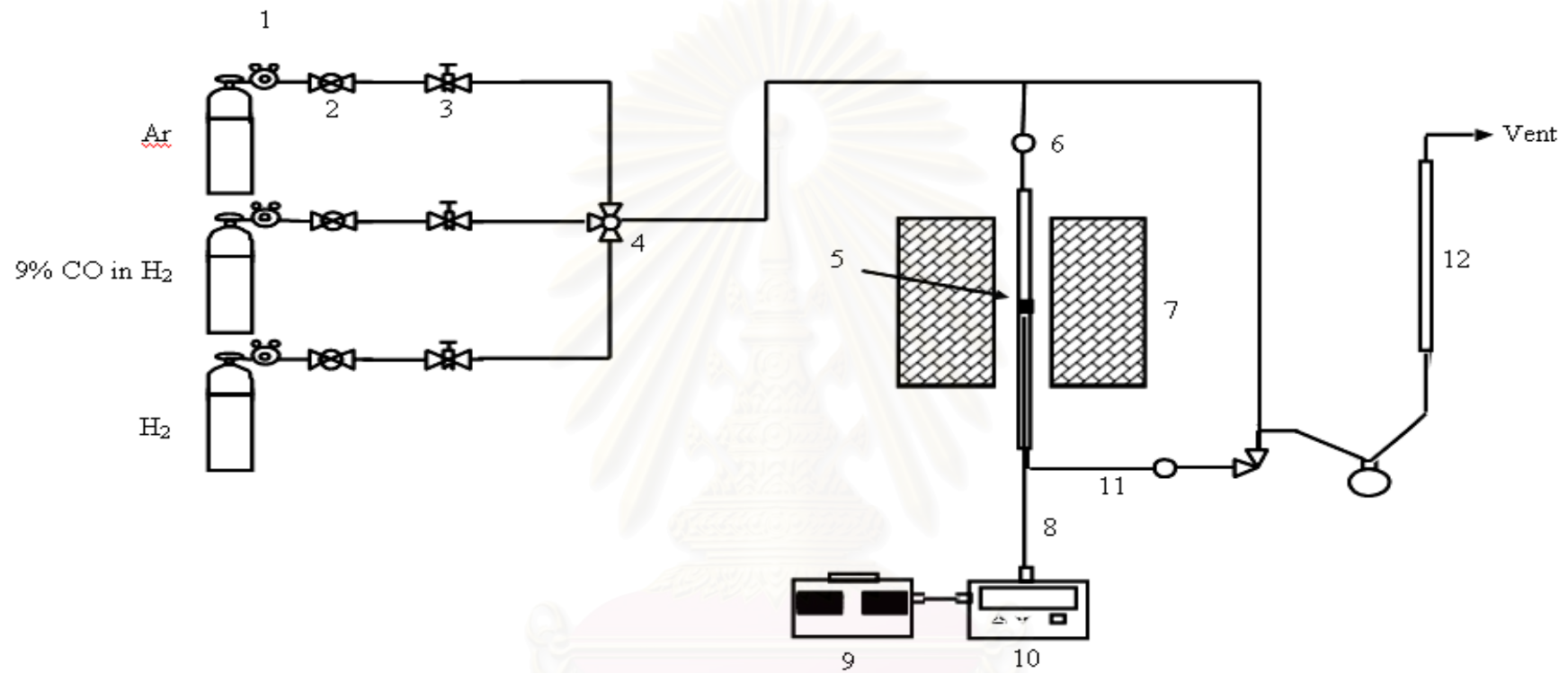
1. Using 0.2 g of catalyst packed in the middle of the stainless steel microreactor, which is located in the electrical furnace.
2. A flow rate of Ar = 8 CC/min, 9% CO in H₂ = 22 CC/min and H₂ = 50 CC/min in a fixed-bed flow reactor. A relatively high H₂/CO ratio was used to minimize deactivation due to carbon deposition during reaction.
3. The catalyst sample was re-reduce *in situ* in flowing H₂ at 350 °C for 3 h prior to CO hydrogenation.

4. CO hydrogenation was carried out at 220 °C and 1 atm total pressure in flowing 9% CO in H₂.

5. The effluent was analyzed using gas chromatography technique. [Thermal conductivity detector (TDC) was used for separation of carbon monoxide (CO) and methane (CH₄) and flame ionization detector (FID) were used for separation of light hydrocarbon such as methane (CH₄), ethane (C₂H₆), propane (C₃H₈), etc.] In all cases, steady-state was reached within 6 h.



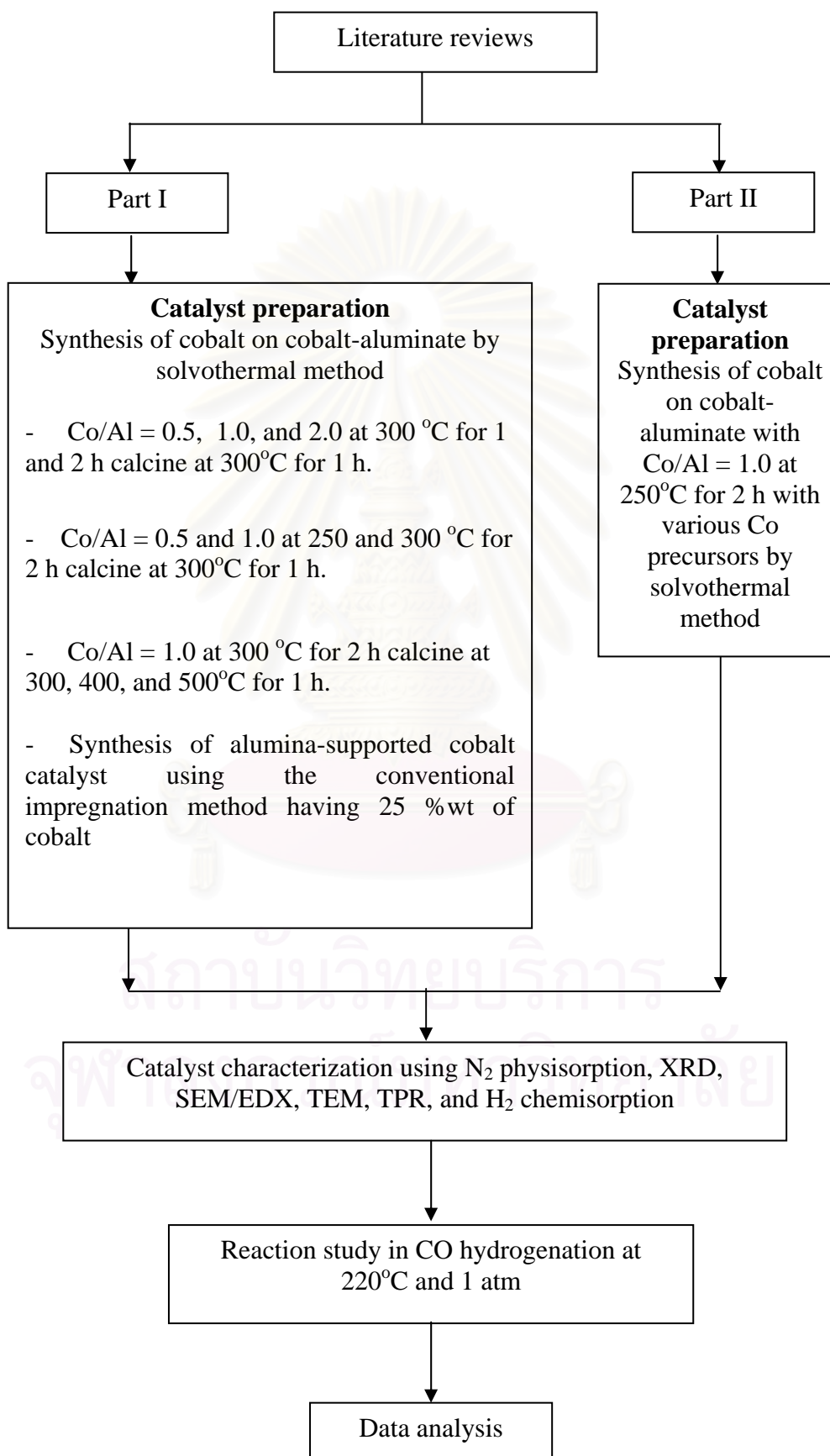
สถาบันวิทยบริการ
จุฬาลงกรณ์มหาวิทยาลัย



- | | | | |
|---------------------------------|----------------------------|-------------------|-----------------------|
| 1. Pressure Regulator | 2. On-Off Valve | 3. Metering Valve | 4. 3-way Valve |
| 5. Catalyst Bed | 6. Sampling point | 7. Furnace | 8. Thermocouple |
| 9. Variable Voltage Transformer | 10. Temperature Controller | 11. Heating Line | 12. Bubble Flow Meter |

Figure 4.1 Flow diagram of CO hydrogenation system

RESEARCH METHODOLOGY



CHAPTER V

RESULTS AND DISCUSSION

This thesis was conducted in order to investigate the characteristics and catalytic properties of cobalt on cobalt-aluminate catalysts in one-pot via the solvothermal process for CO hydrogenation. In this chapter, the experimental results and discussions are described. The results and discussions are divided into two sections. Section 5.1 (Part I) described characteristics and catalytic activity towards CO hydrogenation of the cobalt on cobalt-aluminate catalysts that was synthesized with various Co/Al molar ratios, temperature and time during solvothermal process, and temperature of calcination. Section 5.2 (Part II) described characteristics and catalytic activity towards CO hydrogenation of the cobalt on cobalt-aluminate catalysts that was synthesized with various cobalt precursors.

5.1 Cobalt on cobalt-aluminate catalyst with various Co/Al molar ratios, temperature and time during solvothermal process, and temperature of calcination.

(Part I)

5.1.1 Effect of Co/Al molar ratio and holding time during synthesis

The present study focused on synthesis of the cobalt on cobalt-aluminate using the solvothermal process. The excess cobalt precursor was added in order to obtain the cobalt oxides on cobalt-aluminate after calcination of samples. Therefore, the Co/Al molar ratios (0.5, 1.0, and 2.0) and the holding times (1 and 2 h) during solvothermal process were varied. After solvothermal synthesis, all samples were calcined at 300°C for 1 h prior to characterization and reaction study.

After calcination, all catalyst samples were characterized by means of N₂ physisorption, XRD, SEM/EDX, TEM, and TPR.

5.1.1.1 BET surface area

The BET surface areas of samples obtained from N₂ physisorption are listed in **Table 5.1**.

Table 5.1 BET surface areas of the calcined cobalt on cobalt-aluminate catalysts with various Co/Al molar ratios and holding time during synthesis

Samples	BET surface area (m ² /g)
Co/Al_0.5_1h	139
Co/Al_0.5_2h	139
Co/Al_1.0_1h	131
Co/Al_1.0_2h	137
Co/Al_2.0_1h	100
Co/Al_2.0_2h	103
Impregnated Co/Al ₂ O ₃ _2h	84

It can be observed that increased Co/Al molar ratios apparently resulted in decreased surface areas of samples. However, the holding time during solvothermal process showed only little effect on surface areas of samples. The decreased surface areas of samples with increased Co/Al molar ratios can be attributed to agglomeration of the larger amounts of cobalt oxide formed. Thus, the decreased surface areas of samples were evident when the Co/Al ratios increased. Furthermore, the surface area of the conventional solvothermal-derived alumina-supported cobalt catalyst having 25 wt% of cobalt was less than the cobalt on cobalt-aluminate catalysts in one-pot via the solvothermal process synthesis.

5.1.1.2 X-ray diffraction (XRD)

The XRD patterns for all samples are shown in **Figure 5.1**. All samples exhibited the similar short-broaden XRD peaks at 31, 37, 46, 59 and 65° assigned to Co_3O_4 and CoAl_2O_4 species, which were overlapped (Jongsomjit *et al.*, 2001). This was suggested that all crystallite species were in the highly dispersed form.

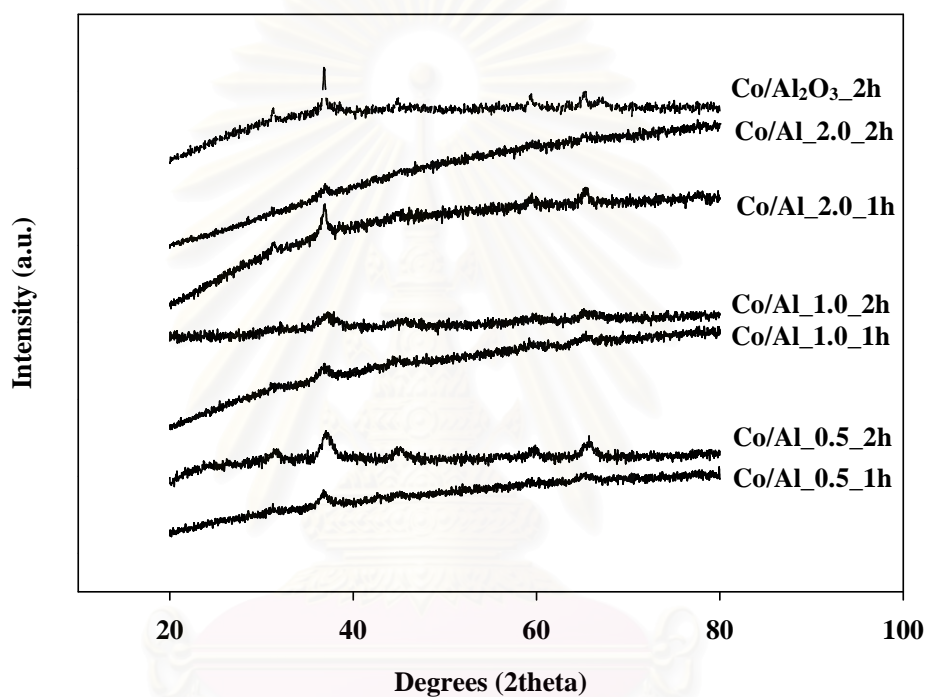


Figure 5.1 XRD pattern of the calcined cobalt on cobalt-aluminate catalysts

5.1.1.3 Scanning electron microscopy (SEM) and Energy dispersive X-ray spectroscopy (EDX)

SEM and EDX were performed to study the morphologies of catalyst samples and the elemental distribution on the external surface of the catalyst granule. It was found that no significant change in morphologies upon different Co/Al molar ratios and holding time during solvothermal process was observed. A typical SEM micrograph and EDX mapping for cobalt on cobalt-aluminate are shown in **Figure 5.2-5.7** and the typical SEM micrograph and EDX mapping for the conventional solvothermal-derived alumina-supported cobalt catalyst having 25 wt% of cobalt are shown in **Figure 5.8**. It can be also observed that cobalt was well distributed on the catalyst granule.

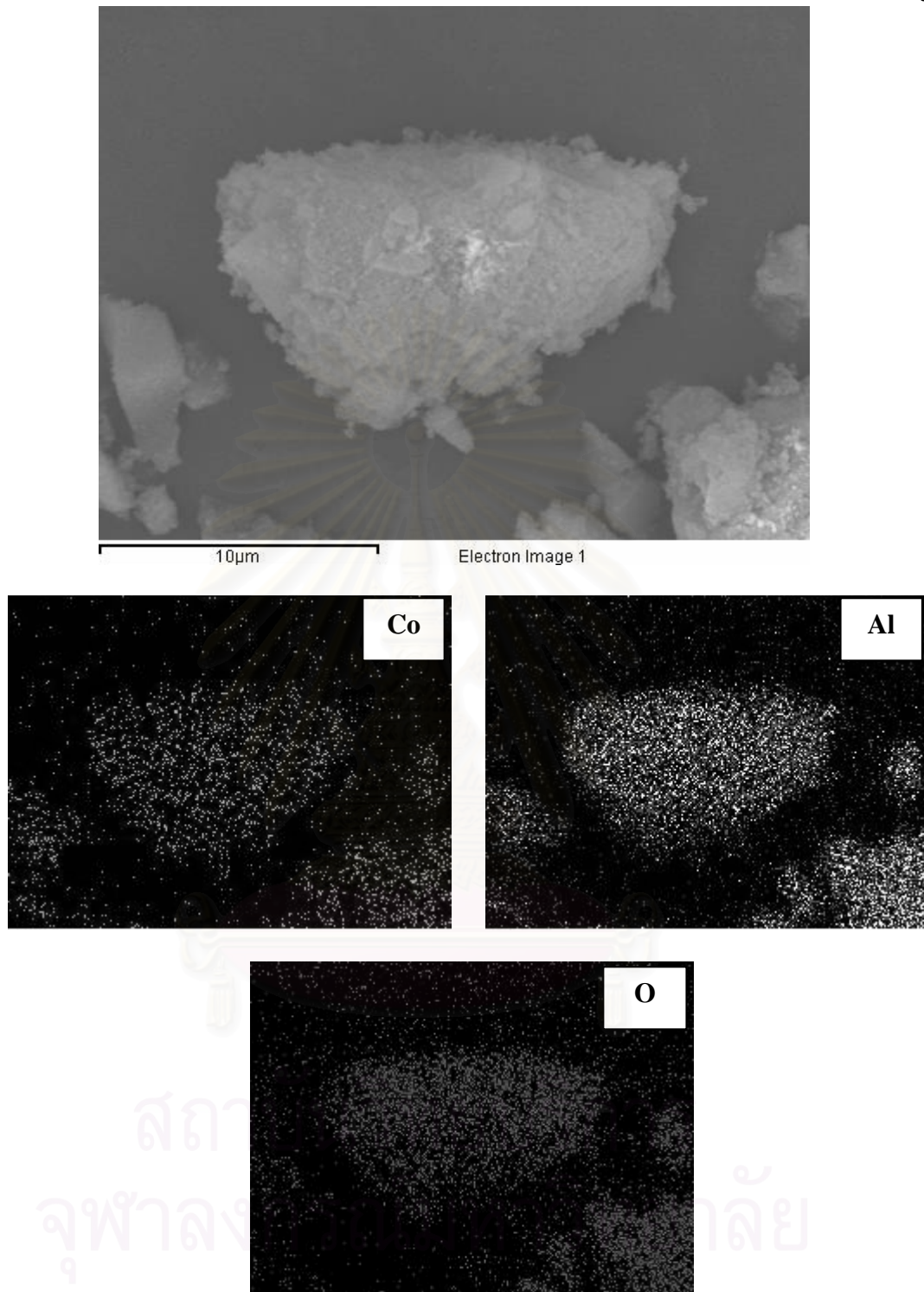


Figure 5.2 SEM micrograph and EDX mapping of Co/Al_{0.5}_1h

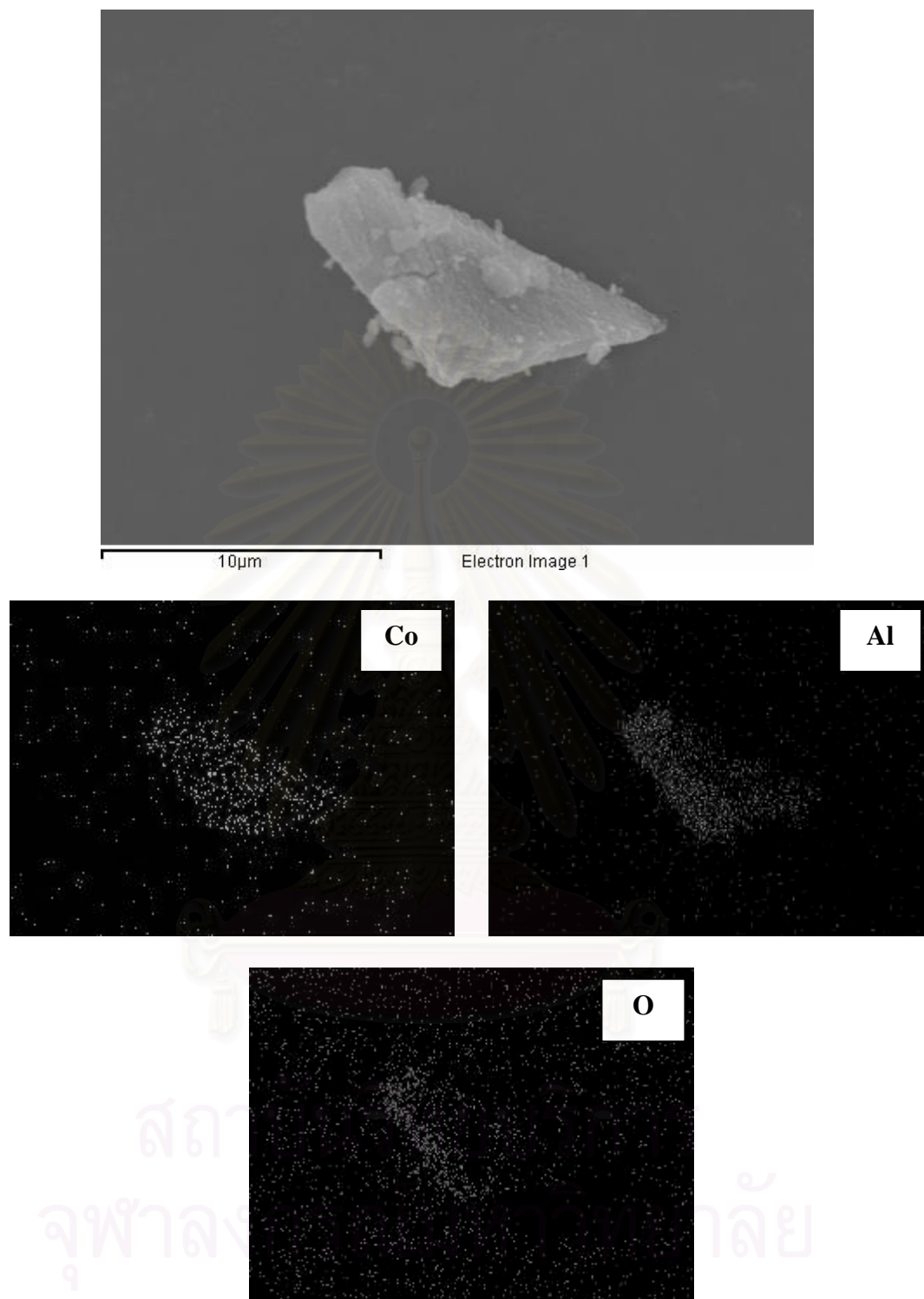


Figure 5.3 SEM micrograph and EDX mapping of Co/Al_{0.5}_2h

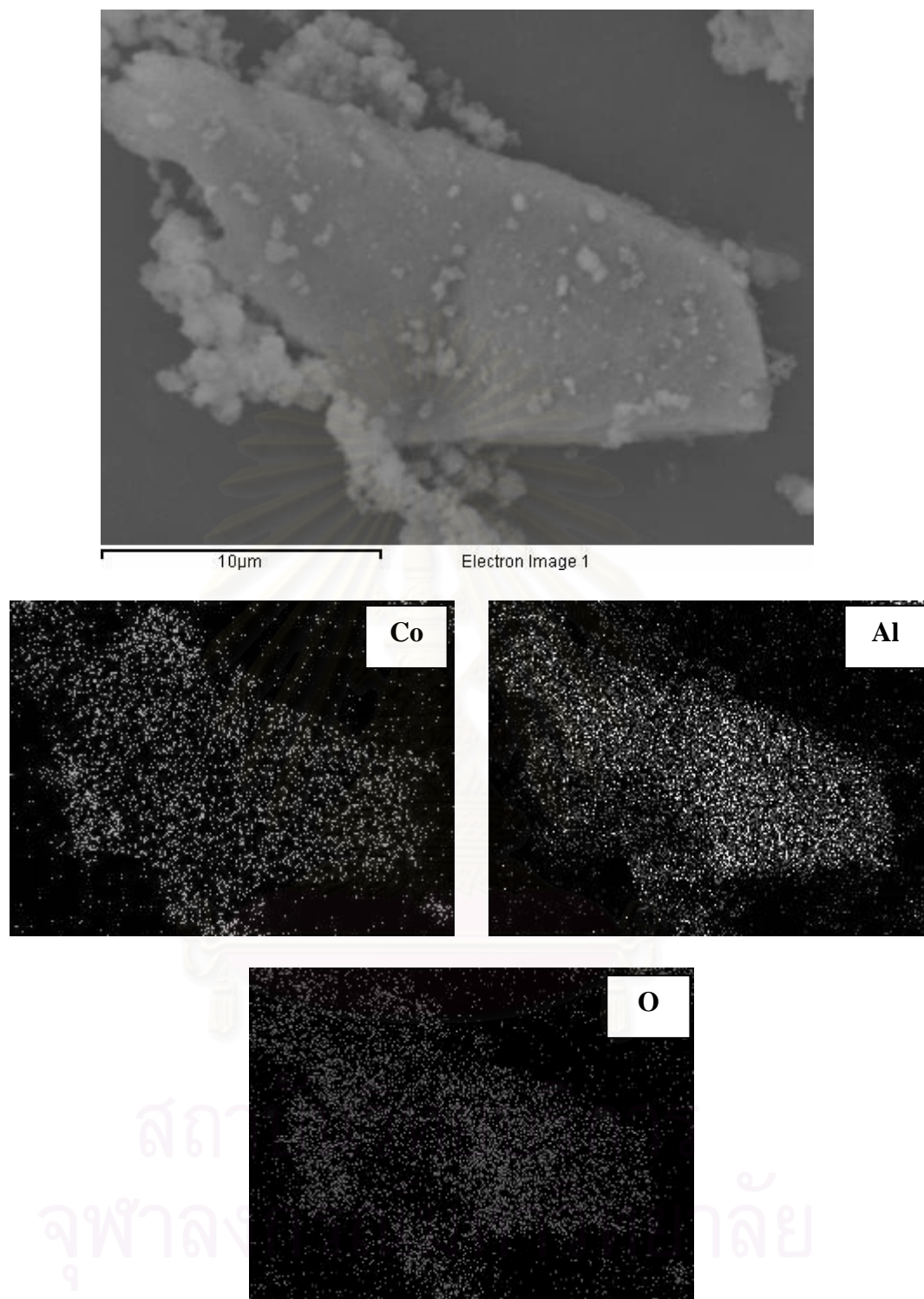


Figure 5.4 SEM micrograph and EDX mapping of Co/Al_{1.0}_1h

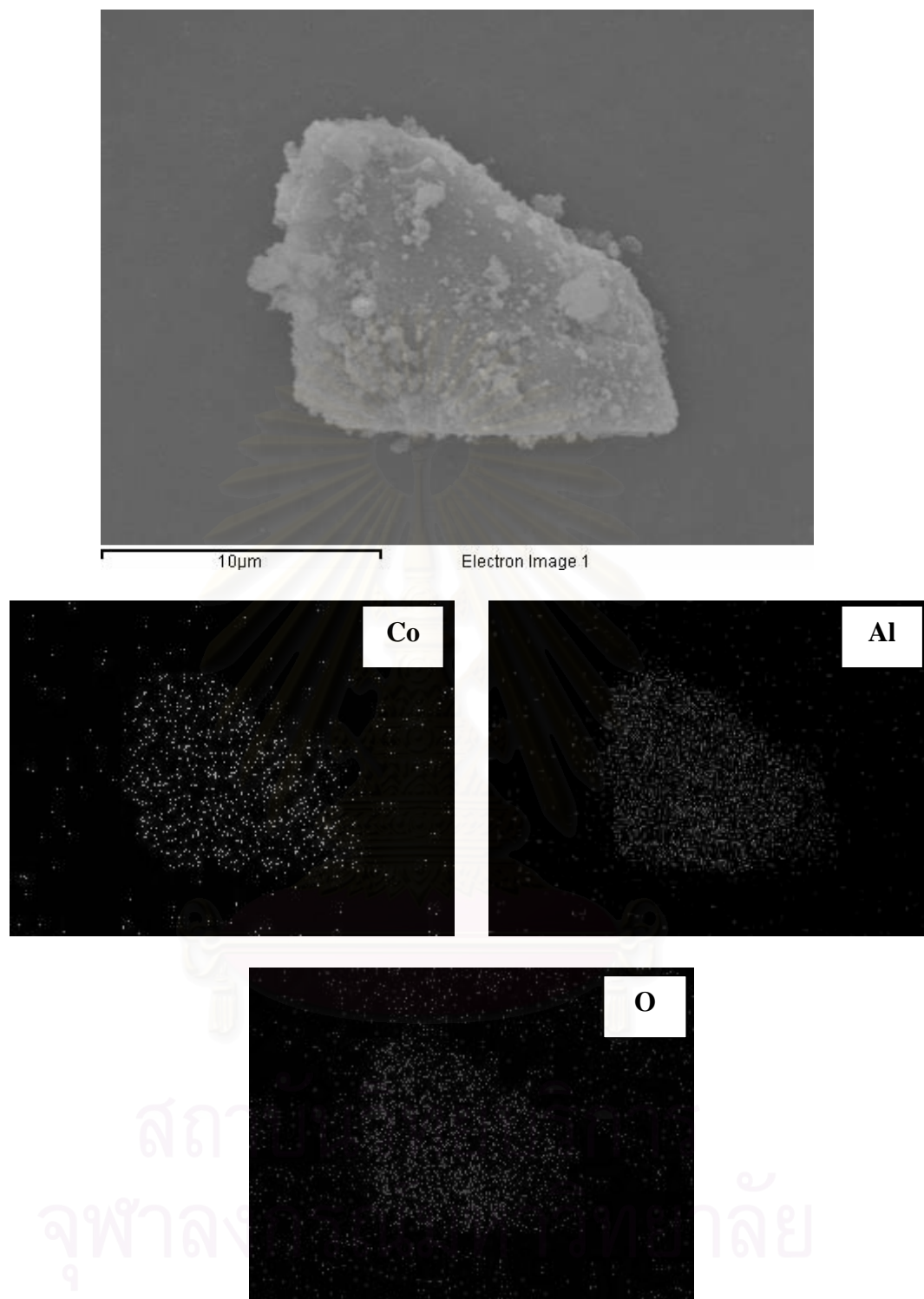


Figure 5.5 SEM micrograph and EDX mapping of Co/Al_{1.0}_2h

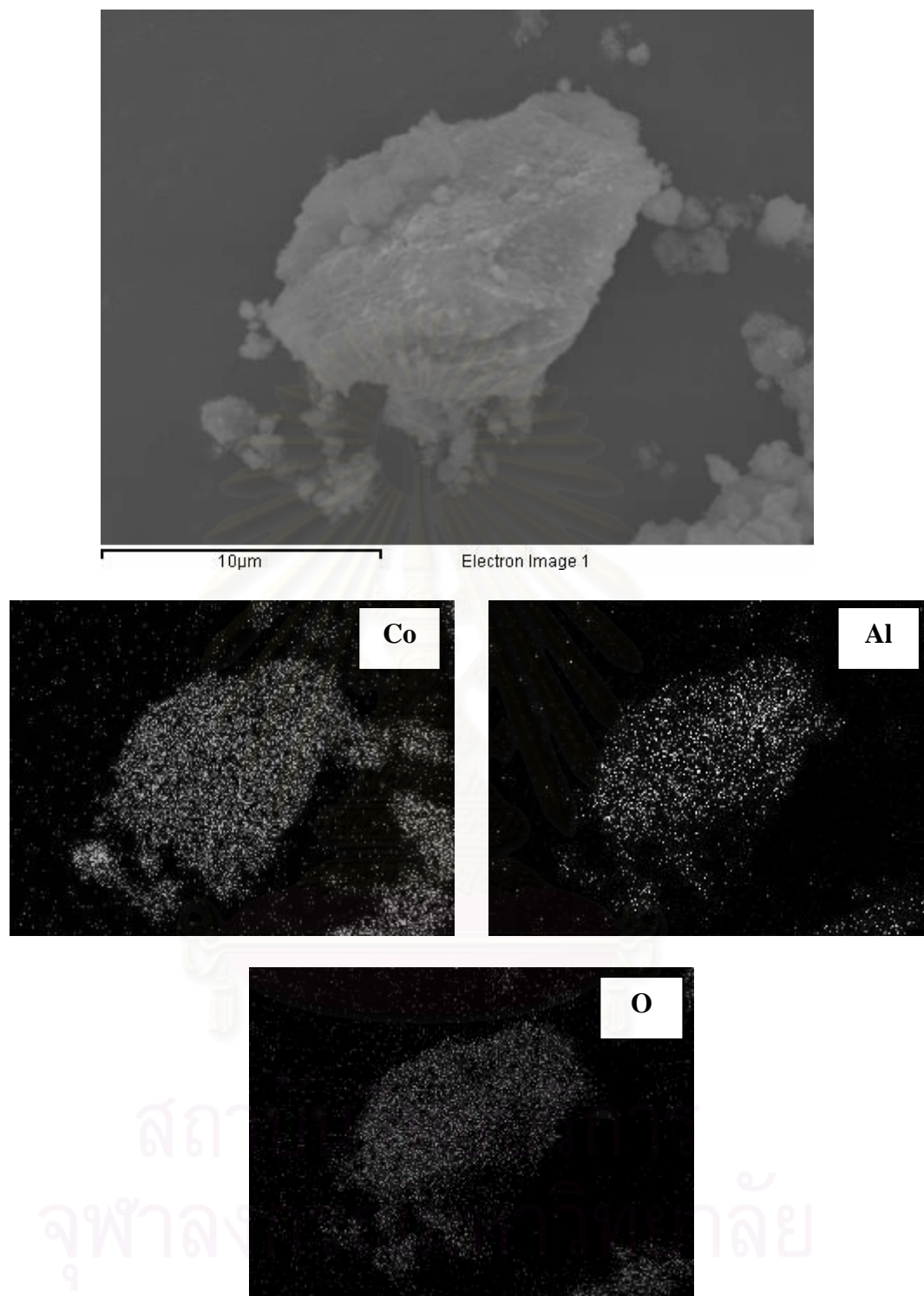


Figure 5.6 SEM micrograph and EDX mapping of Co/Al_{2.0}_1h

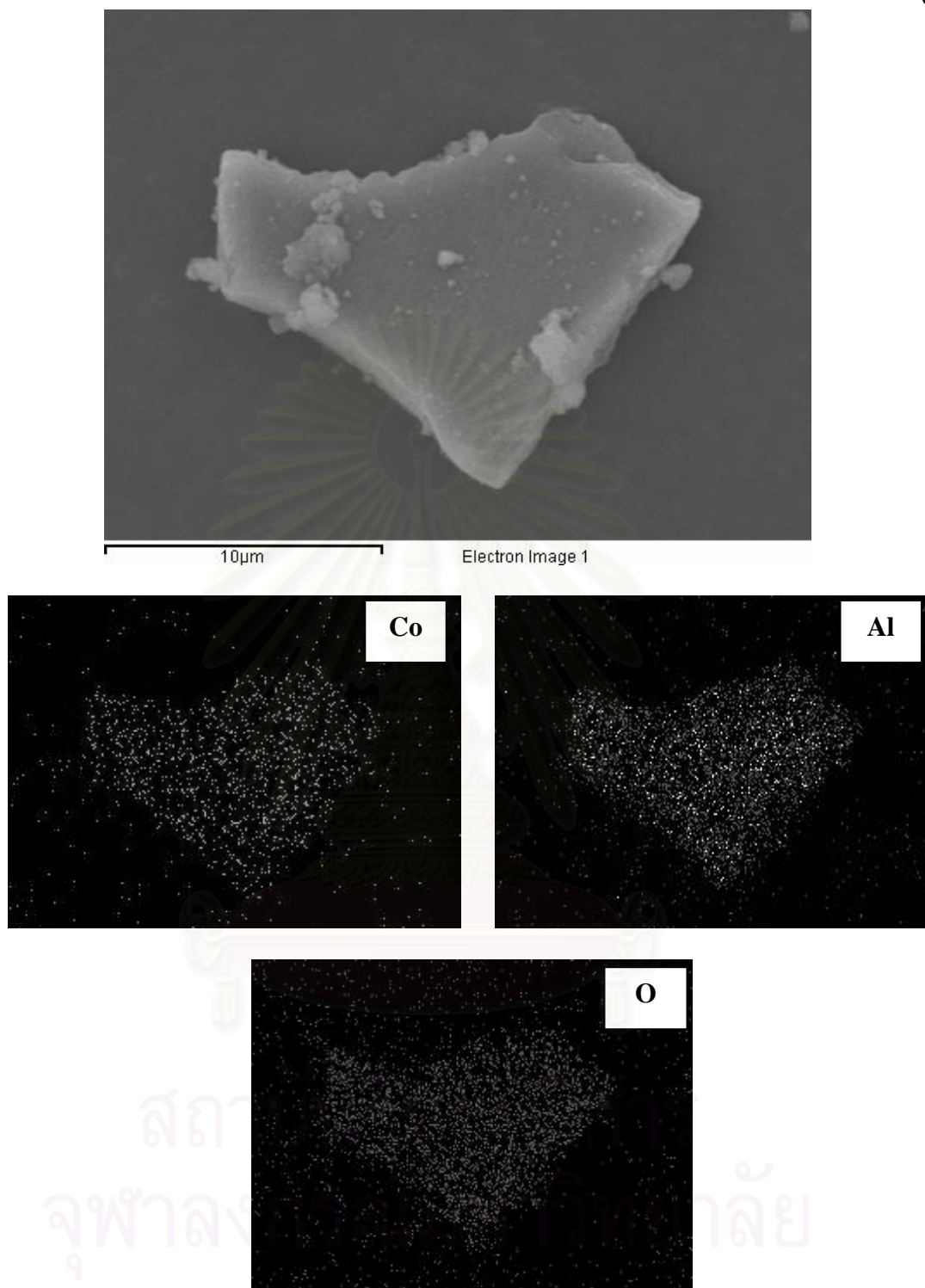


Figure 5.7 SEM micrograph and EDX mapping of Co/Al_{2.0}_2h

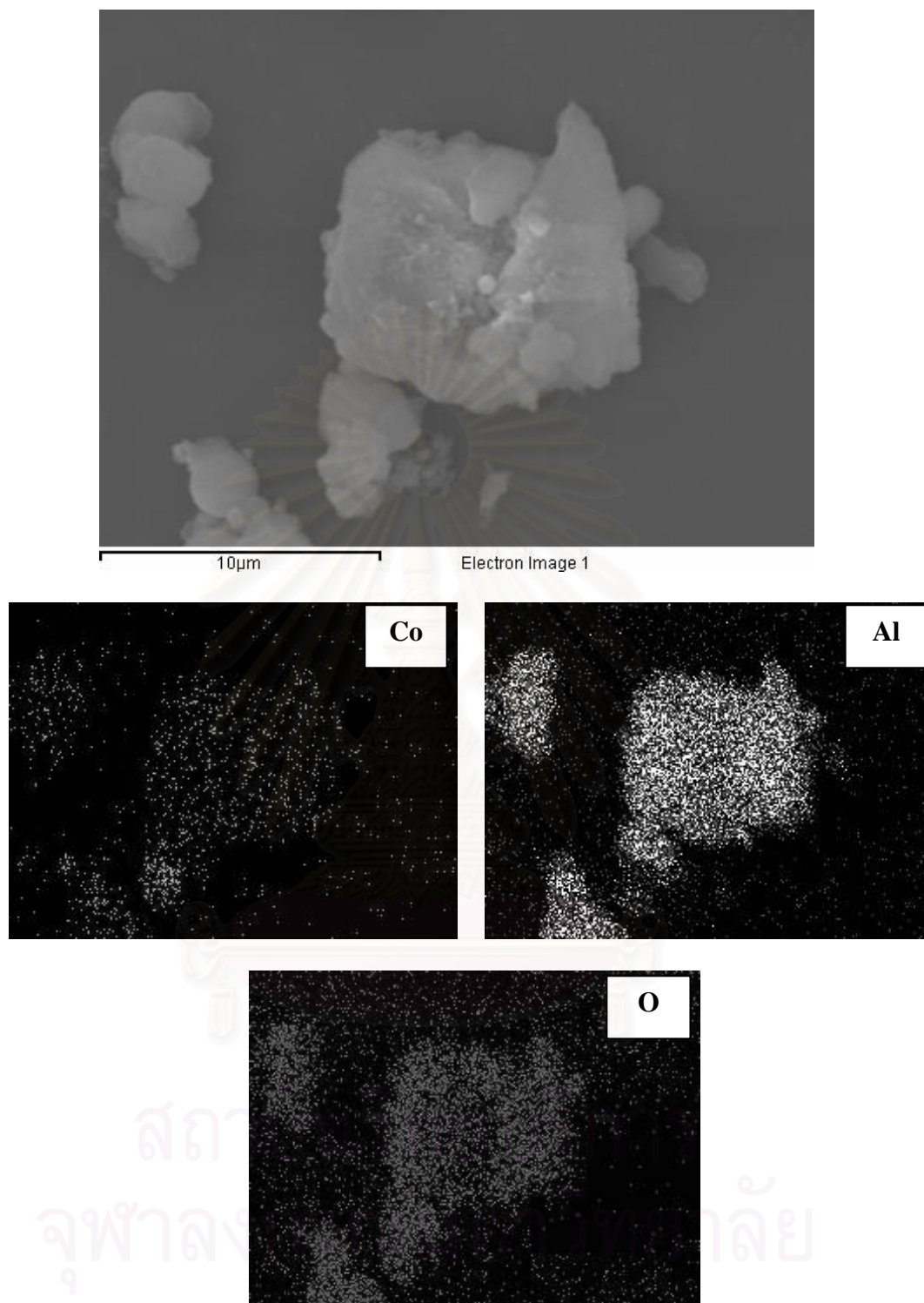


Figure 5.8 SEM micrograph and EDX mapping of Co/Al₂O₃_2h

5.1.1.4 Transmission Electron Microscopy (TEM)

In order to determine the dispersion of cobalt oxide species and crystallite size of them, the more powerful technique, such as TEM was performed. The TEM micrographs for cobalt on cobalt-aluminate samples are shown in **Figure 5.9-11** and the TEM micrographs for the conventional solvothermal-derived alumina-supported cobalt catalyst having 25 wt% of cobalt samples are shown in **Figure 5.12**. The dark spots represented the cobalt species dispersing on the catalyst granule. Based on TEM micrographs, all samples exhibited the agglomeration of cobalt species.

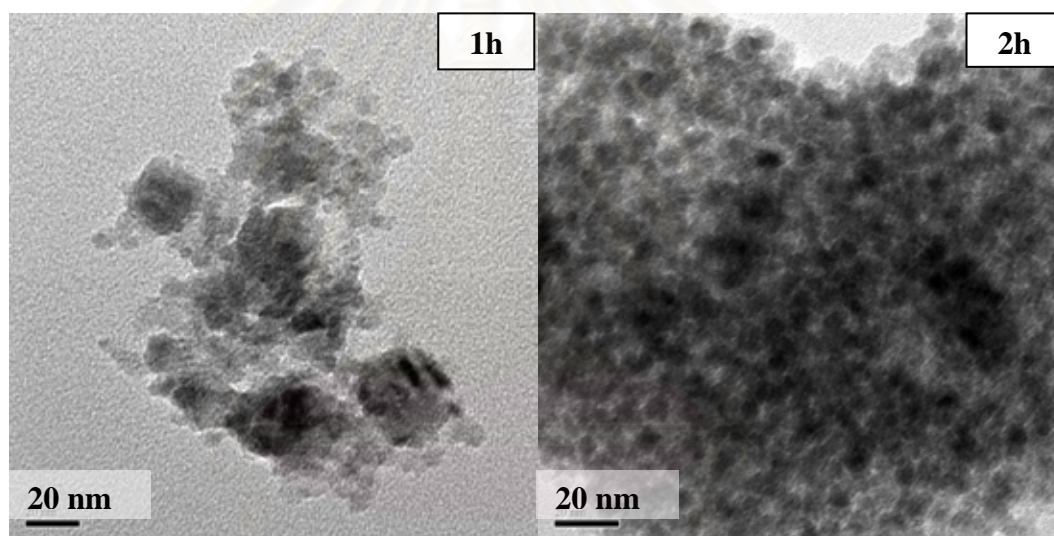


Figure 5.9 TEM micrograph of Co/Al_{0.5}_1h and Co/Al_{0.5}_2h

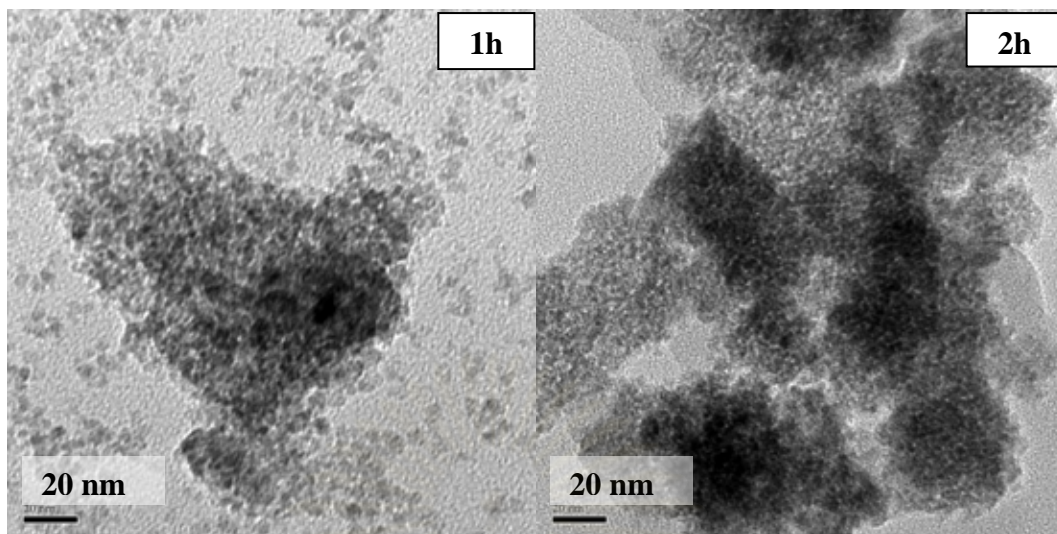


Figure 5.10 TEM micrograph of Co/Al_{1.0}_1h and Co/Al_{1.0}_2h

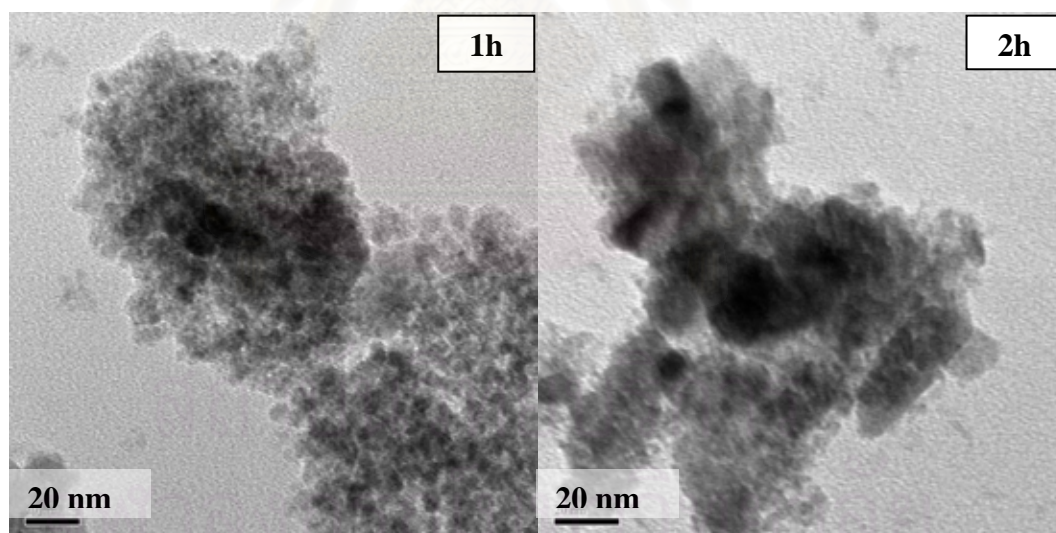


Figure 5.11 TEM micrograph of Co/Al_{2.0}_1h and Co/Al_{2.0}_2h

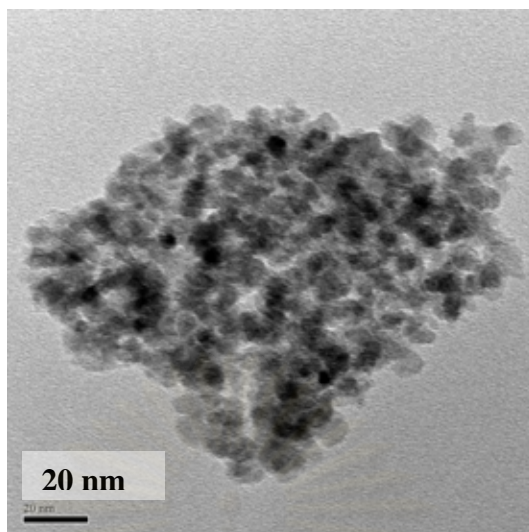
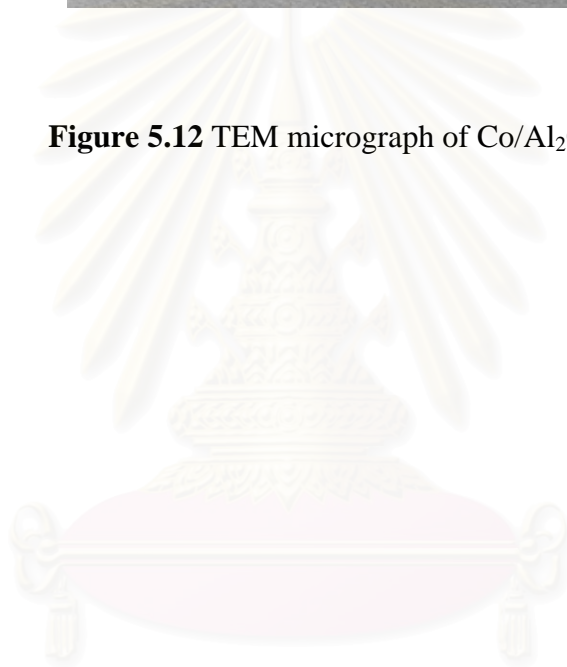


Figure 5.12 TEM micrograph of Co/Al₂O₃_2h



สถาบันวิทยบริการ
จุฬาลงกรณ์มหาวิทยาลัย

5.1.1.5 Temperature programmed reduction (TPR)

TPR was performed in order to determine the reduction behaviors. The TPR profiles for all catalyst samples are shown in **Figure 5.13**. It was found that mostly the one reduction peak below 400°C was observed and assigned to the overlap of two step reduction of Co_3O_4 to CoO and, then to Co metal (Jongsomjit *et al.*, 2001, 2004, 2005). Upon the TPR conditions, the two-step reduction may or may not be observed. In fact, the TPR peak locations are affected by reduction kinetics. The kinetics of reduction can be affected by a wide range of variables, including particle size, support interaction, and reduction gas composition (Jongsomjit *et al.*, 2001, 2002). The effects of particle size and support interaction can be superimposed on each other. Thus, while a decrease in metal oxide particle size can result in faster reduction due to greater surface area/volume ratio, smaller particles may interact more with the support, slowing reduction. Based on the TPR profiles of sample, the reduction peak at high temperature (ca. above 600°C) was also observed. This peak can be assigned to the reduction of non-stoichiometric cobalt-aluminate, which is more difficult than the reduction of Co_3O_4 species (Jongsomjit *et al.*, 2001). According to the TPR results, it can be concluded that increased Co/Al molar ratios resulted in increased Co_3O_4 species, which facilitated the reduction behavior of catalyst samples. Thus, the larger reduction peaks at low reduction temperature (ca. below 400°C) for Co/Al_2.0_1h and Co/Al_2.0_2h samples were evident. No significant change on the reduction behaviors upon changing the holding time during solvothermal process was observed.

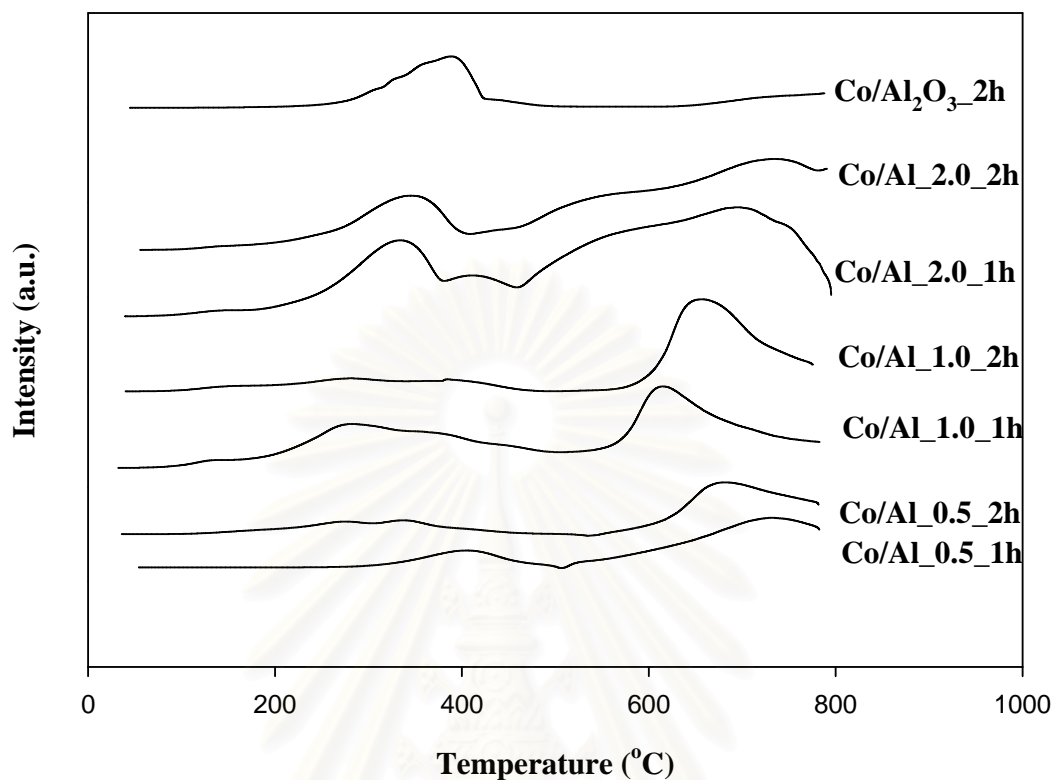


Figure 5.13 TPR profiles for the calcined cobalt on cobalt-aluminate catalysts with various Co/Al molar ratios and holding time during synthesis and TPR profile for alumina supported cobalt catalyst

5.1.1.6 Reaction study in CO hydrogenation

In order to determine the catalytic behaviors of the samples having different Co/Al ratios and holding time during solvothermal synthesis, CO hydrogenation ($H_2/CO = 1$) was performed to determine the overall activity and product selectivity of the samples. In fact, hydrogenation of CO under methanation condition was carried out at 220°C at atmospheric pressure. A flow rate of $H_2/CO/Ar = 20/2/8$ cc/min in a fixed-bed flow reactor was used. The relatively high H_2/CO ratio was employed to minimize deactivation due to carbon deposition during reaction. The resulted reaction study is shown in **Table 5.2**. For a comparative study, the activity and selectivity for the conventional solvothermal-derived alumina-supported cobalt catalyst having 25 wt% of cobalt was also measured as listed in **Table 5.2**.

Table 5.2 Reaction study of cobalt on cobalt aluminate with various Co/Al molar ratios and holding time during synthesis

Samples	Rate ($\times 10^2$ gCH ₂ /g.cat.h)	Selectivity to CH ₄ (%)	Selectivity to C ₂ -C ₄ (%)
Co/Al_0.5_1h	29.5	99.4	0.6
Co/Al_0.5_2h	21.0	99.8	0.2
Co/Al_1.0_1h	30.3	99.4	0.6
Co/Al_1.0_2h	30.1	99.7	0.3
Co/Al_2.0_1h	33.3	99.6	0.4
Co/Al_2.0_2h	32.6	99.8	0.2
Impregnated Co/Al ₂ O ₃ _2h	25.8	99.7	0.3

It was found that increased Co/Al molar ratios of cobalt on cobalt-aluminate catalysts apparently resulted in increased activity without changing the product selectivity. Increased activities can be attributed to more reducible cobalt oxide species at lower reaction temperature with increased Co/Al molar ratios as mentioned in the TPR results. The holding time during solvothermal synthesis seemed to have only little effect on activity for the samples having Co/Al molar ratios of 1.0 and 2.0.

However, the holding time during solvothermal synthesis was found to have a significant effect on the catalyst sample having Co/Al molar ratio of 0.5 where the activities dramatically decreased with increasing the holding time. This was probably due to more non-reducible cobalt-aluminate formed resulting in lower amount of the reducible cobalt oxide species as also seen in **Figure 5.13** during the TPR measurement. On the other word, the longer holding time, the larger amount of non-reducible cobalt-aluminate was formed. Considering the activity of the conventional solvothermal-derived alumina-supported cobalt catalyst having 25 wt% of cobalt, it exhibited lower activity due to the further formation of non-reducible cobalt-aluminate (at temperature < 800°C) (Jongsomjit *et al.*, 2001, 2003, 2003) during reduction and/or reaction period without changing the product selectivity.



สถาบันวิทยบริการ
จุฬาลงกรณ์มหาวิทยาลัย

5.1.2 Effect of temperature during solvothermal process

The present study focused on the influence of temperatures during solvothermal process on characteristics and catalytic properties of the cobalt on cobalt-aluminate synthesized by the solvothermal process. The excess cobalt precursor was employed in order to obtain the cobalt oxides on cobalt-aluminate after calcination of samples. Therefore, the Co/Al = 0.5 and 1.0 was synthesized at 250 and 300 °C for 2 h by solvothermal process. After solvothermal synthesis, all samples were calcined at 300 °C for 1 h prior to characterization and reaction study.

After calcination at different temperatures, all samples were characterized by means of N₂ physisorption, XRD, SEM/EDX, TEM, and TPR.

5.1.2.1 BET surface area

The BET surface areas of samples obtained from N₂ physisorption are listed in **Table 5.3**.

Table 5.3 BET surface areas of the calcined cobalt on cobalt-aluminate catalysts with various temperature during solvothermal process.

Samples	BET surface area (m ² /g)
Co/Al_0.5_250°C	114
Co/Al_0.5_300°C	139
Co/Al_1.0_250°C	130
Co/Al_1.0_300°C	137

It was found that increased temperatures during solvothermal process resulted in increased surface areas of samples. The increased surface area was probably due to the formation of cobalt-aluminate that has very small particles.

5.1.1.2 X-ray diffraction (XRD)

The XRD patterns for cobalt on cobalt aluminate samples are shown in **Figure 5.14**. All samples exhibited the similar short-broaden XRD peaks at 31, 37, 46, 59 and 65° assigned to Co_3O_4 and CoAl_2O_4 species, which were overlapped (Jongsomjit *et al.*, 2001). The observed short-broaden peaks suggested the good dispersion of Co_3O_4 and CoAl_2O_4 species.

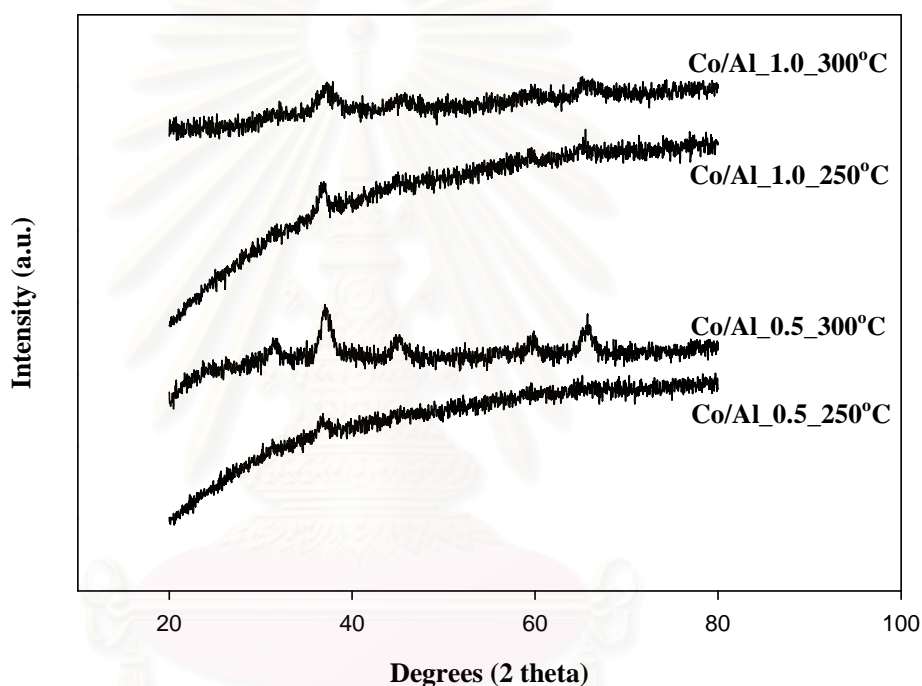


Figure 5.14 XRD pattern of the calcined cobalt on cobalt-aluminate catalysts with various temperature during solvothermal process

5.1.2.3 Scanning electron microscopy (SEM) and Energy dispersive X-ray spectroscopy (EDX)

SEM and EDX were performed in order to study the morphologies of catalyst samples and the elemental distribution on the external surface of the sample granule. It was found that there was no significant change in morphologies upon different temperatures during solvothermal process used. A typical SEM micrograph and EDX mapping for cobalt on cobalt-aluminate Co/Al_{0.5}_300°C and Co/Al_{1.0}_300°C are shown in **Figure 5.3, 5.5** and Co/Al_{0.5}_250°C and Co/Al_{1.0}_250°C are shown in **Figure 5.15-5.16**. It can be also observed that cobalt was well distributed on the sample granule.

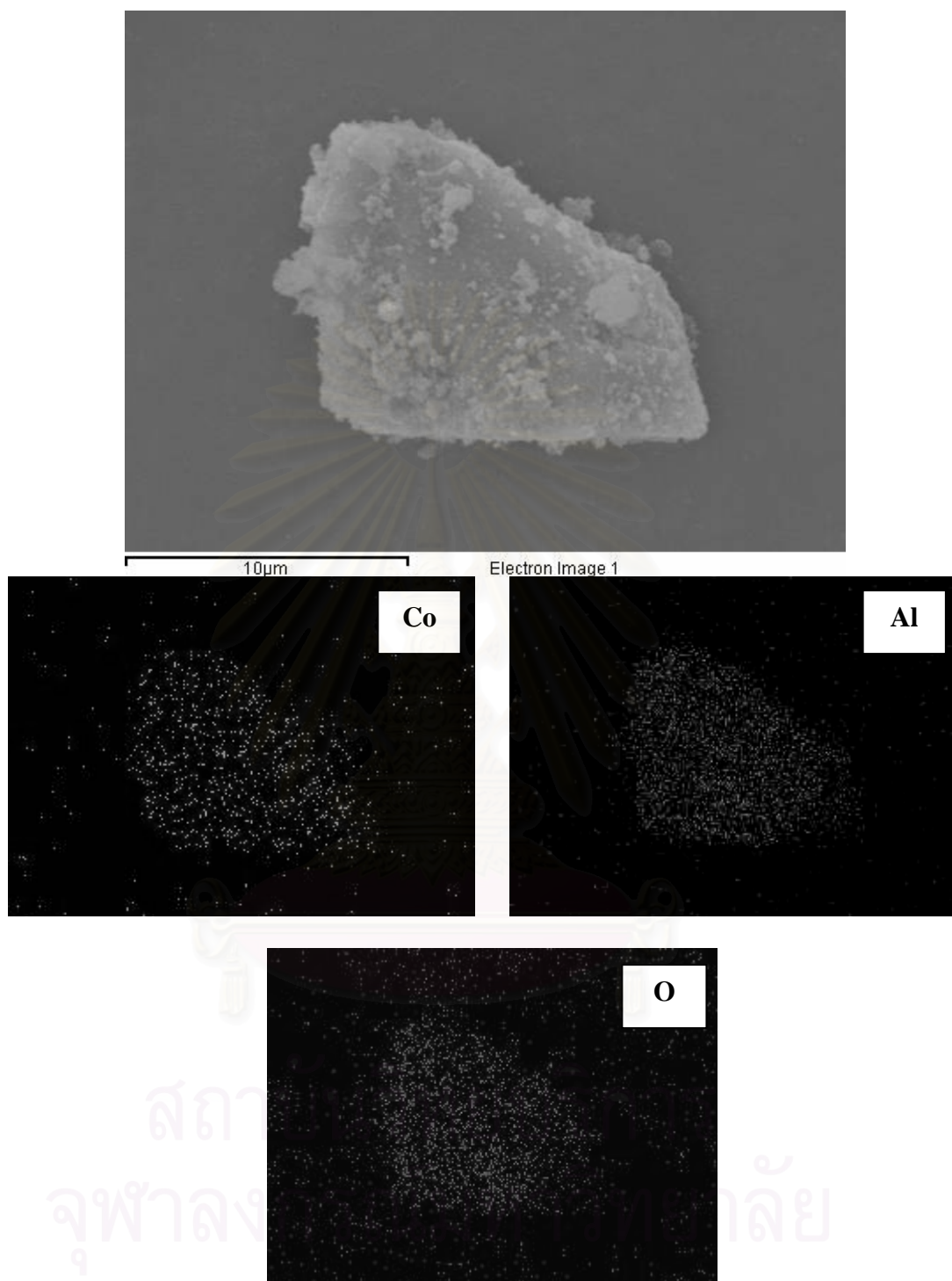


Figure 5.15 SEM micrograph and EDX mapping of Co/Al_{0.5}_250°C

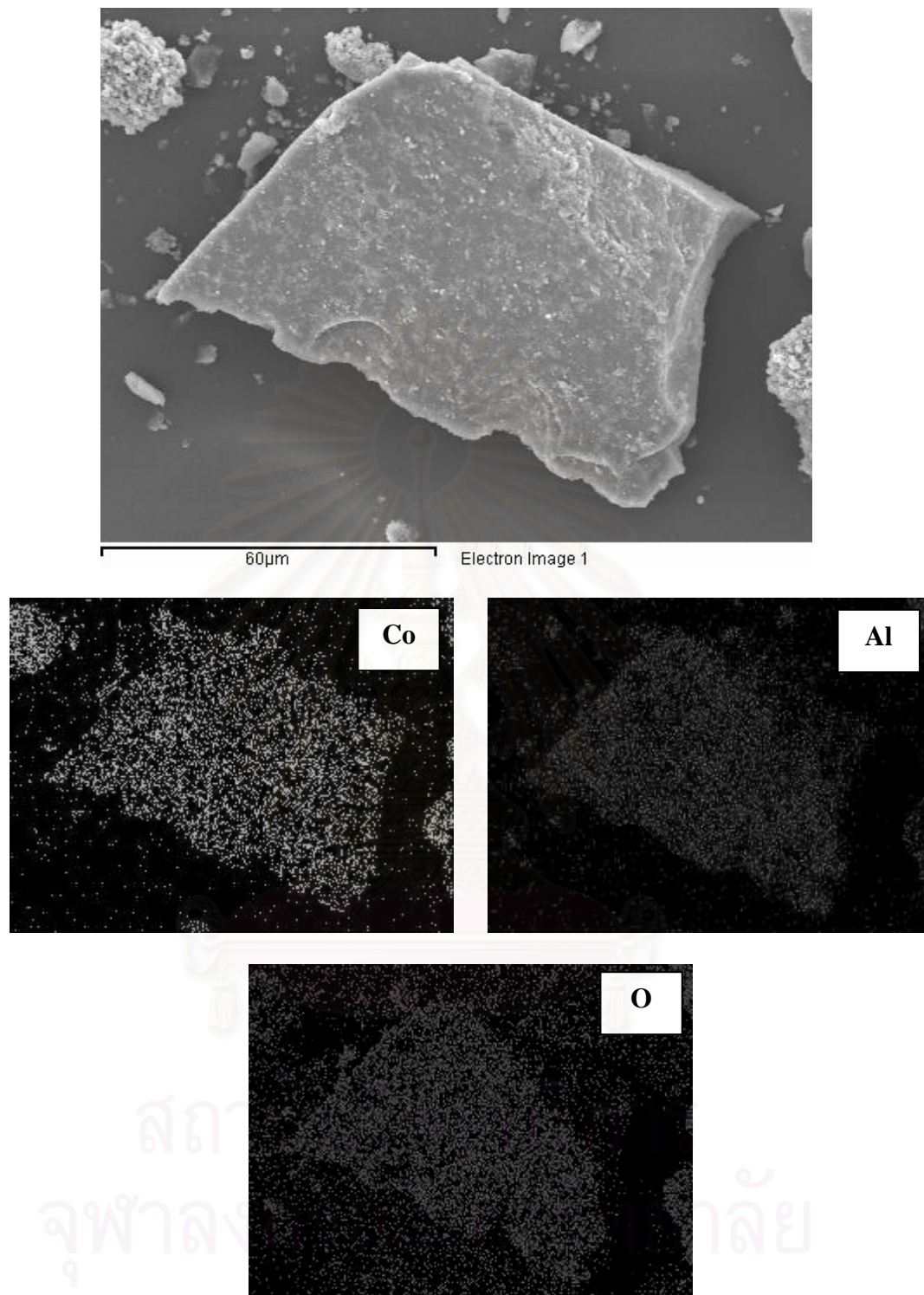


Figure 5.16 SEM micrograph and EDX mapping of Co/Al_{1.0}_250°C

5.1.2.4 Transmission Electron Microscopy (TEM)

In order to determine the dispersion of cobalt oxide species and crystallite size of them, the more powerful technique, such as TEM was performed. The TEM micrograph for all sample are shown in **Figure 5.17**. The dark spots represented the cobalt species dispersing on the sample granule. It was found that the dispersion of cobalt oxide species was good. The crystallite size of cobalt was very small (less than 10 nm) and agglomerated as the polycrystals.

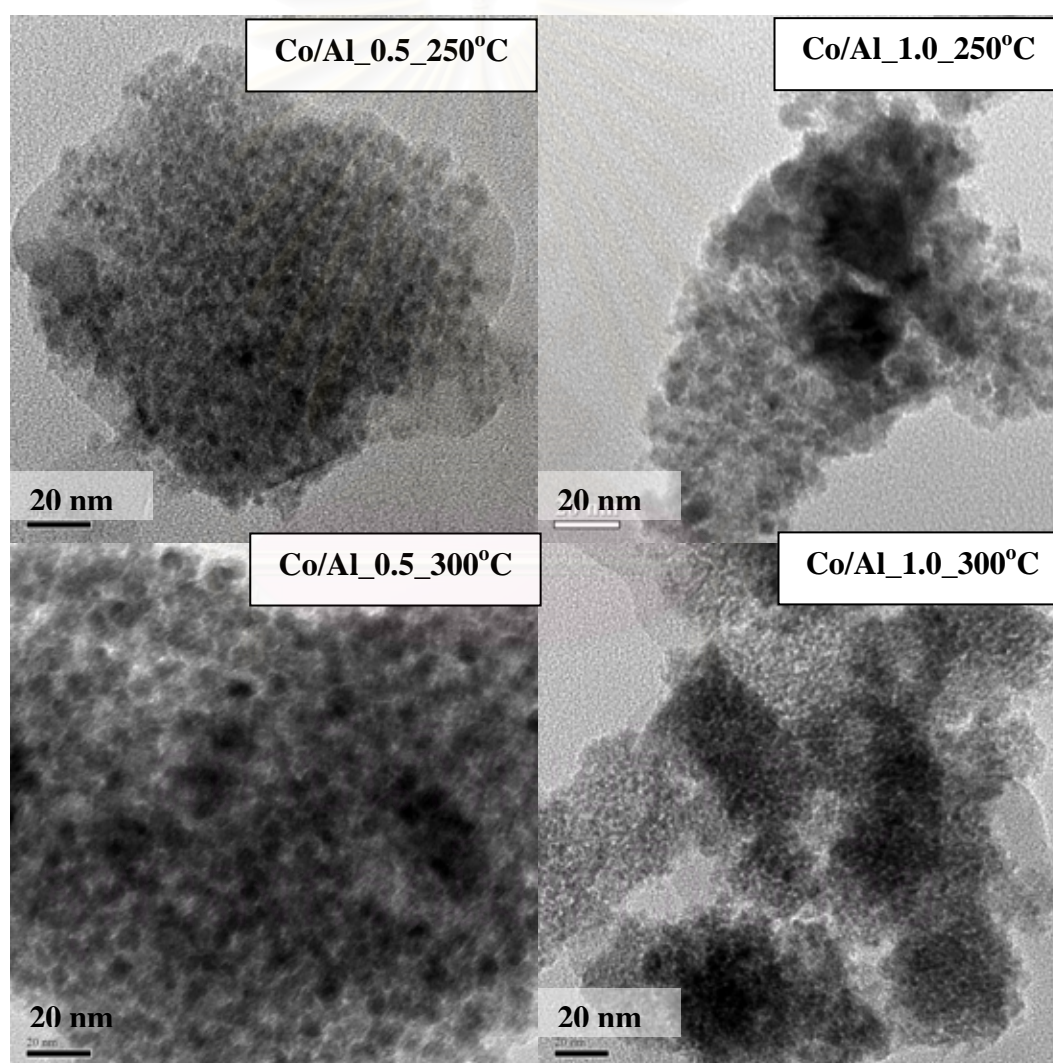


Figure 5.17 TEM micrograph of cobalt on cobalt-aluminate catalysts with various temperature during solvothermal process.

5.1.2.5 Temperature programmed reduction (TPR)

TPR was performed in order to determine the reduction behaviors. The TPR profiles for all catalyst samples are shown in **Figure 5.18**. It was found that mostly the one reduction peak below 400°C was observed and assigned to the overlap of two step reduction of Co_3O_4 to CoO and, then to Co metal (Jongsomjit *et al.*, 2001, 2004, 2005). Upon the TPR conditions, the two-step reduction may or may not be observed. In fact, the TPR peak locations are affected by reduction kinetics. The kinetics of reduction can be affected by a wide range of variables, including particle size, support interaction, and reduction gas composition (Jongsomjit *et al.*, 2001, 2002). The effects of particle size and support interaction can be superimposed on each other. Thus, while a decrease in metal oxide particle size can result in faster reduction due to greater surface area/volume ratio, smaller particles may interact more with the support, slowing reduction. Based on the TPR profiles of sample, the reduction peak at high temperature (ca. above 600°C) was also observed. This peak can be assigned to the reduction of non-stoichiometric cobalt-aluminate, which is more difficult than the reduction of Co_3O_4 species (Jongsomjit *et al.*, 2001). According to the TPR results, it can be concluded that increased temperature during solvothermal process resulted in decreased Co_3O_4 species, which facilitated the reduction behavior of catalyst samples.

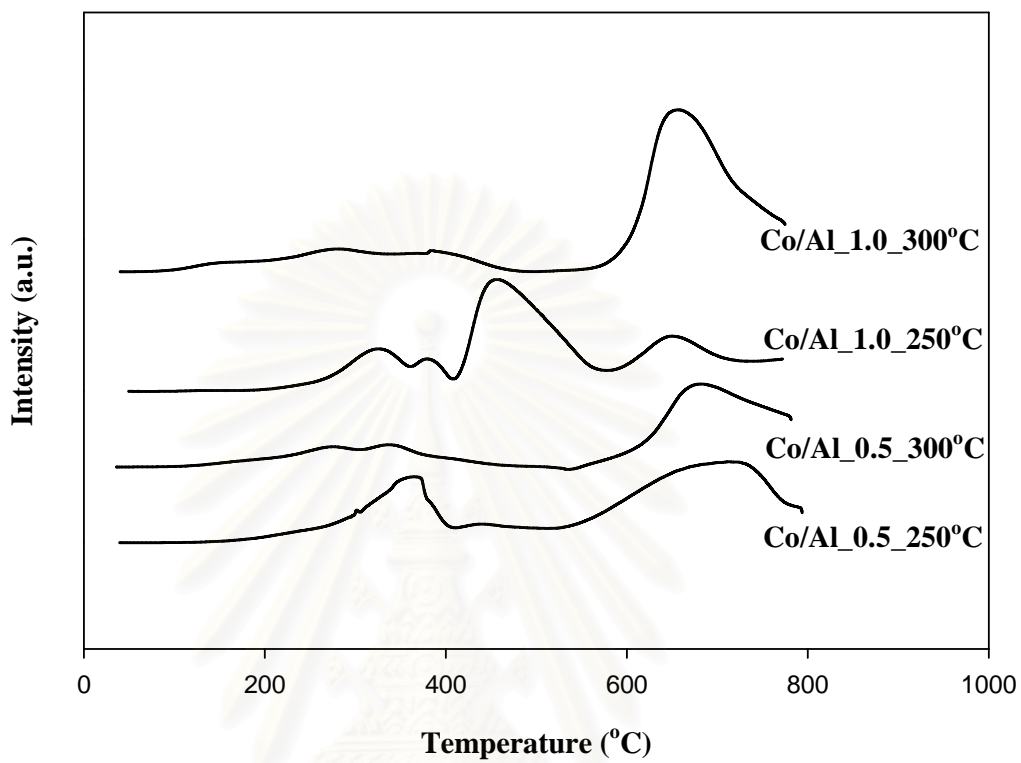


Figure 5.18 TPR profiles for the calcined cobalt on cobalt-aluminate catalysts with various temperature during solvothermal process.

สถาบันวิทยบริการ
จุฬาลงกรณ์มหาวิทยาลัย

5.1.2.7 Reaction study in CO hydrogenation

CO hydrogenation ($H_2/CO = 1$) under methanation condition was performed to determine the overall activity and product selectivity of the samples. In fact, hydrogenation of CO under was carried out at 220°C at atmospheric pressure. A flow rate of $H_2/CO/Ar = 20/2/8$ cc/min in a fixed-bed flow reactor was used. The relatively high H_2/CO ratio was employed to minimize deactivation due to carbon deposition during reaction. The resulted reaction study is also shown in **Table 5.4**. It was found that decreased temperature during solvothermal process resulted in increased activity. The reaction results were in agreement with the TPR study as mentioned above. It can be attributed to more reducible cobalt oxide species occurred. Considering the product selectivity, it revealed that different temperatures during solvothermal process did not affect on the selectivity of product during methanation where methane was still the product majority in the effluent.

Table 5.4 Reaction study of cobalt on cobalt aluminate with various temperature during solvothermal process

Samples	Rate ($\times 10^2$ gCH ₂ /g.cat. h)	Selectivity to CH ₄ (%)	Selectivity to C ₂ -C ₄ (%)
Co/Al_0.5_250°C	31.94	99.7	0.3
Co/Al_0.5_300°C	21.00	99.8	0.2
Co/Al_1.0_250°C	37.36	99.9	0.1
Co/Al_1.0_300°C	30.10	99.7	0.3

5.1.3 Effect of calcination temperature

The present study focused on the influence of different calcination temperatures on characteristics and catalytic properties of the cobalt on cobalt-aluminate synthesized by the solvothermal process. The excess cobalt precursor was employed in order to obtain the cobalt oxides on cobalt-aluminate after calcination of samples. Therefore, the Co/Al = 1.0 was synthesized at 300 °C for 2 h by solvothermal process. After solvothermal synthesis, all samples were calcined at varied from 300, 400 and 500°C for 1 h prior to characterization and reaction study.

After calcination at different temperatures, all samples were characterized by means of N₂ physisorption, XRD, SEM/EDX, TEM, TPR and H₂ chemisorption.

5.1.3.1 BET surface area

The BET surface areas of samples obtained from N₂ physisorption are listed in **Table 5.5**.

Table 5.5 BET surface areas of the calcined cobalt on cobalt-aluminate catalysts with various calcination temperature

Samples	BET surface area (m ² /g)
Co/Al_300°C	137
Co/Al_400°C	125
Co/Al_500°C	111

It was found that increased calcination temperatures apparently resulted in decreased surface areas of samples. The decreased surface area was probably due to the agglomeration of cobalt oxide species or sintering of the pores.

5.1.3.2 X-ray diffraction (XRD)

The XRD patterns for cobalt on cobalt aluminate samples are shown in **Figure 5.19**. All samples exhibited the similar short-broaden XRD peaks at 31, 37, 46, 59 and 65° assigned to Co_3O_4 and CoAl_2O_4 species, which were overlapped (Jongsomjit *et al.*, 2001). The observed short-broaden peaks suggested the good dispersion of Co_3O_4 and CoAl_2O_4 species.

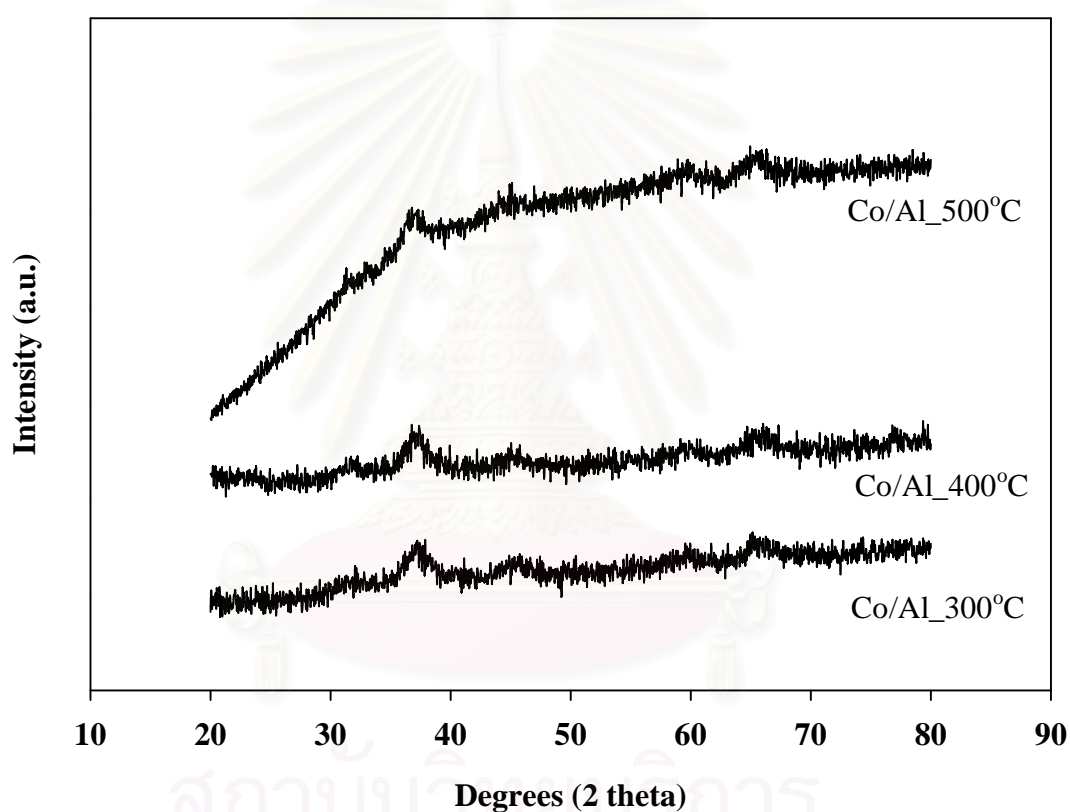


Figure 5.19 XRD pattern of the calcined cobalt on cobalt-aluminate catalysts with various calcination temperature

5.1.3.3 Scanning electron microscopy (SEM) and Energy dispersive X-ray spectroscopy (EDX)

SEM and EDX were performed in order to study the morphologies of catalyst samples and the elemental distribution on the external surface of the sample granule. It was found that there was no significant change in morphologies upon different calcination temperatures used. A typical SEM micrograph and EDX mapping for cobalt on cobalt-aluminate are shown in **Figure 5.20-5.22**. It can be also observed that cobalt was well distributed on the sample granule.



สถาบันวิทยบริการ
จุฬาลงกรณ์มหาวิทยาลัย

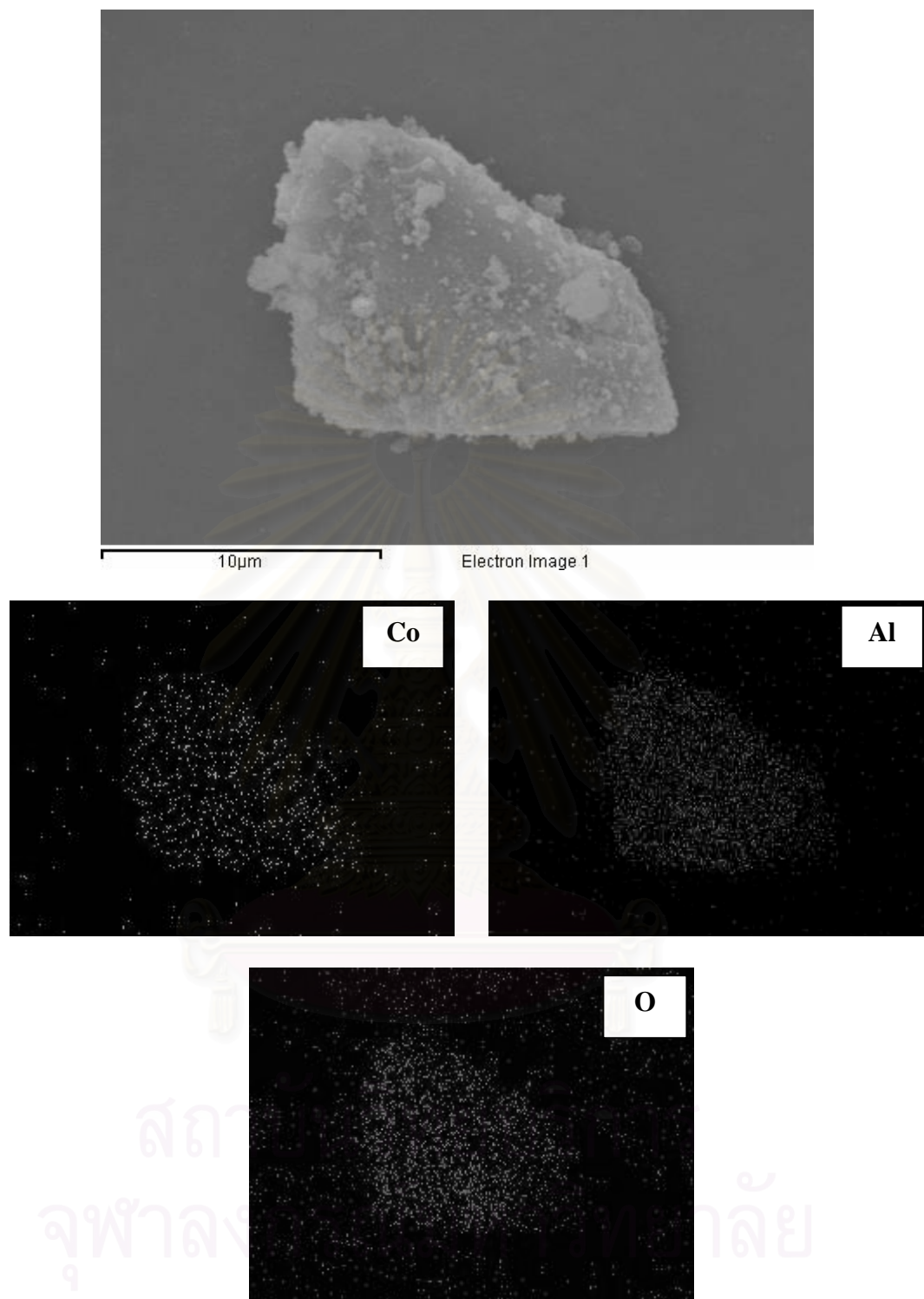


Figure 5.20 SEM micrograph and EDX mapping of Co/Al_{300°C}

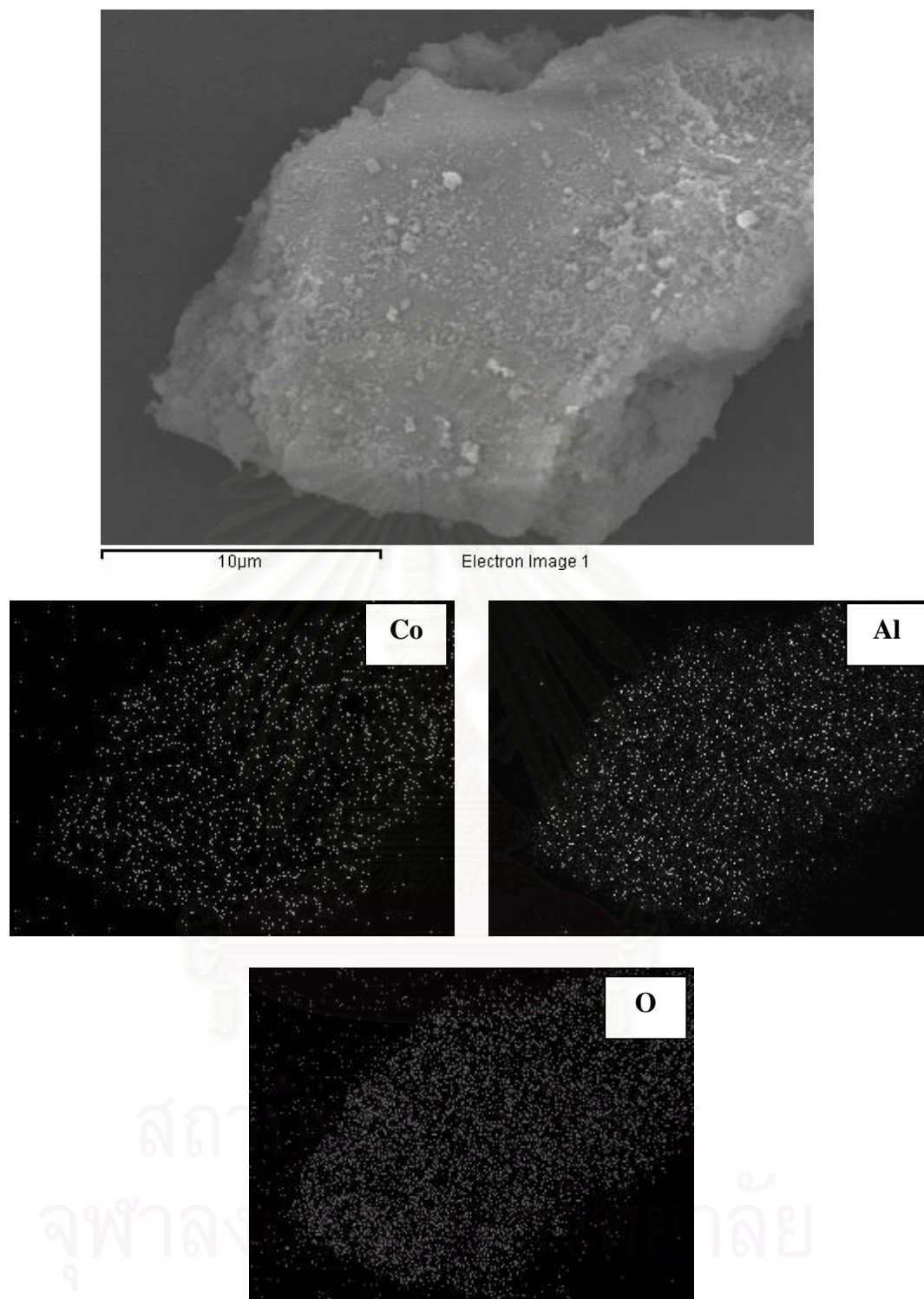


Figure 5.21 SEM micrograph and EDX mapping of Co/Al₄₀₀°C

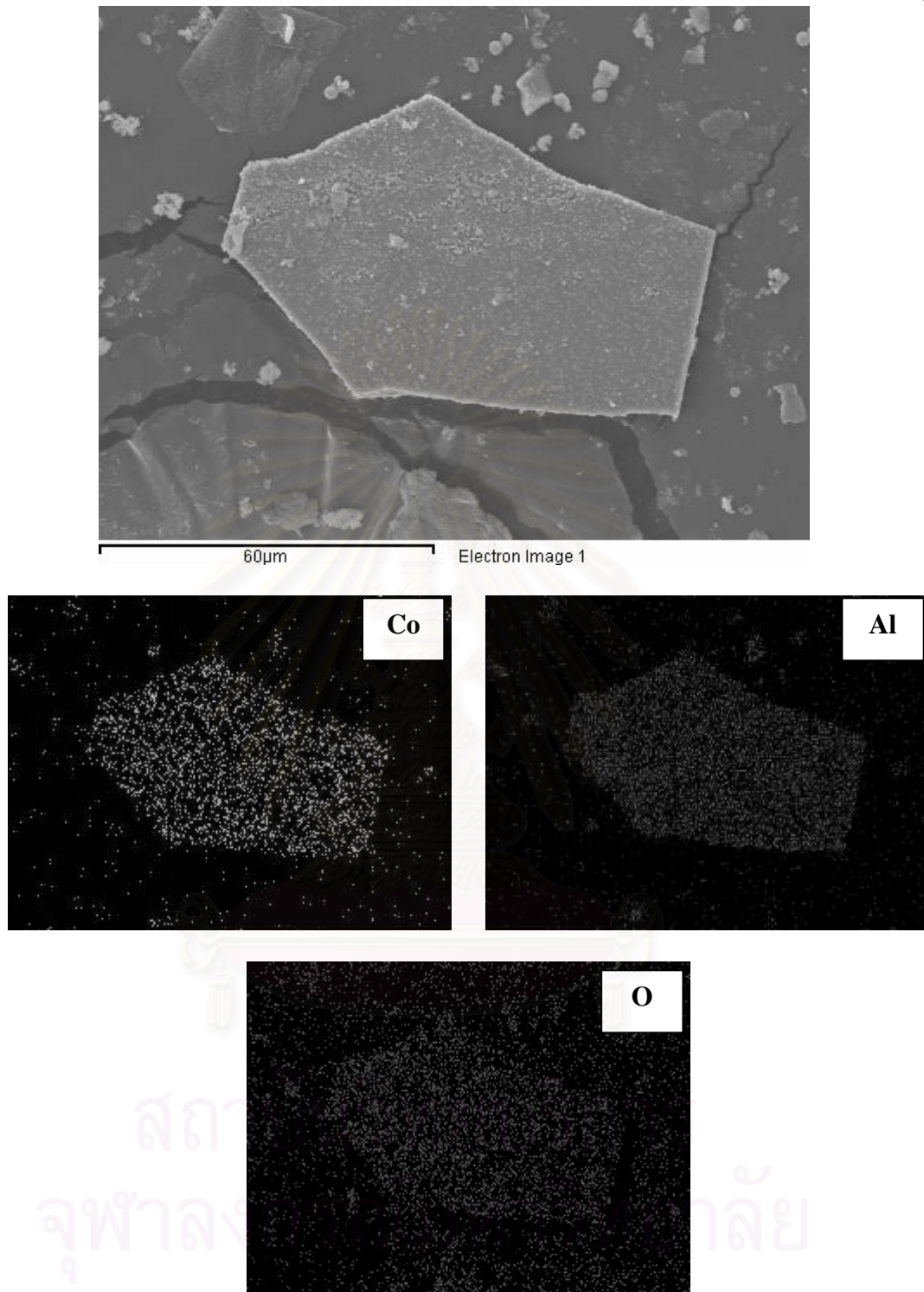


Figure 5.22 SEM micrograph and EDX mapping of Co/Al_500°C

5.1.3.4 Transmission Electron Microscopy (TEM)

In order to determine the dispersion of cobalt oxide species and crystallite size of them, the more powerful technique, such as TEM was performed. The TEM micrograph for all sample are shown in **Figure 5.23**. The dark spots represented the cobalt species dispersing on the sample granule. It was found that the dispersion of cobalt oxide species was good. The crystallite size of cobalt was very small (less than 10 nm) and agglomerated as the polycrystals.

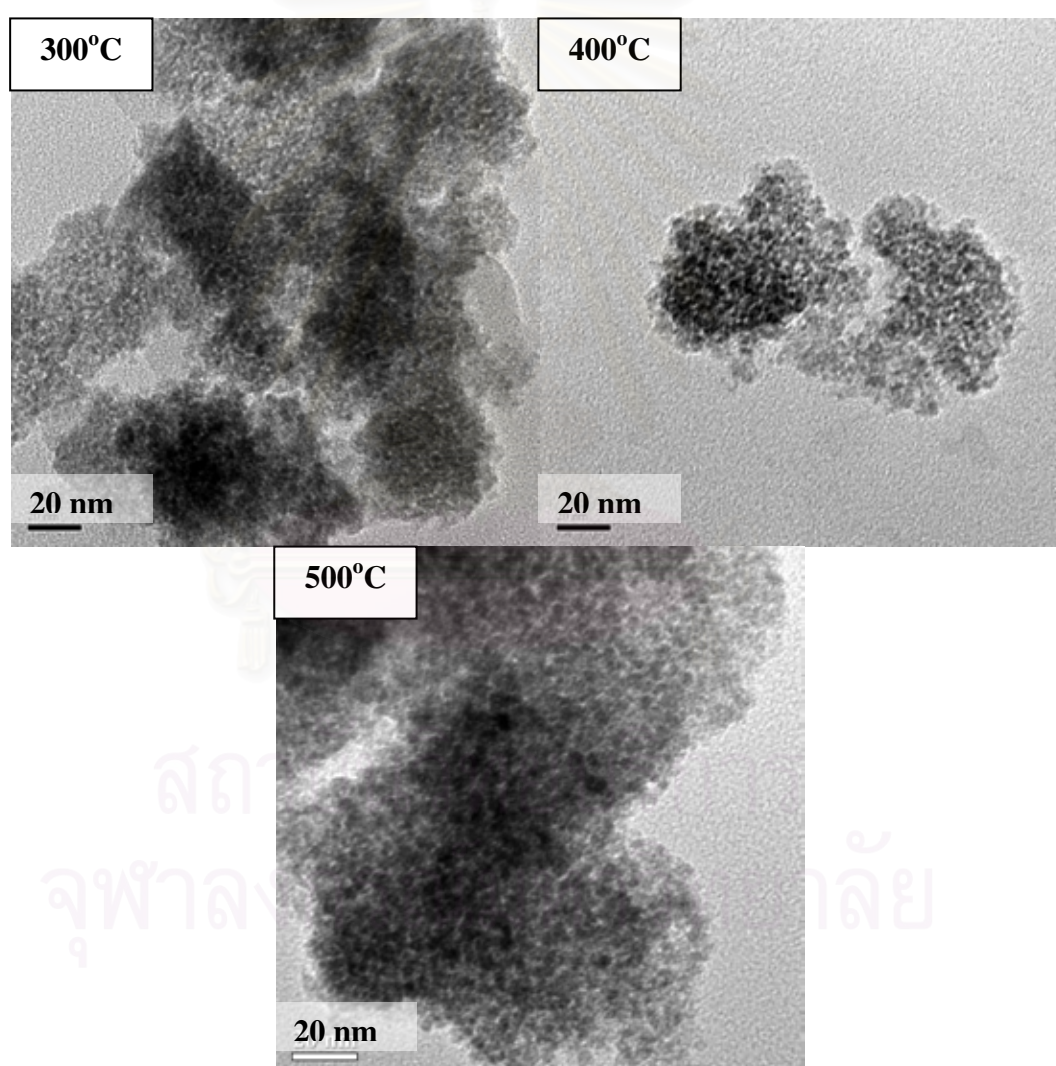


Figure 5.23 TEM micrograph of cobalt on cobalt-aluminate catalysts with various calcination temperature

5.1.3.5 Temperature programmed reduction (TPR)

TPR was performed in order to determine the reduction behaviors. The TPR profiles for cobalt on cobalt-aluminate catalyst samples are shown in **Figure 5.24**. It indicated that all samples exhibited only one reduction peak at ca. 650°C, which was assigned to the overlap of two step reduction of Co_3O_4 to CoO and then to Co metal (Jongsomjit, B). Upon the TPR conditions, the two-step reduction may or may not be observed. In fact, the TPR peak locations are affected by reduction kinetics. The kinetics of reduction can be affected by a wide range of variables, including crystallite size, support interaction, and reduction gas composition (Jongsomjit *et al.*, 2001, 2002, 2003). The effects of particle size and support interaction can be superimposed on each other. Thus, while a decrease in metal oxide crystallite size can result in faster reduction due to greater surface area/volume ratio, the smaller crystallite size may interact more with the support, slowing reduction. According to the TPR results, it can be concluded the cobalt oxide species formed on all samples were similar. However, the amounts of H_2 consumed, which was related to the reducibility of each sample were slightly different as seen from the area below TPR profiles. It can be observed that the sample calcined at 400°C exhibited the highest reducibility among other samples (The relative areas of samples calcined at 400, 500 and 300°C were at 1.00: 0.96: 0.93, respectively). In order to confirm this, the catalyst samples were tested under methanation condition to measure the activity for CO hydrogenation.

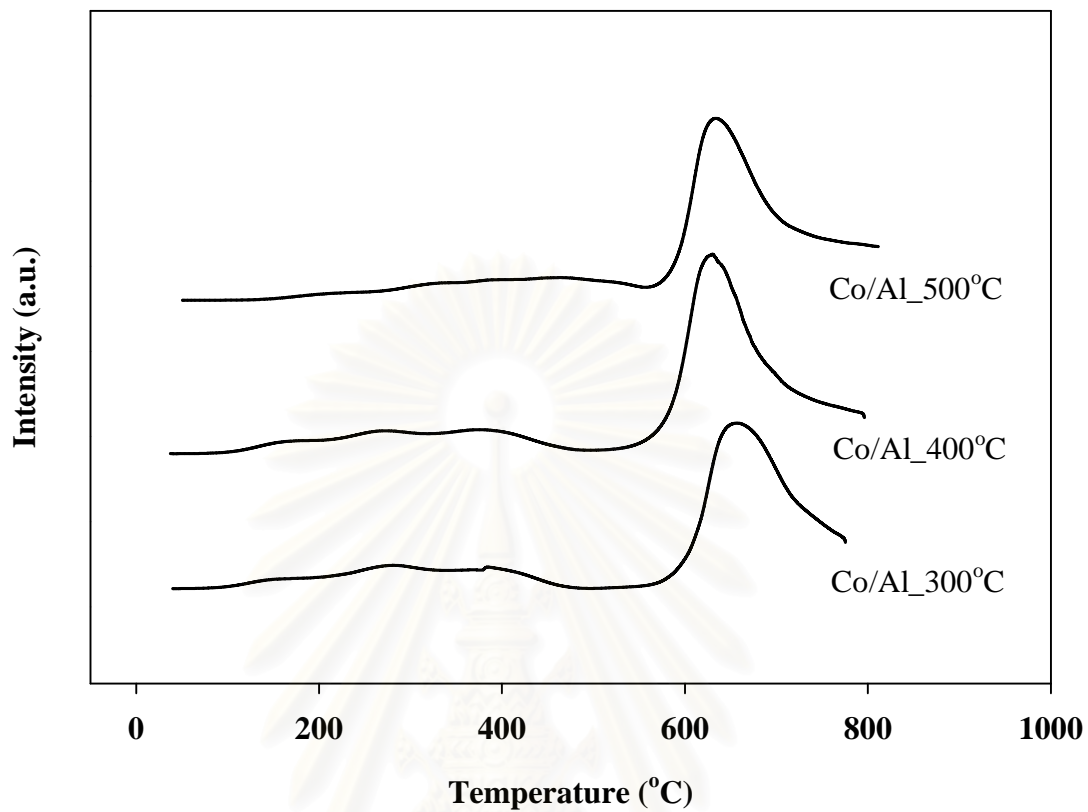


Figure 5.24 TPR profiles for the calcined cobalt on cobalt-aluminate catalysts with various calcination temperature

สถาบันวิทยบริการ
จุฬาลงกรณ์มหาวิทยาลัย

5.1.3.6 H₂ chemisorption

The resulted H₂ chemisorption is illustrated in **Table 5.6**. The H₂ adsorbed increased with increasing calcination temperature to about 400 °C and dramatically decreased when continuously increased the calcination temperature.

5.1.2.7 Reaction study in CO hydrogenation

CO hydrogenation (H₂/CO = 1) under methanation condition was performed to determine the overall activity and product selectivity of the samples. In fact, hydrogenation of CO under was carried out at 220°C at atmospheric pressure. A flow rate of H₂/CO/Ar = 20/2/8 cc/min in a fixed-bed flow reactor was used. The relatively high H₂/CO ratio was employed to minimize deactivation due to carbon deposition during reaction. The resulted reaction study is also shown in **Table 5.6**. It was found that the sample calcined at 400°C exhibited the highest activity during methanation. The reaction results were in agreement with the TPR and H₂ chemisorption study as mentioned above. Considering the product selectivity, it revealed that different calcination temperatures did not affect on the selectivity of product during methanation where methane was still the product majority in the effluent.

Table 5.6 H₂ chemisorption and reaction study of cobalt on cobalt aluminate with various calcination temperature

Samples	Total H ₂ chemisorption (μmol/g cat)	Rate (x10 ² gCH ₂ /g.cat.h)	Selectivity to CH ₄ (%)	Selectivity to C ₂ -C ₄ (%)
Co/Al_300°C	5.2	30	99.7	0.3
Co/Al_400°C	5.6	37	99.6	0.4
Co/Al_500°C	4.8	14	99.8	0.2

5.2 Cobalt on cobalt-aluminate catalyst with various cobalt precursor (Part II)

In the present study, the effect of different cobalt precursors, such as cobalt (II) acetylacetonate, cobalt (II) acetate, cobalt (II) nitrate and cobalt (II) chloride employed to synthesize the cobalt dispersed on cobalt-aluminate catalysts using the solvothermal process was investigated. After calcination of samples, they were further characterized by means of N₂ physisorption, XRD, SEM/EDX, TEM and TPR. The samples were also tested under methanation condition in order to measure the activity and product distribution.

5.2.1 BET surface area

All the calcined samples were measured for the BET surface areas using the N₂ physisorption. The BET surface areas are listed in **Table 5.5**. It was found that the BET surface areas of samples obtained from different cobalt precursors were in the range of 61-130 m²/g within the order of CoAA > CoCL > CoN > CoAC.

Table 5.7 BET surface areas of the calcined cobalt on cobalt-aluminate catalysts with various cobalt precursors

Samples	BET Surface Area (m ² /g)
CoAA	130
CoAC	61
CoN	85
CoCL	124

5.2.2 X-ray diffraction (XRD)

The XRD patterns for all samples are shown in **Figure 5.25**. It indicated that the CoAA, CoAC and CoN samples exhibited the similar short-broaden XRD peaks at 31, 37, 46, 59 and 65° assigned to Co_3O_4 and CoAl_2O_4 species, which were overlapped (Jongsomjit *et al.*, 2001). The observed short-broaden peaks suggested the good dispersion of Co_3O_4 and CoAl_2O_4 species. However, the XRD patterns for CoCL sample showed a short-broaden XRD peaks at 28, 37, 39, 49, 66 and 73° indicating the other forms of cobalt oxide species, such as Co_2O_3 and the CoCl_2 remains.

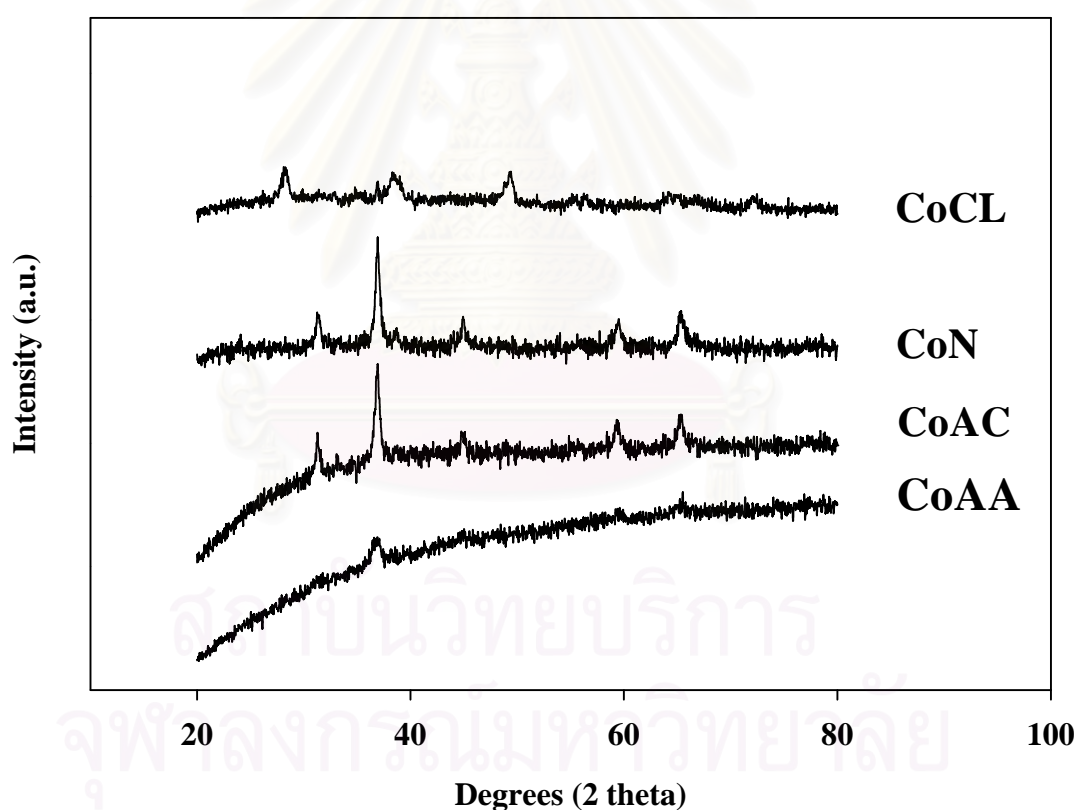


Figure 5.25 XRD pattern of the calcined cobalt on cobalt-aluminate catalysts with various cobalt precursors

5.2.3 Scanning electron microscopy (SEM) and Energy dispersive X-ray spectroscopy (EDX)

SEM and EDX were performed to study the morphologies of catalyst samples and the elemental distribution on the external surface of the catalyst granule. It was found that no significant change in morphologies was observed upon different cobalt precursors employed. A typical SEM micrograph and EDX mapping for cobalt on cobalt-aluminate are shown in **Figure 5.26-5.29**. It was also observed that cobalt was well distributed on the catalyst granule.



สถาบันวิทยบริการ
จุฬาลงกรณ์มหาวิทยาลัย

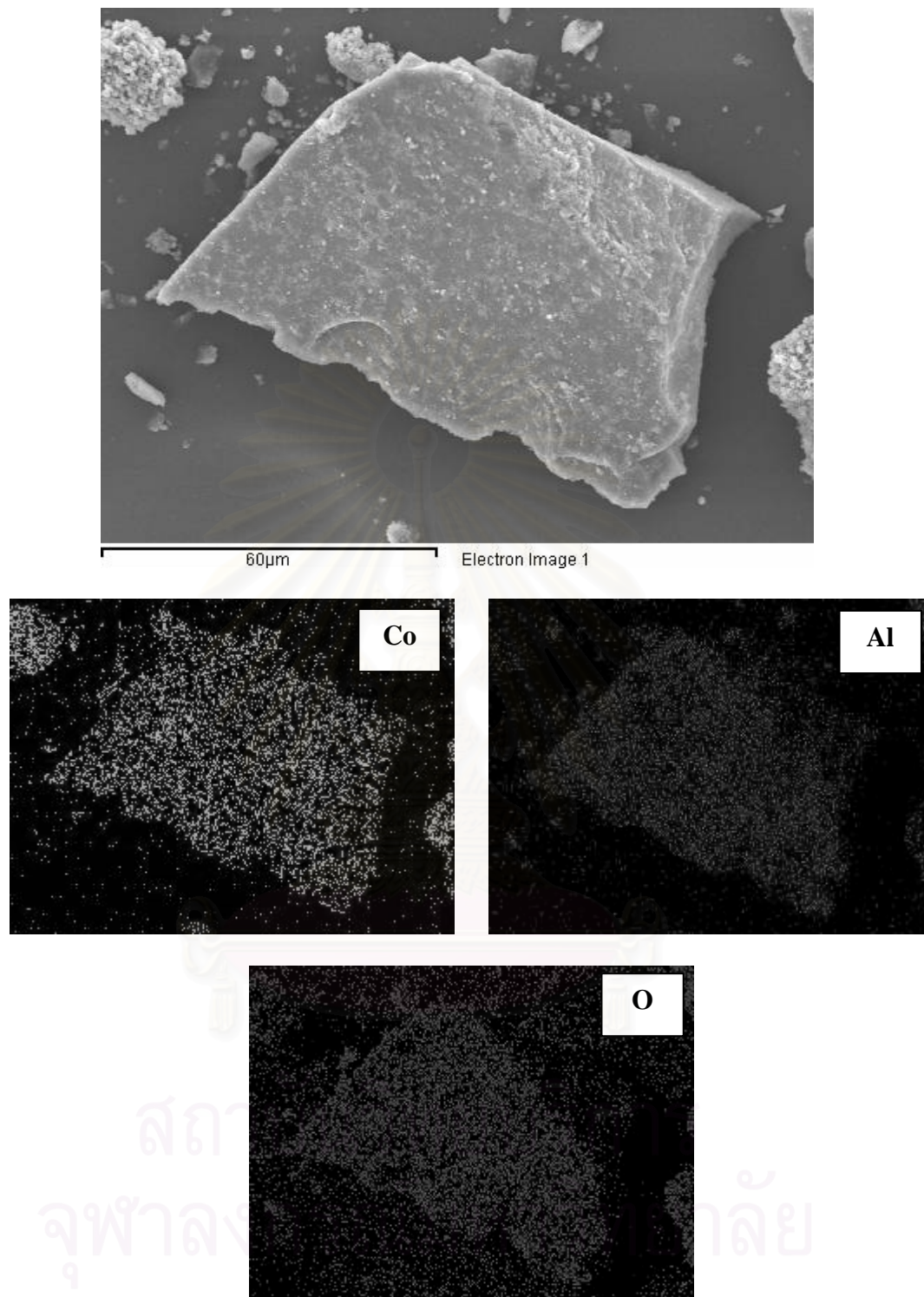


Figure 5.26 SEM micrograph and EDX mapping of CoAA

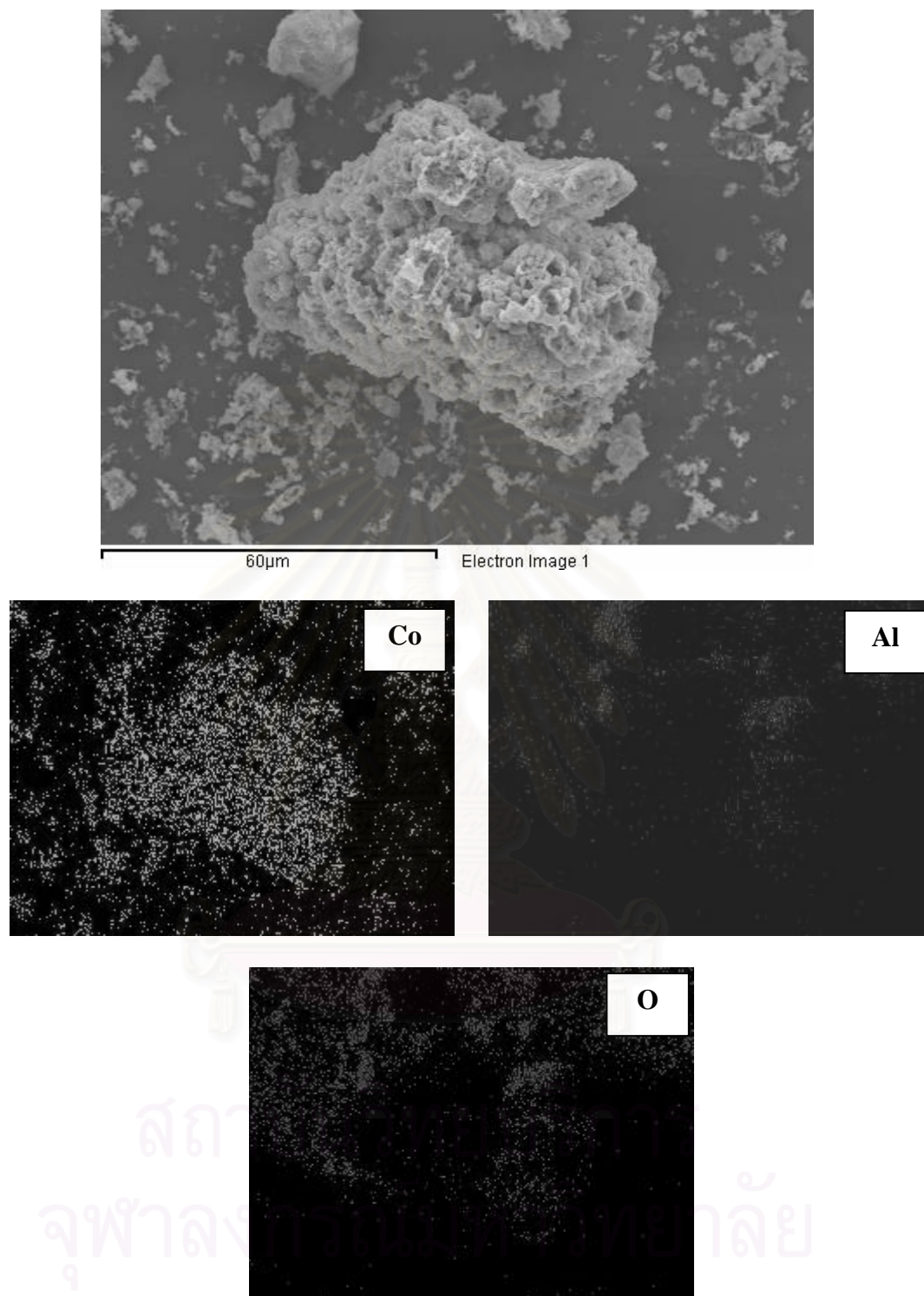


Figure 5.27 SEM micrograph and EDX mapping of CoAC

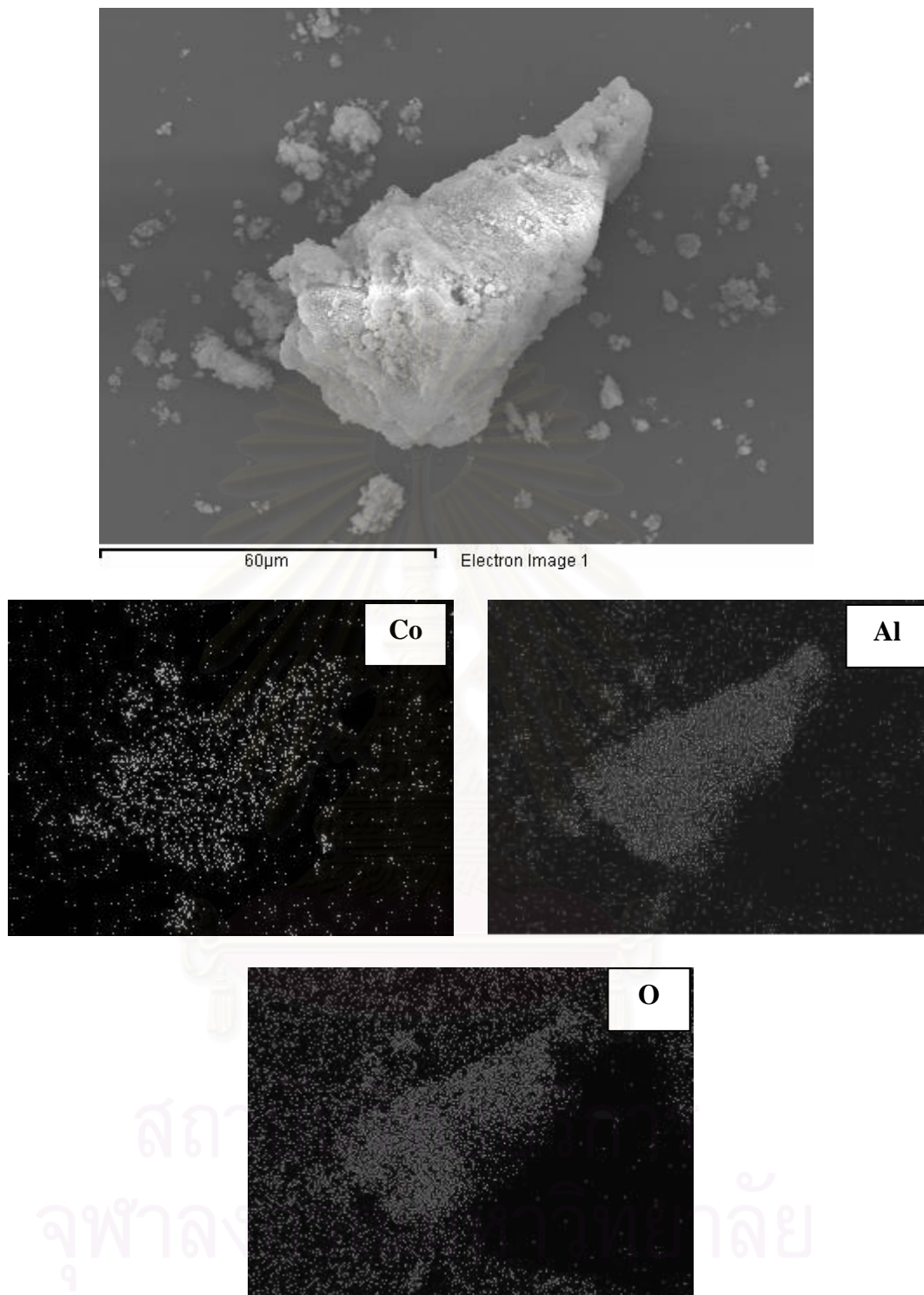


Figure 5.28 SEM micrograph and EDX mapping of CoN

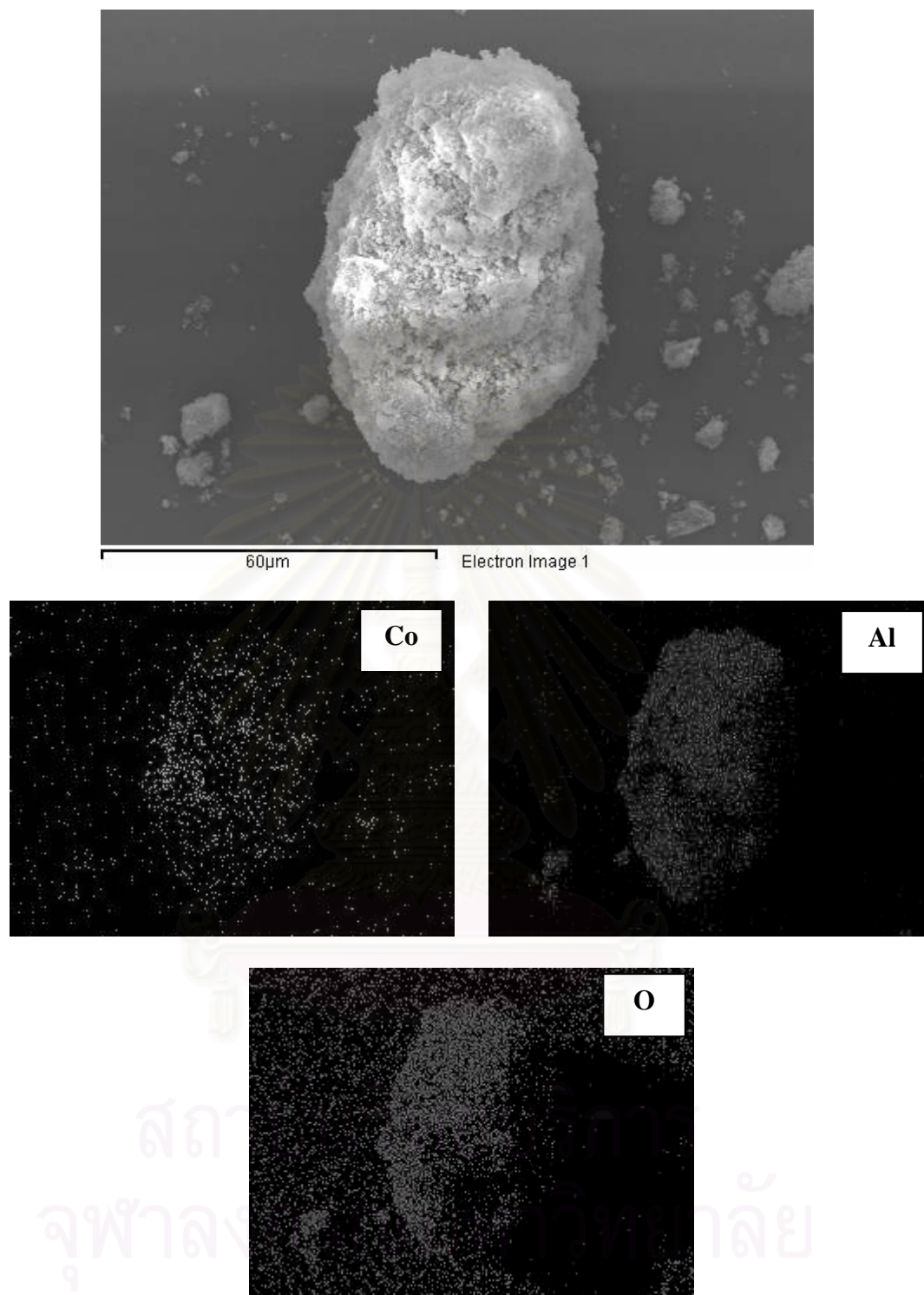


Figure 5.29 SEM micrograph and EDX mapping of CoCL

5.2.4 Transmission Electron Microscopy (TEM)

In order to determine the dispersion of cobalt oxide species and crystallite size of them, the more powerful technique, such as TEM was performed. The TEM micrographs for all samples are shown in **Figure 5.30**. The dark spots represented the cobalt species dispersing on the catalyst granule. It was found that different cobalt precursors were result in different crystallite size of cobalt oxide species in the order of CoN > CoCA > CoAA > CoCL. In addition, all samples exhibited the agglomeration of the crystals as seen in the cluster of polycrystals.

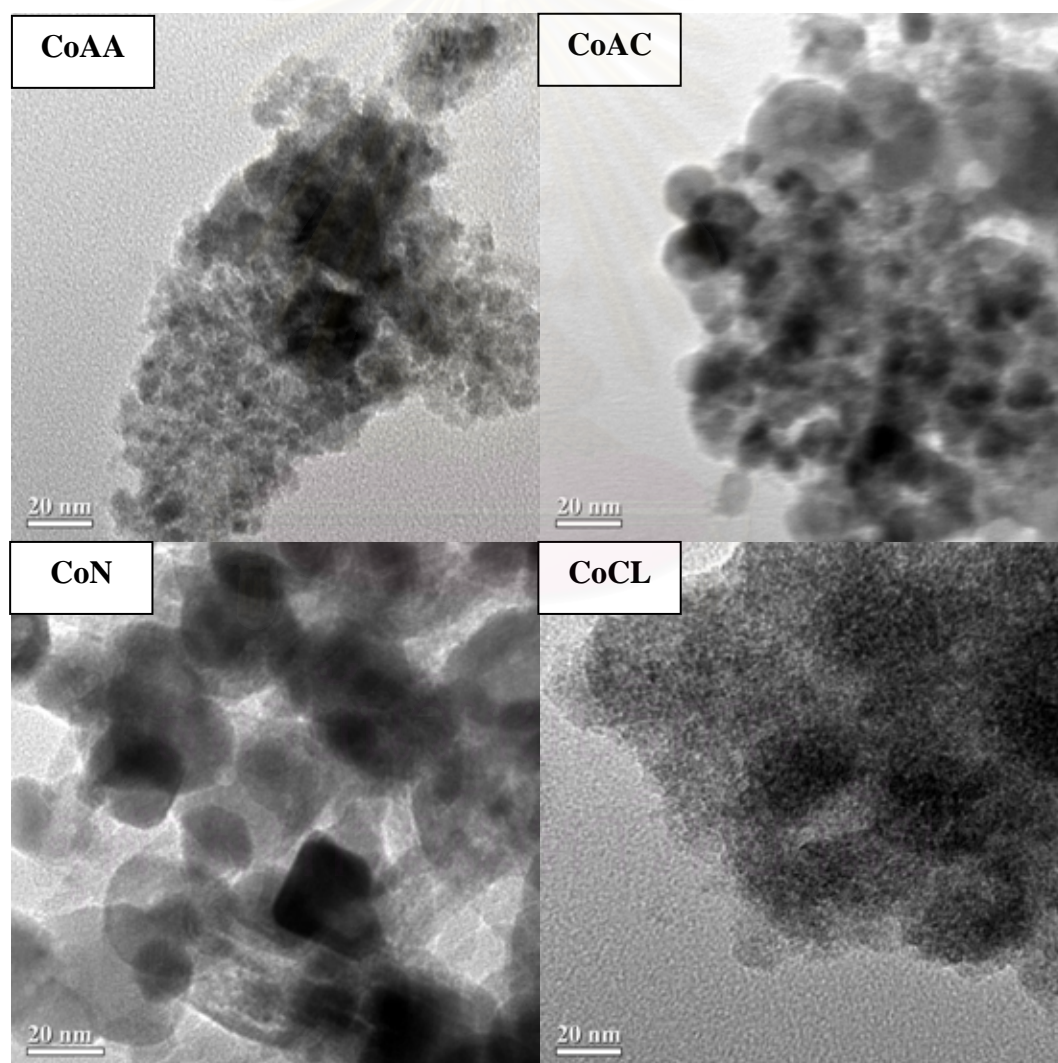


Figure 5.30 TEM micrograph of cobalt on cobalt-aluminate with various cobalt precursors

5.2.5 Temperature programmed reduction (TPR)

It is known that the active form of cobalt catalyst for CO hydrogenation reaction is cobalt metal (Co^0). Thus, reduction of cobalt oxide species is essentially performed in order to transform cobalt oxide species obtained after calcination process into the active cobalt atoms for catalyzing the reaction. Therefore, TPR was performed in order to determine the reduction behaviors and reducibility of cobalt oxide species. The TPR profiles for all catalyst samples are shown in **Figure 5.31**.

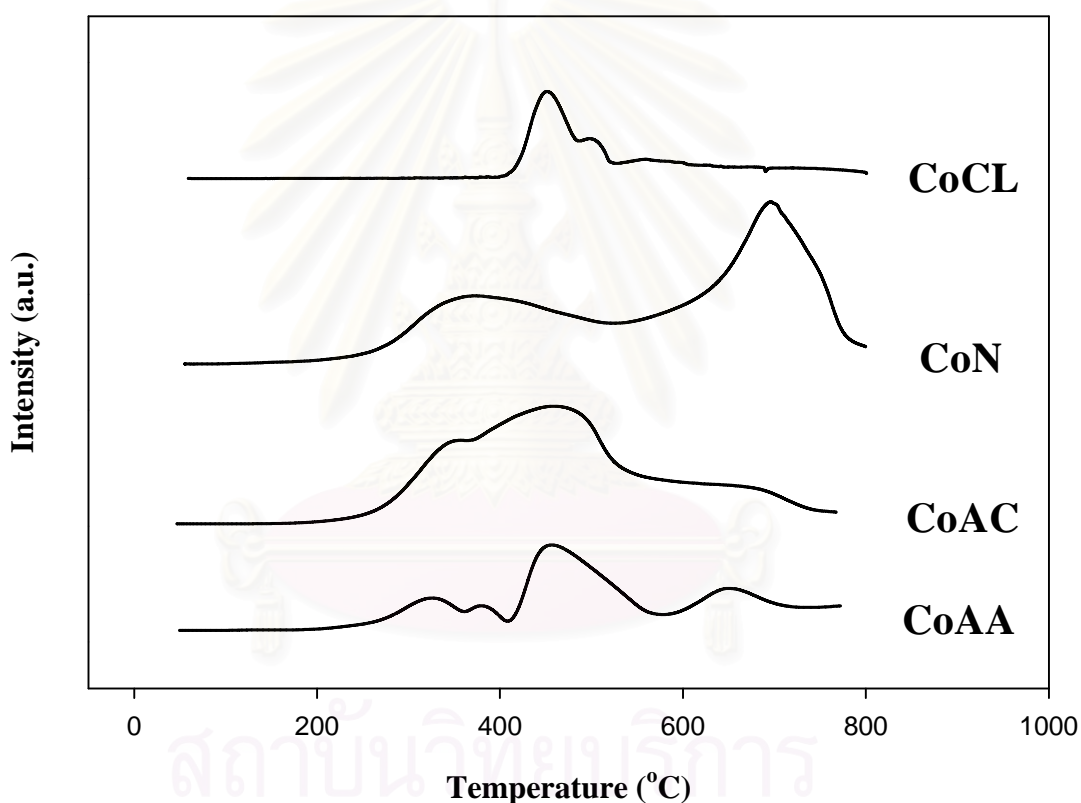


Figure 5.31 TPR profiles for the calcined cobalt on cobalt-aluminate catalysts with various cobalt precursors

It was found that the CoAA and CoAC samples exhibited reduction peaks at ca. 450°C and at ca. 650°C whereas the TPR reduction peaks for the CoN sample were located at ca. 350°C and 700°C . The reduction peak for the CoCL sample was located at ca. 450°C . All the peaks observed were assigned to the overlap of two step

reduction of Co_3O_4 to CoO and, then to Co metal (Jongsomjit *et al.*, 2002, 2004).

Upon the TPR conditions, the two-step reduction may or may not be observed. In fact, the TPR peak locations are affected by reduction kinetics. The kinetics of reduction can be affected by a wide range of variables, including crystallite size, support interaction, and reduction gas composition (Jongsomjit *et al.*, 2001, 2002, 2003). The effects of crystallite size and support interaction can be superimposed on each other. Thus, while a decrease in metal oxide crystallite size can result in faster reduction due to greater surface area/volume ratio, smaller particles may interact more with the support, slowing reduction. As seen from **Figure 5.31**, the amounts of H_2 consumed during TPR, which was related to the reducibility of each sample were different as seen from the area below the TPR profiles. It can be observed that the CoCL sample exhibited the lowest reducibility among other samples even though it rendered the smallest crystallite size of cobalt oxide species as seen from the TEM results. This was suggested that highly dispersed forms of cobalt oxide species be not only the factor that insures the high degree of reducibility (Jongsomjit *et a.*, 2003, 2004). Here, the effect of crystallite size was more pronounced where the smaller particle can interact more retarding reduction. Thus, the larger particle, such as the CoN sample can reduce more based on the TEM and TPR results.

5.2.6 Reaction study in CO hydrogenation

In order to determine the catalytic behaviors of the samples obtained from different cobalt precursors, CO hydrogenation ($H_2/CO = 1$) under methanation condition was performed to determine the overall activity and product selectivity of the samples. In fact, hydrogenation of CO was carried out at 220°C at atmospheric pressure. A flow rate of $H_2/CO/Ar = 20/2/8$ cc/min in a fixed-bed flow reactor was used. The relatively high H_2/CO ratio was employed to minimize deactivation due to carbon deposition during reaction. The resulted reaction study is also shown in **Table 5.8**. The CoN sample exhibited the highest activity among other samples with in agreement as the results from the TPR measurement. The CoAC and CoAA samples also showed adjacent high activity as well. However, the CoCL sample exhibited the lowest activity during methanation due to strong interaction. Considering the product selectivity, it revealed that for the CoN, CoAC and COAA samples, cobalt precursors did not affect on the selectivity of product during methanation where methane was still the product majority in the effluent. On contrary, the selectivity of C_2 - C_4 products apparently increased with the use of $CoCl_2$ as the cobalt precursor. This was suggested that the cobalt oxide species derived from $CoCl_2$ might have different form compared to those obtained from other cobalt precursors as mentioned for the XRD results. The different forms of cobalt oxide species likely respond for the chain growth probability resulting in different C_2 - C_4 selectivity during methanation.

Table 5.8 Reaction study of cobalt on cobalt aluminate with various cobalt precursors

Samples	Rate ($\times 10^2 \text{gCH}_2/\text{g.cat.h}$)	Selectivity to CH_4 (%)	Selectivity to $\text{C}_2\text{-C}_4$ (%)
CoAA	37	99.5	0.5
CoAC	41	99.9	0.1
CoN	69	99.9	0.1
CoCL	1	89.9	10.1



สถาบันวิทยบริการ
จุฬาลงกรณ์มหาวิทยาลัย

CHAPTER VI

CONCLUSIONS AND RECOMMENDATIONS

In this chapter, section 6.1 provides the conclusions obtained from the experimental results of the synthesis of cobalt on cobalt-aluminate catalysts on various Co/Al molar ratios, temperature and time during solvothermal process, temperature of calcination, and cobalt precursors. Additionally, recommendations for further study are given in section 6.2.

6.1 Conclusions

The cobalt on cobalt-aluminate catalyst can be synthesized in one-pot via solvothermal process. The obtained catalysts exhibited higher activities than that obtained from the conventional solvothermal-derived alumina-supported cobalt catalyst without changing the product selectivity. It probably due to unstable of cobalt-aluminate that can be reduced further. It was found that increased Co/Al molar ratios apparently resulted in increased activities during methanation, whereas the holding time during solvothermal synthesis seemed to have only little effect on the activities upon the high molar ratios of Co/Al. However, at low molar ratio of Co/Al (0.5), the increased holding time can result in dramatically decreased activity and the decreased temperature during solvothermal synthesis can result in dramatically increased activity due to decreased amount of non-reducible cobalt-aluminate formed based on the TPR study. The calcination temperature had effects on the characteristics and catalytic properties of cobalt on cobalt-aluminate synthesized by the solvothermal process. The sample calcined at 400°C exhibited the highest activity among other samples due to increased reducibility, active sites and dispersion. Increased calcination temperature could result in decreased surface area and dispersion consequently.

The different cobalt precursors, such as cobalt (II) acetylacetonate, cobalt (II) acetate, cobalt (II) nitrate and cobalt (II) chloride, were employed to synthesize the

cobalt on cobalt-aluminate catalysts. It revealed that the CoN sample exhibited the highest activity during methanation due to high reducibility and large crystallite size having fewer interactions. The similar trend was observed for the CoAC and CoAA samples. However, the CoCL sample had the lowest activity, but highest selectivity to C₂-C₄ products. This was likely attributed to the different form of cobalt oxide species obtained from CoCl₂ as seen from XRD.

6.2 Recommendations

1. The effect of conditions to synthesize cobalt on cobalt-aluminate for carbon monoxide hydrogenation catalysts should be further investigated.

2. Besides Co metal, other metals such as Ni, Fe and etc. should be investigated with the catalysts synthesized in one-pot via solvothermal process for carbon monoxide hydrogenation.

3. Besides cobalt on cobalt-aluminate, such as cobalt on cobalt-silicate and etc. should be investigated with the catalysts that was synthesized in one-pot via solvothermal process for carbon monoxide hydrogenation.

4. Mixed support should be investigated with the catalysts that were synthesized in one-pot via solvothermal process for carbon monoxide hydrogenation.

สถาบันวิทยบริการ
จุฬาลงกรณ์มหาวิทยาลัย

REFERENCES

- Arean, C.O., Mentrui, M.P., Platero, E.E., Xamena, F.X.L.I., and Parra, J. B. Sol-gel method for preparing high surface area CoAl_2O_4 and $\text{Al}_2\text{O}_3\text{-CoAl}_2\text{O}_4$ spinels. Mater. Lett. 39 (1999): 22-27.
- Bacon, G.E. and Roberts, F.F. Neutron-diffraction studies of magnesium ferritealuminate powders. Acta Cryst. 6 (1953): 57-62.
- Brady, R.C., Pettit, R. Mechanism of the Fischer-Tropsch reaction. The chain propagation step. J. Am. Chem. Soc. 103 (1981): 1287-1289.
- Chamtal, S, Larbot, A., Persin, M., Sarrazin, J., Sghyar, M., and Rafiq, M. Cobalt spinel CoAl_2O_4 via sol-gel process: elaboration and surface properties. Mater. Res. Bull. 35 (2000): 2515-2523.
- Chen-Bin, W., Chih-Wei, T., Hsin-Chi, T., and Shu-Hua, C. Characterization and Catalytic Oxidation of Carbon Monoxide Over Supported Cobalt Catalysts. Catal Lett. 107 (2006): 223-230.
- Cho, W.S., and Kakihana, M. Crystallization of ceramic pigment CoAl_2O_4 nanocrystals from Co-Al metal organic precursor. J. Alloy. Compd. 287 (1999): 87-90.
- Chokkaram, S., Srinivasan, R., and Milburn, D. R. Conversion of 2-octanol overnickel-alumina, cobalt-alumina, and alumina catalysts. J. Mol. Catal. A-Chem. 121 (1997): 157-169.
- Edelstein, A., and Cammarata, R.C. Synthesis, Properties and Applications, Nanomaterials. Institute of physics Publishing, Bristol and Philadelphia, 1996.
- Elbashir, N. O., Dutta, P., Manivannan, A., Seehra, M. S., Roberts, C. B. Impact of cobalt-based catalyst characteristics on the performance of conventional gas-phase and supercritical-phase Fischer-Tropsch synthesis. Appl. Catal. A, 285 (2005): 169-180.
- Enache, D.I., Rebours, B., Roy-Auberger, M., Revel, R. In Situ XRD Study of the Influence of Thermal Treatment on the Characteristics and the Catalytic Properties of Cobalt-Based Fischer-Tropsch Catalysts. J. Catal. 205 (2002): 346-353.

- Elbashir, N. O., Dutta, P., Manivannan, A., Seehra, M. S., Roberts, C. B. Impact of cobalt-based catalyst characteristics on the performance of conventional gas-phase and supercritical-phase Fischer–Tropsch synthesis. Appl. Catal. A 285(1-2) (2005): 169-180.
- Girardon, J.S., Lermontov, A.S., Gengembre, L., Chernavskii, P.A., Constant, A.G., Khodakov, A.Y. Effect of cobalt precursors and pretreatment conditions on the structure and catalytic performance of cobalt silica-supported Fischer-Tropsch catalysts. J. Catal. 230 (2005): 339-352.
- Hosseini, S. A., Taeb, A., Feyzi, F. Evaluation of Ru-promoted Co/gamma-Al₂O₃ catalysts in Fischer–Tropsch synthesis in a CSTR. Catal. Comm. 6 (2005)
- Huang, C.J., Fei, J.H., D.J., and Zheng, X.M. The Dramatic Effect of Metal Precursor on the Catalytic Performance of Co/SiO₂ Catalyst for CO₂ reforming of CH₄. Chinese Chem. Lett. 11 (2000) : 181-184.
- Jacobs, G., Das, T., Zhang, Y.Q., Li, J.L., Racoillet, G., Davis, B.H. Fischer-Tropsch synthesis: support, loading, and promoter effects on the reducibility of cobalt catalysts. Mater. Chem. Phys. 89 (2005): 395-401.
- Jongsomjit, B., Panpranot, J., and Goodwin, Jr., J.G. Co-support Compound Formation in Alumina-Supported Cobalt Catalysts. J. Catal. 204 (2001): 98-109.
- Jongsomjit, B., and Goodwin, Jr., J.G. Co-support Compound Formation in Co/Al₂O₃ catalysts: effect of reduction gas containing CO. Catal. Today 77 (2002):191-204.
- Jongsomjit, B., Panpranot, J., and Goodwin, Jr., J.G. Effect of zirconia-modified alumina on the properties of Co/γ-Al₂O₃ catalysts J. Catal. 215 (2003): 66-77
- Jongsomjit, B., Sakdamnusun, C., Goodwin, Jr., J.G., and Praserttham, P. Co-support Compound Formation in Titania-Supported Cobalt Catalysts. Catal. Lett. 94 (2004): 209-215.
- Jongsomjit, B., Sakdamnusun, C., Praserttham, P. Dependence of crystalline phases in titania on catalytic properties during CO hydrogenation of Co/TiO₂ catalysts Mater. Chem. Phys. 89 (2005): 395-401.

- Jongsomjit, B., Wongsalee, T., Praserttham, P. Characteristics and catalytic properties of Co/TiO₂ for various rutile:anatase ratios Catal. Commun. 6 (2005): 705-710.
- Kim-Nga, N., and Kim-Chi, D. Synthesis, Characterization and Catalytic Activity of CoAl₂O₄ and NiAl₂O₄ Spinel - Type Oxides for NO_x Selective Reduction. Advances in Technology of Materials and Materials Processing, 6 (2004): 336-343.
- Kanyanucharat, A. Determination of the thermal stability of CoAl₂O₄, ZnAl₂O₄ and NiAl₂O₄ single nanocrystals. Masters's thesis, Faculty of Engineering, Chulalongkorn University, (2002).
- Kogelbaure, A., Webber, J.C., and Goodwin, Jr., J.G. The formation of cobalt silicates in Co/SiO₂ under hydrothermal condition. Catal Lett. 34 (1995): 259-267.
- Kraum, M., and Bearns, M. Fisher-Tropsch synthesis: the influence of various cobalt compounds applied in the preparation of supported cobalt catalysts on their performance. Appl. Catal. A. 186 (1999). 189-200.
- Lin, J., Zhan, X., Zhang, Y., Jacobs, G., Das, T., and Davis, B.H. Fischer-Tropsch synthesis: effect of water on the deactivation of Pt promoted Co/Al₂O₃ catalysts. Appl. Catal. A: General 228 (2002): 203-212.
- Martinez, A., Lopez, C., Marquez, F., Diaz, I. Fischer-Tropsch synthesis of hydrocarbons over mesoporous Co/SBA-15 catalysts: the influence of metal loading, cobalt precursor, and promoters. J.catal. 220 (2003): 486-499.
- Melo, D.M.A., Cunha, J.D., Fernandes, J.D.G., Bernardi, M.I., Melo, M.A.F., and Martinelli, A.E. Evaluation of CoAl₂O₄ as ceramic pigments. Materials Research Bulletin. 38 (2003): 1559-1564.
- Meyer, F., Dieratein, A., Beck, Ch., Hartl, W., Hempelmann, R., Mathur, S., and Veith, M. Size-controlled synthesis of nanoscaled aluminum spinels using heterobimetallic alkoxide precursors via water/oil microemulsions. Nanostructured Mater. 12 (1999): 71-74.
- Mekasuwandumrong, O., Silveston, P.L., Praserttham, P., Inoue, M., Pavarajarn, V., and Tanaklrungsank, W. Synthesis of thermally stable micro spherical γ -alumina by thermal decomposition of alumina isopropoxide in mineral oil. Inorg. Chem. Commun. 6 (2003): 930-934.

- Mimani, T. Instant synthesis of nanoscale spinel aluminates. J. Alloy. Compd. 315 (2001): 123-128
- Mochizuki, T., Koizumi, N., Hamabe, Y., Hara, T., Takizawa, H., and Yamada, M. J. of Japan Petroleum Institute. 50 (2007): 262
- Niemela, M.K., Krause, A.O.I., Vara, T., Kiviaho, J.J., and Reinikainen, M.K.O. The effect of the precursor on the characteristics of Co/SiO₂ catalysts. Appl. Catal. A. 147 (1996): 325-345.
- Nobuntu N., Neil, J.C. The effect of cobalt and zinc precursors on Co (10%)/Zn (x%)/TiO₂ (x = 0, 5) Fischer-Tropsch catalysts. J. of Molecular Catal. A: Chemical 225 (2005): 137-142.
- Ohgushi, T. and Umeno, S. Low temperature synthesis of dispersed fine particle of cobalt aluminate - a new application of zeolite. Bull. Chem. Soc. Jap. 60 (1987): 4457-4458.
- Ohtsuka, Y., Takahashi, Y., Noguchi, M., I Arai, T., Takasaki, S., Tsubouchi, N., Wangl, Y. Novel utilization of mesoporous molecular sieves as supports of cobalt catalysts in Fischer-Tropsch synthesis. Catal. Today. 89 (2004): 419-429.
- Othmer, K. Encyclopedia of chemical technology. Vol 6. 4th ed. New york: A Wiley Interscience Publication, John Wiley&Son, 1991.
- Panpranot, J., Kaewkun, and S., Praserthdam. Metal-support interaction in mesoporous silica supported cobalt Fischer-Tropsch catalysts. React. Kinet. Catal. Lett. 85 (2005): 299-304.
- Panpranot, J., Kaewkun, S., Praserthdam, P., and Goodwin, Jr., J.G. Effect of cobalt precursors on the dispersion of cobalt on MCM-41. Catal. Lett. 91 (2003): 95-102.
- Rosynek, M.P., and Polansky, C.A. Effect of cobalt source on the reduction properties of silica-supported cobalt catalysts. Appl. Catal. 73 (1991): 97-112.
- Sangthonganothai, P. Solvothermal synthesis of spinel-type zinc gallate and zinc aluminate powder. Masters's thesis, Faculty of Engineering, Chulalongkorn University, (2000).

- Sirijaruphan, A., Horvath, A., Goodwin, Jr., J.G., and Oukaci, R. Cobalt aluminate formation in alumina-supported cobalt catalysts: effects of cobalt reduction state and water vapor. Catal Lett. 91 (2003): 89-94
- Soled, S.L., Iglesia, E., Fiato, R.A., Baumgartner, J.E., Vroman, H.B. and Miseo, S. Paper 293, 18th North American Catalysis Society Meeting, Cancun, Mexico, 1–6 June 2003.
- Steen, E.V., Sewell, G.S., Makhothe, R.A., Micklethwaite, C., Manstein, H., Lange, M.D., and O’Connor, C.T. TPR Study on the Preparation of Impregnated Co/SiO₂ Catalysts. J. Catal. 162 (1996) : 220-229.
- Steynberg, A.P., Espinoza, R.L., Jager, B., Vosloo, A.C. High temperature Fischer-Tropsch synthesis in commercial practice. Appl. Catal. A. 186 (1999): 41-54.
- Steynberg, A.P., Nel, W.U., Desmet, M.A. Large Scale Production of High Value Hydrocarbons Using Fischer-Tropsch Technology. Stud. Surf. Sci. Catal. 147 (2004): 37-42.
- Sun, S.L., Tsubaki, N. and Fujimoto, K. The reaction performances and characterization of Fischer-Tropsch synthesis Co/SiO₂ catalysts prepared from mixed cobalt salts. Appl. Catal. A. 202 (2002): 121-131.
- Thormahlen, P., Fridell, E., Cruise, N., Skoglundh, M., and Palmqvist, A. The influence of CO₂, C₃H₆, NO, H₂, H₂O or SO₂ on the low-temperature oxidation of CO on a cobalt-aluminate spinel catalyst (Co_{1.66}Al_{1.34}O₄). Appl Catal B: Environmental 31 (2001)
- Voß, M., Borgmann, D., and Wedler, G. Characterization of alumina, silica, and titania supported cobalt catalysts, J.Catal. 212 (2002): 10-21.
- Young, R.S. COBALT: Its Chemistry, Metallurgy, and Uses. New York: Reinhold Publishing Corporation, 1960.
- Zayat, M. and Levy, D. Blue CoAl₂O₄ particles prepared by the sol-gel and citrate-gel methods. Chem.Mater. 12 (2000): 2763-2769.
- Zayat, M. and Levy, D. Surface Area Study of High Area Cobalt Aluminate Particles Preticles Prepared by the Sol-Gel Method. Sol-Gel Science and Technology. 25 (2002): 201-206.



APPENDICES

สถาบันวิทยบริการ
จุฬาลงกรณ์มหาวิทยาลัย

APPENDIX A

CALCULATION FOR CATALYST PREPARATION

In this study, cobalt on cobalt aluminate and alumina support were prepared by solvothermal method which using toluene as a solvent.

A.1 Calculation of cobalt on cobalt-aluminate preparation

Preparation of cobalt on cobalt-aluminate with various molar ratios of Co/Al (0.5, 1.0 and 2.0) and cobalt precursors (Cobalt (II) acetylacetonate, Cobalt (II) acetate, Cobalt (II) nitrate and Cobalt (II) chloride) by solvothermal method is shown as follow:

Reagent:	- Aluminium isopropoxide (AIP, $[(CH_3)_2CHO]_3Al$)
	Molecular weight = 204.25 g/mol
	- Aluminum, Al
	Atomic weight = 26.9815 g/mol
Precursors:	- Cobalt (II) acetylacetonate $[CH_3COCH=C(O-)CH_3]_2Co$
	Molecular weight = 257.15 g/mol
	- Cobalt (II) acetate tetrahydrate $(C_2H_3O_2)_2Co \cdot 4H_2O$
	Molecular weight = 249.08 g/mol
	- Cobalt (II) nitrate hexahydrate $Co(NO_3)_2 \cdot 6H_2O$
	Molecular weight = 291.03 g/mol
	- Cobalt (II) chloride hexahydrate $CoCl_2 \cdot 6H_2O$
	Molecular weight = 237.93 g/mol
	- Cobalt, Co
	Atomic weight = 58.933 g/mol

Calculation:

Cobalt (II) acetylacetonate**Co/Al = 0.5**

Aluminium isopropoxide 15 g were used for preparation cobalt on cobalt-aluminate.

Aluminium isopropoxide 15 g consisted of aluminum equal to:

$$\begin{aligned} \text{Aluminum} &= \frac{15}{204.25} \times (26.9815) \text{ g} \\ &= 1.9815 \text{ g} \\ &= \frac{1.9815}{26.9815} \text{ mol} \\ &= 0.07344 \text{ mol} \end{aligned}$$

For Co/Al = 0.5, 0.07344 mole of aluminum

$$\begin{aligned} \text{Cobalt required} &= 0.07344 \times 0.5 \text{ mol} \\ &= 0.03672 \text{ mol} \\ &= 0.03672 \times 58.933 \text{ g} \\ &= 2.1640 \text{ g} \end{aligned}$$

Cobalt 2.1640 g was prepared from cobalt (II) acetylacetonate

$$\begin{aligned} &= \frac{2.1640}{58.933} \times 257.15 \text{ g} \\ &= 9.4425 \text{ g} \end{aligned}$$

Co/Al = 1.0

Aluminium isopropoxide 15 g were used for preparation cobalt on cobalt-aluminate.

$$\text{Aluminum} = 0.07344 \text{ mol}$$

For Co/Al = 1.0, 0.07344 mole of aluminum

$$\begin{aligned} \text{Cobalt required} &= 0.07344 \times 1.0 \text{ mol} \\ &= 0.07344 \text{ mol} \\ &= 0.07344 \times 58.933 \text{ g} \\ &= 4.3280 \text{ g} \end{aligned}$$

Cobalt 4.3290 g was prepared from cobalt (II) acetylacetonate

$$\begin{aligned} &= \frac{4.3280}{58.933} \times 257.15 \text{ g} \\ &= 18.8851 \text{ g} \end{aligned}$$

Co/Al = 2.0

Aluminium isopropoxide 15 g were used for preparation cobalt on cobalt-aluminate.

$$\text{Aluminum} = 0.07344 \text{ mol}$$

For Co/Al = 1.0, 0.07344 mole of aluminum

$$\begin{aligned} \text{Cobalt required} &= 0.07344 \times 2.0 \text{ mol} \\ &= 0.14688 \text{ mol} \\ &= 0.14688 \times 58.933 \text{ g} \\ &= 8.6561 \text{ g} \end{aligned}$$

Cobalt 8.6561 g was prepared from cobalt (II) acetylacetonate

$$\begin{aligned} &= \frac{8.6561}{58.933} \times 257.15 \text{ g} \\ &= 37.7703 \text{ g} \end{aligned}$$

Cobalt (II) acetate**Co/Al = 1.0**

Aluminium isopropoxide 15 g were used for preparation cobalt on cobalt-aluminate.

$$\text{Aluminum} = 0.07344 \text{ mol}$$

For Co/Al = 1.0, 0.07344 mole of aluminum

$$\text{Cobalt required} = 4.3280 \text{ g}$$

Cobalt 4.3280 g was prepared from cobalt (II) acetate

$$\begin{aligned} &= \frac{4.3280}{58.933} \times 249.08 \text{ g} \\ &= 18.2923 \text{ g} \end{aligned}$$

Cobalt (II) nitrate**Co/Al = 1.0**

Aluminium isopropoxide 15 g were used for preparation cobalt on cobalt-aluminate.

$$\text{Aluminum} = 0.07344 \text{ mol}$$

For Co/Al = 1.0, 0.07344 mole of aluminum

$$\text{Cobalt required} = 4.3280 \text{ g}$$

Cobalt 4.3280 g was prepared from cobalt (II) nitrate

$$\begin{aligned} &= \frac{4.3280}{58.933} \times 291.03 \text{ g} \\ &= 21.3730 \text{ g} \end{aligned}$$

Cobalt (II) chloride

Co/Al = 1.0

Aluminium isopropoxide 15 g were used for preparation cobalt on cobalt-aluminate.

$$\text{Aluminum} = 0.07344 \text{ mol}$$

For Co/Al = 1.0, 0.07344 mole of aluminum

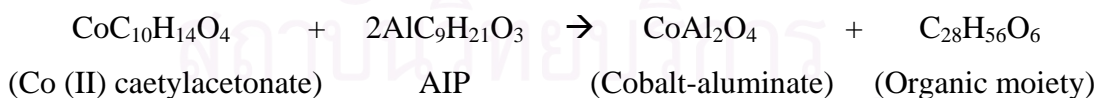
$$\text{Cobalt required} = 4.3280 \text{ g}$$

Cobalt 4.3280 g was prepared from cobalt (II) nitrate

$$\begin{aligned} &= \frac{4.3280}{58.933} \times 237.93 \text{ g} \\ &= 17.4734 \text{ g} \end{aligned}$$

A.2 Calculation of cobalt excess and % cobalt loading

Preparation of cobalt-aluminate (CoAl_2O_4) which the ratio of Co/Al is equal to 0.5 is assumed for complete conversion of CoAl_2O_4 formation.



Co/Al = 0.5

0.0367 mol	0.07344 mol	0.0367 mol
MW 257.15 g/mol	204.25 g/mol	176.856 g/mol
9.4425 g	15 g	6.4906 g

$$\text{Co} = 2.1640 \text{ g}$$

Co/Al = 1.0, cobalt equal to 4.3280 g

The weight of cobalt excess in Co/Al = 1 is 2.1640 g

$$\begin{aligned} \text{The weight of cobalt excess} &= \frac{2.1640}{2.1640 + 6.4906} \times 100 \\ &= 25 \% \text{ wt} \end{aligned}$$

A.3 Calculation of cobalt loading

Preparation of 25% wtCo/Al₂O₃ by the incipient wetness impregnation method are shown as follows:

Reagent: - Cobalt (II) acetylacetonate [CH₃COCH=C(O-)CH₃]₂Co
 Molecular weight = 257.15 g/mol
 Cobalt (Co), Atomic weight = 58.933 g/mol
 - Support: Al₂O₃

Based on 100 g of catalyst used, the composition of the catalyst will be as follows:

$$\begin{aligned} \text{Cobalt} &= 25 \text{ g} \\ \text{Al}_2\text{O}_3 &= 100 - 25 = 75 \text{ g} \end{aligned}$$

For 1 g of support (Al₂O₃)

$$\text{Cobalt required} = 1 \times \frac{25}{75} = 0.333 \text{ g}$$

Cobalt 0.333 g was prepared from cobalt (II) acetylacetonate.

$$\begin{aligned} \text{Cobalt (II) acetylacetonate required} &= \frac{0.333}{58.933} \times 257.15 \\ &= 1.4530 \text{ g} \end{aligned}$$

Since the pore volume of Al₂O₃ support is 1 ml/g. Thus, the total volume of impregnation solution which must be used is 1 ml for Al₂O₃ by the requirement of incipient wetness impregnation method, the ethanol is added until equal pore volume for dissolve cobalt (II)acetylacetonate.

APPENDIX B

CALCULATION FOR TOTAL H₂ CHEMISORPTION

Calculation of the total H₂ chemisorption and metal dispersion of the catalyst, a stoichiometry of H/Co = 1, measured by H₂ chemisorption is as follows:

Let the weight of catalyst used	=	W	g
Integral area of H ₂ peak after adsorption	=	A	unit
Integral area of 45 μl of standard H ₂ peak	=	B	unit
Amounts of H ₂ adsorbed on catalyst	=	B-A	unit
Volume of H ₂ adsorbed on catalyst	=	45 × [(B - A) / B]	μl
Volume of 1 mole of H ₂ at 100°C	=	28.038	μl
Mole of H ₂ adsorbed on catalyst	=	[(B - A) / B] × [45 / 28.038]	mole

$$\begin{aligned} \text{Total H}_2 \text{ chemisorption} &= [(B - A) / B] \times [45 / 28.038] \times [1 / W] \text{ mole/g of catalyst} \\ &= N \text{ mole/g of catalyst} \end{aligned}$$

สถาบันวิทยบริการ
จุฬาลงกรณ์มหาวิทยาลัย

APPENDIX C

CALIBRATION CURVES

This appendix showed the calibration curves for calculation of composition of reactant and products in CO hydrogenation reaction. The reactant is CO and the main product is methane. The other products are linear hydrocarbons of heavier molecular weight that are C₂-C₄ such as ethane, ethylene, propane, propylene and butane.

The thermal conductivity detector, gas chromatography Shimadzu model 8A was used to analyze the concentration of CO by using Molecular sieve 5A column.

The VZ10 column are used with a gas chromatography equipped with a flame ionization detector, Shimadzu model 14B, to analyze the concentration of products including of methane, ethane, ethylene, propane, propylene and butane. Conditions uses in both GC are illustrated in Table C.1.

Mole of reagent in y-axis and area reported by gas chromatography in x-axis are exhibited in the curves. The calibration curves of CO, methane, ethane, ethylene, propane, propylene and butane are illustrated in the following figures.

Table C.1 Conditions use in Shimadzu modal GC-8A and GC-14B.

Parameters	Condition	
	Shimadzu GC-8A	Shimadzu GC-14B
Width	5	5
Slope	50	50
Drift	0	0
Min. area	10	10
T.DBL	0	0
Stop time	50	60
Atten	0	0
Speed	2	2
Method	41	41
Format	1	1
SPL.WT	100	100
IS.WT	1	1

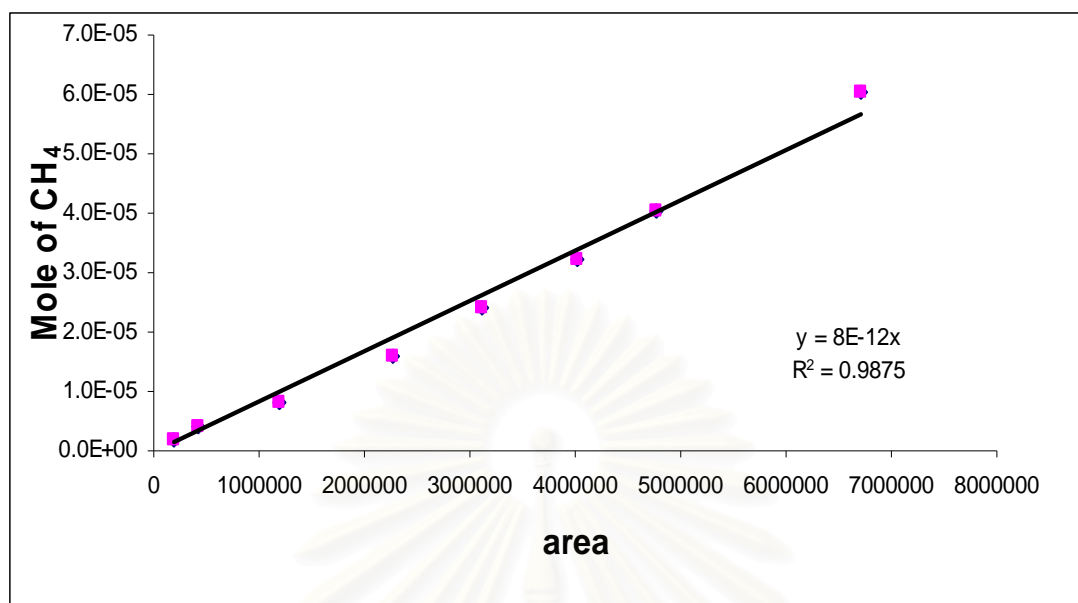


Figure C.1 The calibration curve of methane.

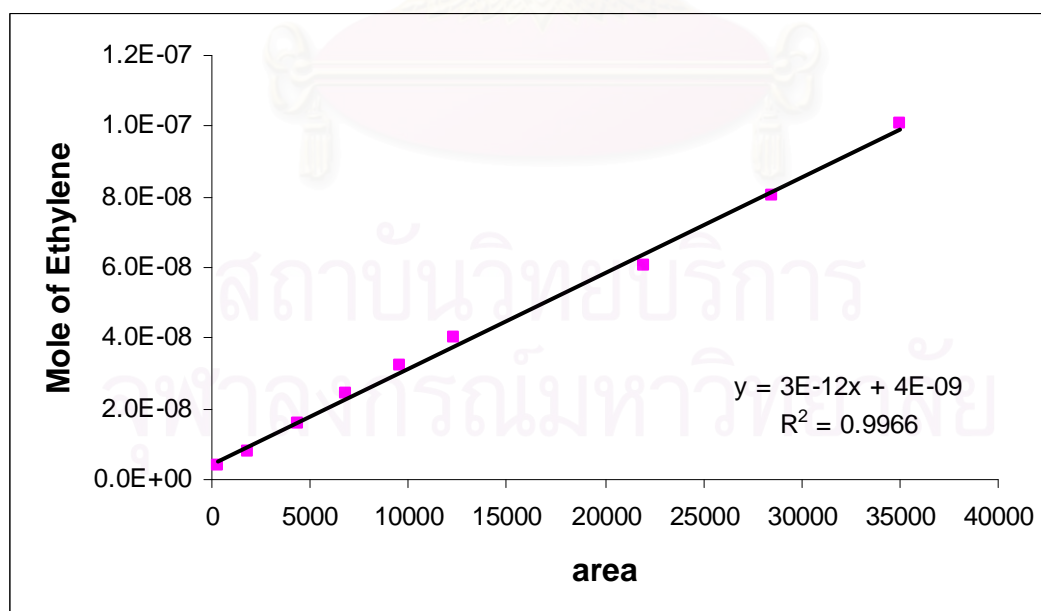


Figure C.2 The calibration curve of ethylene.

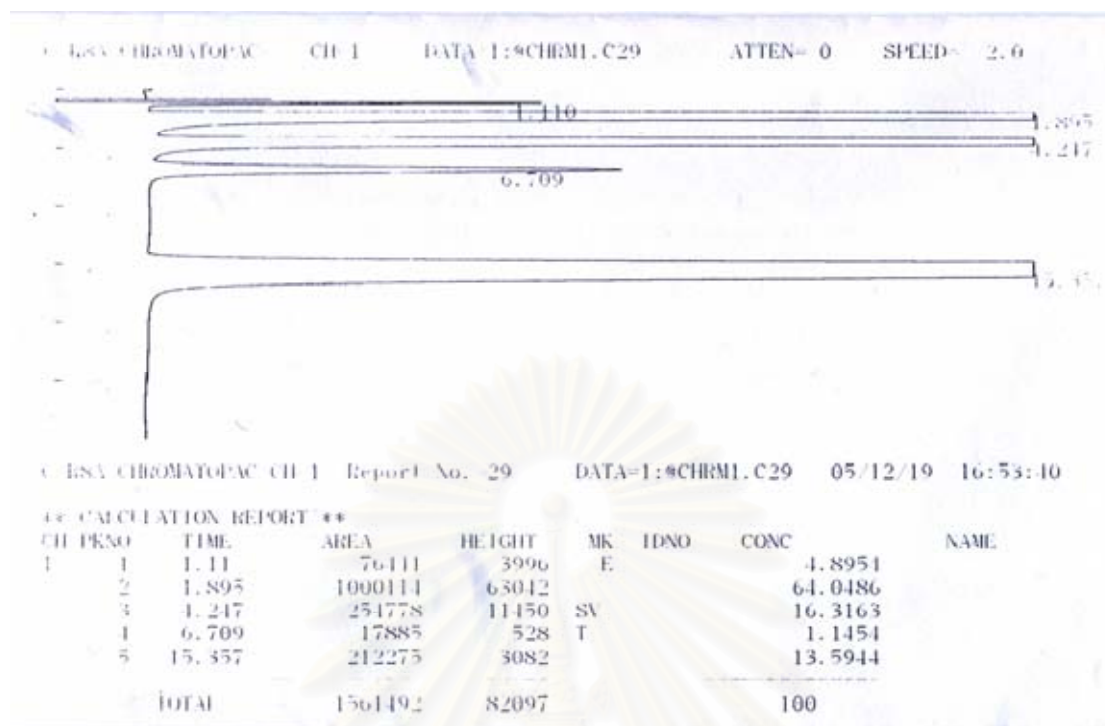


Figure C.3 The chromatograms of catalyst sample from thermal conductivity detector, gas chromatography Shimadzu model 8A (Molecular sieve 5A column).

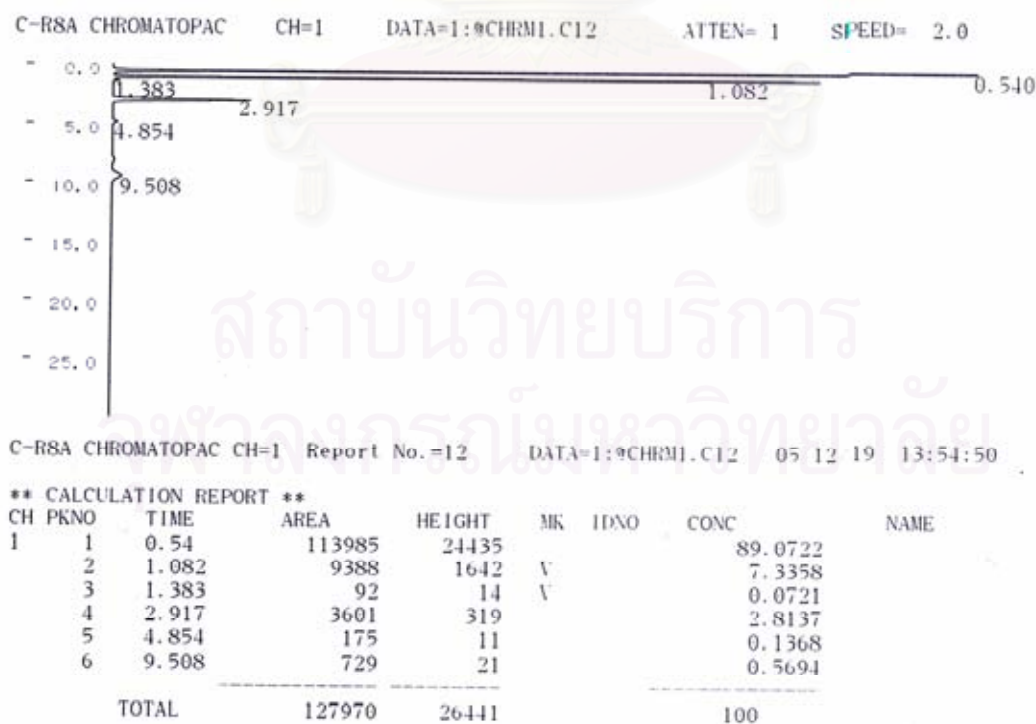


Figure C.4 The chromatograms of catalyst sample from flame ionization detector, gas chromatography Shimadzu model 14B (VZ10 column).

APPENDIX D

CALCULATION OF CO CONVERSION, REACTION RATE AND SELECTIVITY

The catalyst performance for the CO hydrogenation was evaluated in term of activity for CO conversion, reaction rate and selectivity.

CO conversion is defined as moles of CO converted with respect to CO in feed:

$$\text{CO conversion (\%)} = \frac{100 \times [\text{mole of CO in feed} - \text{mole of CO in product}]}{\text{mole of CO in feed}} \quad (\text{i})$$

Reaction rate was calculated from CO conversion that is as follows:

Let the weight of catalyst used	=	W	g
Flow rate of CO	=	2	cc/min
Reaction time	=	60	min
Weight of CH ₂	=	14	g
Volume of 1 mole of gas at 1 atm	=	22400	cc

$$\text{Reaction rate (g CH}_2\text{/g of catalyst)} = \frac{[\% \text{ conversion of CO} / 100] \times 60 \times 14 \times 2}{W \times 22400} \quad (\text{ii})$$

Selectivity of product is defined as mole of product (B) formed with respect to mole of CO converted:

$$\text{Selectivity of B (\%)} = 100 \times [\text{mole of B formed} / \text{mole of total products}] \quad (\text{iii})$$

Where B is product, mole of B can be measured employing the calibration curve of products such as methane, ethane, ethylene, propane, propylene and butane

$$\text{mole of CH}_4 = (\text{area of CH}_4 \text{ peak from integrator plot on GC-14B}) \times 8 \times 10^{12} \quad (\text{iv})$$

APPENDIX E

CHEMISORPTION DATA

Table E.1 chemisorption data

Samples	Total H ₂ chemisorption ($\mu\text{mol/g cat}$)
Co/Al_0.5_1h	17.5
Co/Al_0.5_2h	8.1
Co/Al_0.5_250°C	25.5
Co/Al_1.0_1h	21.6
Co/Al_1.0_2h	5.2
Co/Al_1.0_250°C	36.0
Co/Al_300°C	5.2
Co/Al_400°C	5.6
Co/Al_500°C	4.8
Co/Al_2.0_1h	48.8
Co/Al_2.0_2h	66.7
Co/Al ₂ O ₃ _2h	4.8
CoAA	36.0
CoAC	85.9
CoN	42.6
CoCL	26.6

APPENDIX F

LIST OF PUBLICATIONS

- **Proceeding**

1. Sirirat Rojanapipatkul, Bunjerd Jongsomjit, and Piyasan Ptaserthdam, “Synthesis of cobalt on cobalt-aluminate and its catalytic properties for carbon monoxide hydrogenation”, Proceeding of the 17th Thailand Chemical Engineering and Applied Chemistry Conference, Chiangmai Thailand, Oct., 2007.

- **International Papers**

1. Sirirat Rojanapipatkul, Piyasan Praserthdam, and Bunjerd Jongsomjit, “Synthesis of cobalt on cobalt-aluminate via solvothermal method and its catalytic properties for carbon monoxide hydrogenation”, Submitted to Catalysis Communications, Jan., 2008.
2. Sirirat Rojanapipatkul, Piyasan Praserthdam, and Bunjerd Jongsomjit, “Influence of calcination temperatures on the characteristics of cobalt on cobalt-aluminate catalysts synthesized by the solvothermal process”, Submitted to Materials Letters, Jan., 2008.
3. Sirirat Rojanapipatkul and Bunjerd Jongsomjit, “Effect of cobalt precursors on the physico-chemical properties of cobalt dispersed on cobalt-aluminate synthesized by the solvothermal process”, Submitted to Materials Chemistry and Physics , Jan., 2008.

VITA

Miss Sirirat Rojanapipatkul was born on 19th September 1983, in Bangkok, Thailand. She finished high school from Horwang school, Bangkok in 2002, and received her Bachelor degree of Chemical Technology from Faculty of Science, Chulalongkorn University, Thailand in March 2006. She continued her Master's study at the department of Chemical Engineering, Faculty of Engineering, Chulalongkorn University in 2006.



สถาบันวิทยบริการ
จุฬาลงกรณ์มหาวิทยาลัย